A sea anemone and its microbiome

–

Identification of factors determining the microbiome establishment in the metaorganism *Nematostella vectensis*

Inaugural-Dissertation

zur Erlangung des Doktorgrades
der Mathematisch-Naturwissenschaftlichen Fakultät
der Heinrich-Heine-Universität Düsseldorf

vorgelegt von
Hanna Domin
aus Salzgitter

Düsseldorf, November 2022

aus dem Institut für Zoologie und organismische Interaktionen
der Heinrich-Heine-Universität Düsseldorf

Gedruckt mit der Genehmigung der
Mathematisch-Naturwissenschaftlichen Fakultät der
Heinrich-Heine-Universität Düsseldorf

Berichterstatter:

1. Professor Dr. Sebastian Fraune

2. Professor Dr. Ilka Maria Axmann

Tag der mündlichen Prüfung: 09. Februar 2023

Contents

Abstract

Life on earth is never solitary. No individual is ever alone, but always appearing in intra- or interspecies communities, or both. Every multicellular organism possesses a microbiota, which consists of prokaryotes, unicellular eukaryotes and viruses. The community composition of the microbiota is highly dependent on the host species and its environment. This unit of a host and the entity of all associated microbes in a given environment is called a metaorganism. The metaorganism acts as a biological entity, which can help its host to adapt to a changing environment, fight a microbial intruder or digest molecules indigestible for the host itself. With the emergence of high throughput sequencing, the huge diversity and the capabilities of microbes living in and on macroscopic organisms were revealed. The microbial community assembly and microbial community establishment is a very young and a highly discussed field.

Nematostella vectensis is an emerging model organism especially in interdisciplinary research fields and offers the possibility to research host-bacteria interactions during development and in a changing environment. The microbiome of *Nematostella* is development-specific, each developmental stage from planula larva over juvenile to adult polyp exhibits a distinct bacterial colonization pattern.

In this thesis, I wanted to identify factors contributing to the development-specific microbiome of *Nematostella*. For this, I performed recolonization experiments with juvenile and adult polyps, in which I recolonized polyps with complex microbiomes extracted from specific developmental stages, or with commensal bacterial strains. 16S rRNA sequencing revealed that the bacterial succession during recolonization recapitulates the bacterial succession pattern occurring during natural development. The calculation of bacterial co-occurrence networks indicated dynamic bacteria-bacteria interactions during development. Whole transcriptome sequencing of host RNA and calculation of the metabolic potential of the microbiome revealed host mechanisms as regulator of early recolonization, and bacteria-bacteria interactions as a driver of late recolonization. Additionally, chitin was identified as a promising candidate influencing the community assembly and succession, as *Nematostella* increased its chitin production upon recolonization, while the microbiome was able to degrade chitin and possibly cross-feed on the metabolites.

Abbreviations

°C	degrees Celsius
% (v/v)	volume concentration (volume/volume)
% (w/v)	mass concentration (weight/volume)
A	adenine
Amp	ampicillin
AMP	antimicrobial peptide
bA	bacteria of adult stages
BALO	*Bdellovibrio* and like organism
bJ	bacteria of juvenile stages
bL	bacteria of larval stages
BMP	bone morphogenetic protein
bp	base pairs
C	cytosine
Cas9	CRISPR-associated protein 9
CBD	chitin binding domain
CFU	colony forming unit
ChIP	chromatin Immunoprecipitation
cm	centimeter
CRISPR	clustered regularly interspaced short palindromic repeats
DMSO	dimethyl sulfoxide
DNA	deoxyribonucleic acid
DNase	deoxyribonuclease
dNTP	deoxynucleotide triphosphate
dpr	days post recolonization
EDTA	ethylenediaminetetraacetic acid
EF1a	elongation factor 1alpha
ESV	exact sequence variant
EtOH	ethanol
E. coli	Escherichia coli
et al.	lat: et alii, engl.: and others
G	guanine
g	gram
gDNA	genomic DNA
GF	germ free
GFP	green fluorescent protein
hox	homeobox
hp	hairpin
hpf	hours post fertilization
Ig	immunoglobulin
IL-1R	interleukin-1 receptor
kd	knockdown
L	liter
LB	Luria Bertani (bacterial growth broth)
LED	Light-emitting diode
Log2FC	Log 2 fold change

LRR	leucine-rich repeat
M	molar
MAMP	microbe-associated molecular pattern
MB	marine bouillon or marine broth
mg	milligram
min	minute
mL	milliliter
mm	millimeter
mM	millimolar
mRNA	messenger RNA
MyD88	myeloid Differentiation factor 88
n	number of replicates
NF-κB	nuclear Factor kappa-light-chain-enhancer of activated B cells
nm	nanometer
NM	*Nematostella* Medium
NOD	nucleotide-binding oligomerization domain
µL	microliter
µM	micromolar
µm	micrometer
OD	optical density
OTU	operational taxonomic unit
PAMP	pathogen-associated molecular pattern
PBS	phosphate buffered saline
PCA	principal component analysis
PCoA	principal coordinates analysis
PCR	polymerase chain reaction
PFA	paraformaldehyde
pH	potential of hydrogen
POM	particulate organic matter
ppt	parts per thousand
PRR	pattern-recognition receptor
qRT	quantitative Real Time
QS	quorum sensing
RFP	red fluorescent protein
RNA	ribonucleic acid
RNase	ribonuclease
rpm	rounds per minute
rRNA	ribosomal RNA
RT	room temperature or reverse transcriptase
s	second
SCFA	short chain fatty acid
SOB	super optimal broth
SOC	super optimal broth with glucose
sp.; spp.	species
T	thymine
TAE	tris-acetate-EDTA buffer

TALEN	transcription activator-like effector nuclease
TIR	Toll/Interleukin-1 receptor
TLR	Toll-like receptor
Tm	melting temperature
U	unit
UPGMA	unweighted pair group method with arithmetic mean
UV	ultraviolet light
wt	wildtype

1 Introduction

1.1 Metaorganism Concept

Animals evolved in a world already inhabited by all forms of unicellular life, making it unsurprising that microorganisms also colonized animals (Sieber et al. 2021). This colonization sometimes developed into such a tight relationship that it became an obligate and mutualistic symbiosis, while others remained facultative. With the emergence of genomic tools to study the molecular nature of organisms, the view on microscopic life changed from microbes being primarily pathogens to them also providing benefits to their macroscopic interaction partners (Jaspers et al. 2019). From this, the metaorganism concept emerged, which considers every multicellular organism as a metaorganism: The multicellular host lives in close association with bacteria, archaea, fungi, viruses and other microbial and eukaryotic species in a given environment (**Figure 1-1**) (Bosch and McFall-Ngai 2011).

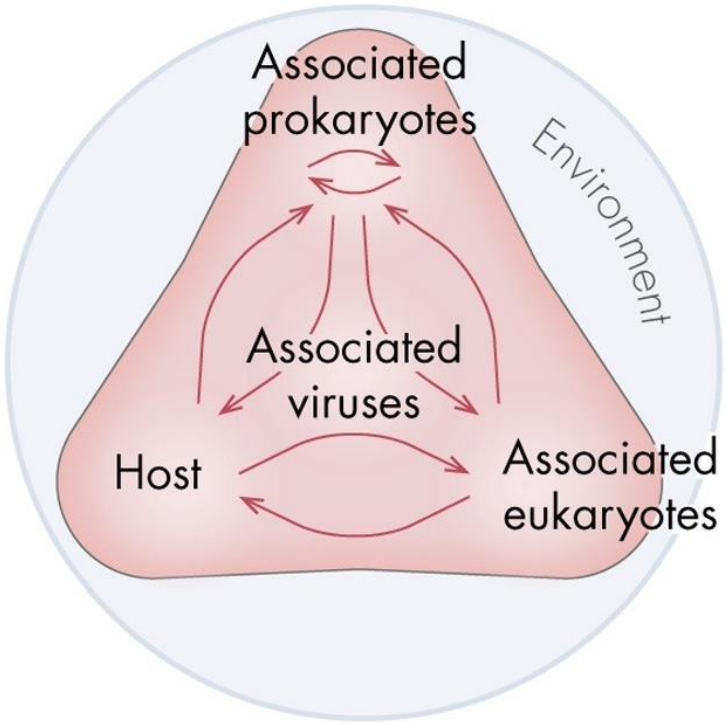

Figure 1-1 *The Metaorganism Concept. The metaorganism consists of a macroscopic host and all associated prokaryotes, eukaryotes and viruses in a given environment* (Jaspers et al. 2019).

With advancement of genomic tools and sequencing technologies, especially in regard to cost, sequencing quantity and sequencing length, with the emergence of metagenomes, meta-transcriptomes and single cell sequencing, it is now possible to study the microbial diversity and the interactions within metaorganisms on a fine scale (Simon et al. 2019).

Microbes can colonize each of the host's surfaces, which interact with their environment, like the skin, gut, mouth and other mucosal epithelia (Huttenhower et al. 2012). However, the host is not a neutral habitat waiting for microbes can settle. Environmental- and host-factors, but also bacteria-bacteria interactions all contribute to shape the host-specific microbiota. For instance, it is not necessarily possible to predict how two commensals will grow on a host by calculating population dynamics of their in-vitro growth, as was shown for two bacterial colonizers of the model organism *Hydra*. Here, the commensal *Curvibacter sp.* was able to outcompete another commensal during host-colonization, even though in-vitro growth experiments suggested the opposite (Li et al. 2015). It was also shown that when the gut microbiome of mice and fish were reciprocally transplanted, the resulting microbiome will more closely resemble the microbiome of the acceptor than the donor, underlining the selective pressures within the gut of the host (Rawls et al. 2006). Examples for mechanisms through which the host can exert influence on its microbiome include quorum quenching, to interfere with bacterial signaling and the production of species-specific sets of antimicrobial peptides (AMPs) which support and maintain a species-specific microbiome (Franzenburg et al. 2013; Pietschke et al. 2017; Weiland-Bräuer et al. 2019).

The metaorganism however is not a static state. It is dependent on factors which confer a nature of fluidity (Jaspers et al. 2019). Therefore, the assemblage of the microbiome is dependent on factors like developmental age (O'Toole and Jeffery 2015), nutrition (David et al. 2014a), antibiotic intake (Schubert, Sinani, and Schloss 2015) and other stress (Karl et al. 2018).

In humans, the microbiome contains one hundred times more genes than the host itself, centuplicating the genomic potential of the human host (Gilbert et al. 2018).The influence of the microbiome on the host is so extensive that some are even talking about the microbiome as an "organ" (Bäckhed et al. 2004; Baquero and Nombela 2012; Clarke et al. 2014; O'Hara and Shanahan 2006). It is complementing its host in many regards of life. Within the metaorganism, microbes can contribute to manifold aspects of the host's life:

It can influence development and reproduction, metabolism and digestion, pathogen defense and immune system maturation, but also ageing, behavior and even speciation (**Figure 1-2**) (Esser et al. 2019).

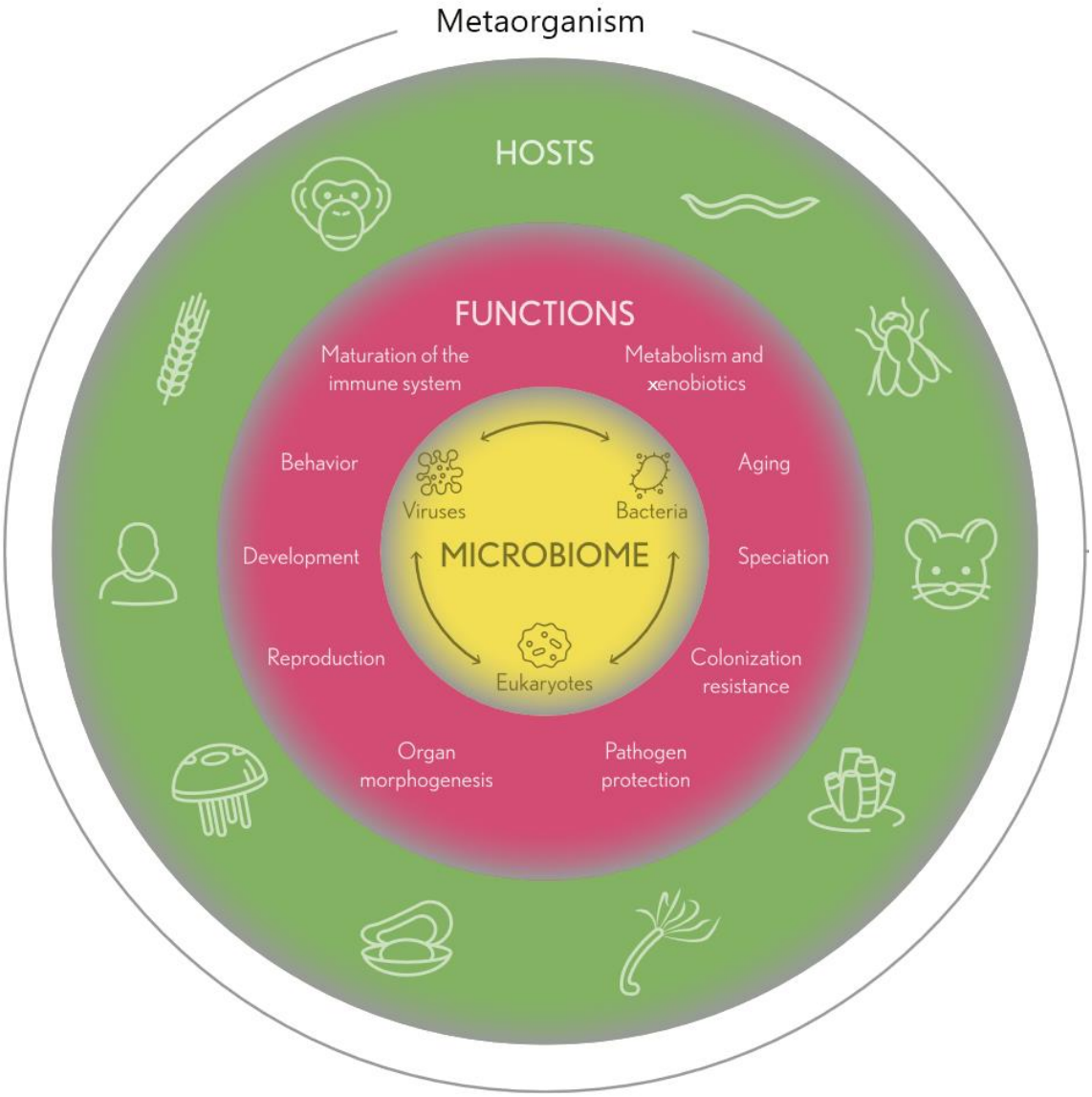

Figure 1-2 *The metaorganism with, examples of hosts and possible members of the microbiome, as well es the functions exhibited by members of the metaorganism* (Esser et al. 2019)*. The hosts range from early-emerging metazoans like sponges and cnidarians to highly complex vertebrates like apes and humans. The functions include influence on behavior development and aging, as well as pathogen protection and colonization resistance.*

It can help with digestion by e.g. degrading dietary polysaccharides, proteins and pyruvate and provide the host with short chain fatty acids (SCFAs), butyrate, propionate and acetate (Oliphant and Allen-Vercoe 2019). It can also influence the fitness of its host by e.g. influencing the fecundity or the length of the life span (Gould et al. 2018).The microbiome

is also highly correlated in metabolism by e.g. regulating gut hormone release or by influencing the body weight (Martin et al. 2019; Turnbaugh et al. 2006). Another important role is in development. Some animals can't undergo its full developmental life cycle in a germ-free state (Weiland-Bräuer et al. 2020). The absence of specific bacteria can also cause neurobehavioral traits like contraction frequency in Hydra (Murillo-Rincon et al. 2017). The impact of the microbiome on the brain is so extensive that the gut-brain-axis concept was expanded to the microbiota-gut-brain axis (Cryan et al. 2019). But the microbiome also influences, primes and trains both the innate and adaptive immune system (Zheng, Liwinski, and Elinav 2020), but also provides a direct defense against pathogens by providing colonization resistance, disease tolerance or even pathogen detainment (Chiu et al. 2017; Fraune et al. 2015; Longford et al. 2019). Bacteria can also act as a factor that allows fast adaptation. So do bacteria confer thermal resistance on a rapid scale in corals by undergoing a rapid change upon environmental changes (Reshef et al. 2006) It is also shown that the absence of bacteria causes developmental and immunological defects (Luczynski et al. 2016; Round and Mazmanian 2009). If these defects are mediated by removal of the microbiome, the wildtype phenotype can often be rescued by conventionalization of the germ-free animals (Nichols and Davenport 2020). Bacteria can also be utilized as a treatment for diseases like recurrent clostridium difficile infection where antibiotic treatment is unsuccessful. In these cases, the microbiome of healthy subjects can be transplanted into infected individuals, curing them in doing so (van Nood et al. 2013).

1.2 Microbial colonization and bacterial interactions

Although there's a lot of descriptive work which bacteria are present in which metaorganism under which circumstances, the assembly and maintenance of specific microbial communities is generally poorly understood (Bang et al. 2018). Most well-established theories regarding the assembly of ecological communities were created mainly from research about animals and plants on a macroscopic scale. Research of community assemblies on a microbial scale was scarce up until recently (Liu et al. 2019).

Bacteria exhibit common ecological relationships like competition and cooperation (Bauer et al. 2018). These ecological interactions fall under one of the three categories: Either they

are positive, negative, or neutral (Faust and Raes 2012). Positive interactions are interactions, in which both partners benefit. This kind of interactions is commonly referred to as mutualism. If two species exhibit negative interactions, it is called competition. If one species benefits while another one has a disadvantage, it is called parasitism or predation. If one species benefits while the other species is not affected, it is called commensalism. And if one species is not affected while the other one has a disadvantage, it is called amenalism (**Figure 1-3**).

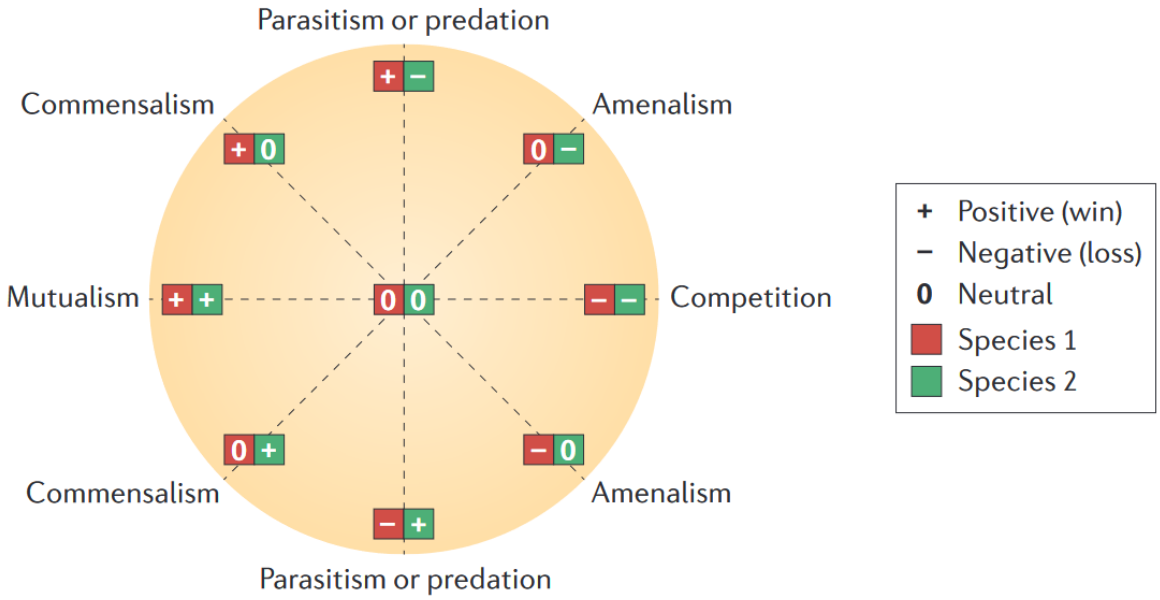

Figure 1-3 *Ecological intra-action compass for all possible pairwise interactions* (Faust and Raes 2012; Lidicker, 1979). *When two species exhibit pure positive interactions, this is called mutualism. Purely negative interactions are called competition. If one species gains while the other one loses, it is called parasitism or predation. In commensalism one species gains while the second species neither gains nor loses. In amensalism one species loses while the other neither gains nor loses.*

These pairwise interactions are important to understand the assembly, succession and stability within a complex bacterial community. Interaction types like competition, mutualism and predation are important factors not just in two-species communities but also in shaping multi-species communities. It was shown that a bacterial community with a high diversity is more likely to be stable if the interactions within the whole community are mostly competitive (Coyte, Schluter, and Foster 2015). Mixed-species biofilms profit from mutualistic interactions, for example by facilitating colonization and aggregation, by metabolic cooperation, and by mediating antibiotic resistance (Elias and Banin 2012). The

presence of predatory bacteria like Bdellovibrio and Like Organisms (BALOs) also seems to be positively correlated with microbiome diversity (Johnke et al. 2019).

While these ecological relationships are important for the assembly of microbial communities, these factors alone are not enough to grant a full understanding of the relationships inside a metaorganism. On this microscopic scale, metabolic dependencies are a crucial part of interspecies interactions (Zelezniak et al. 2015). Primary resources are metabolized first by primary degraders and then by secondary consumers. Metabolic end products can then again be used for primary production of e.g. polysaccharides (**Figure 1-4**).

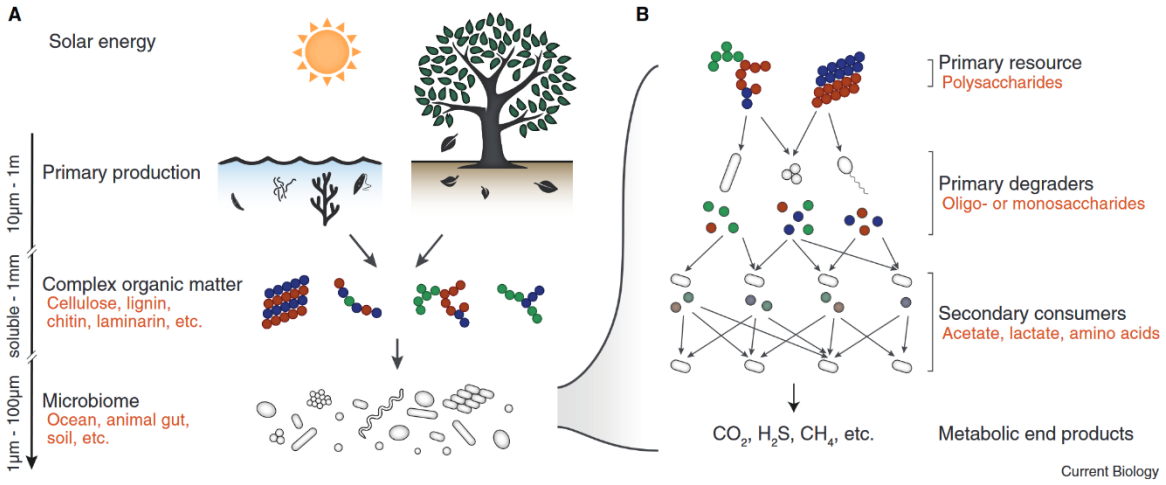

Figure 1-4 *Microbiomes and their metabolic dependencies in the context of the global ecosystem* (Gralka et al. 2020). *In the global ecosystem, primary production results in complex organic matter which can be used as energy resource by the microbiome. The primary resource consisting of polysaccharides can be degraded by primary degraders, resulting in oligo- and monosaccharides. Secondary consumers can process the byproducts of the primary degraders. Metabolic end products then again act as primary sources for primary production.*

The metabolic networks and the interactions within a community are complex. Therefore, first approaches were taken up to create and unify a conceptual framework of microbial community assembly by combining several ecological models like neutral theory, null models, stochastic and deterministic models into one framework and applying them from the macrobial to the microbial scale (Dumbrell et al. 2010; Vellend 2010; Weiher and Keddy 1995). Nemergut *et al* expanded Vellend's try to unify terms into a model, in which community assembly can be represented by four processes: Selection, Diversification, Dispersal and Drift (**Figure 1-5**) (Nemergut et al. 2013; Vellend 2010).

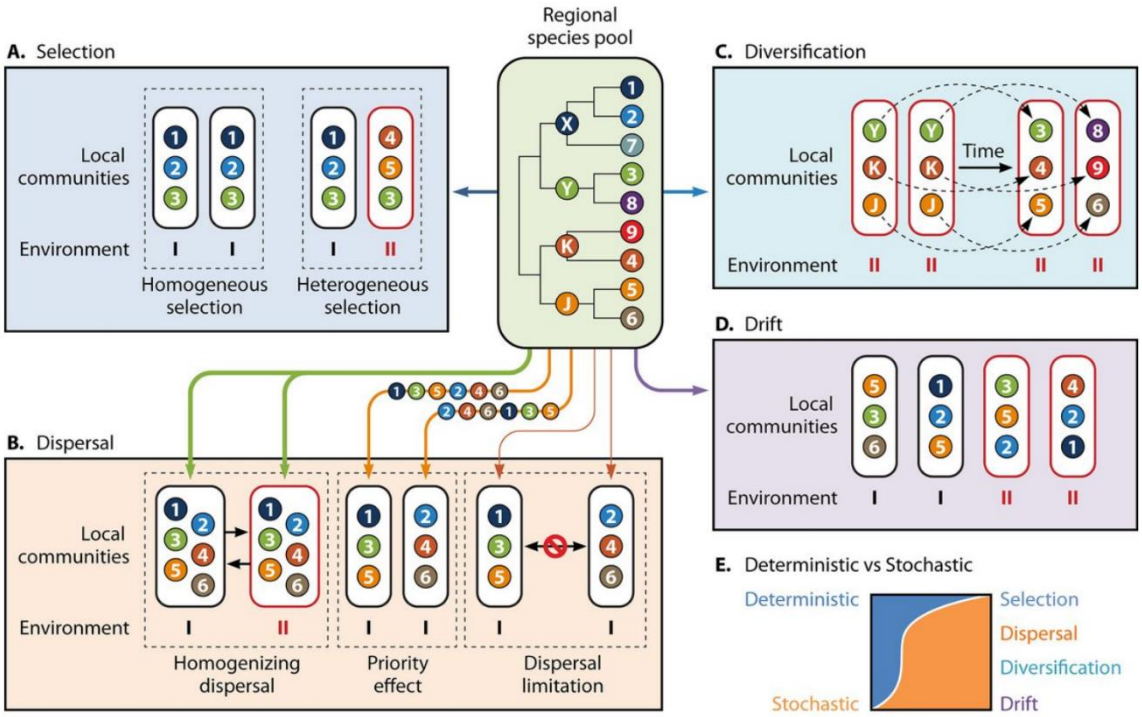

Figure 1-5 *Schematic representation of the four processes influencing community assembly* (Zhou and Ning 2017). *Choosing from a regional species pool, bacteria can be selected in a specific environment via homogenous or heterogeneous selection (**A**). They can disperse through different environments in a homogenizing way, or dispersion can be limited. If priority effects take place, bacteria can just initially disperse and establish themselves (**B**). After arriving in a specific environment, the community can diversify over time (**C**). Bacteria can also drift within their local communities and environments (**D**). Selection is a deterministic effect, while drift is a stochastic one. Dispersal and diversification are intermediate between deterministic and stochastic (**E**).*

Selection and diversification fall under the two processes that are deterministic, while dispersal and drift are mainly stochastic effects. Stochastic effects include events like birth, death, colonization, extinction and speciation (Zhou and Ning 2017). They can be seen in early colonization events in guts but are often accompanied by deterministic effects (McCafferty et al. 2013). If it is not chance that dictates the process of the first colonization events, it is shaped by deterministic factors like the host transcriptome, the environment or the bacteria themselves, as already described in the metaorganism concept (Chapter 1.1).

1.3 *Nematostella vectensis*

1.3.1 Phylogeny and morphology

Nematostella vectensis is a small, burrowing sea anemone of the order Actinaria within the class of Anthozoa. It belongs to the Phylum of Cnidaria and therefore forms the sister group to all Bilateria (**Figure 1-6** A)(Collins 2002; Medina et al. 2001; Wainright et al. 1993).

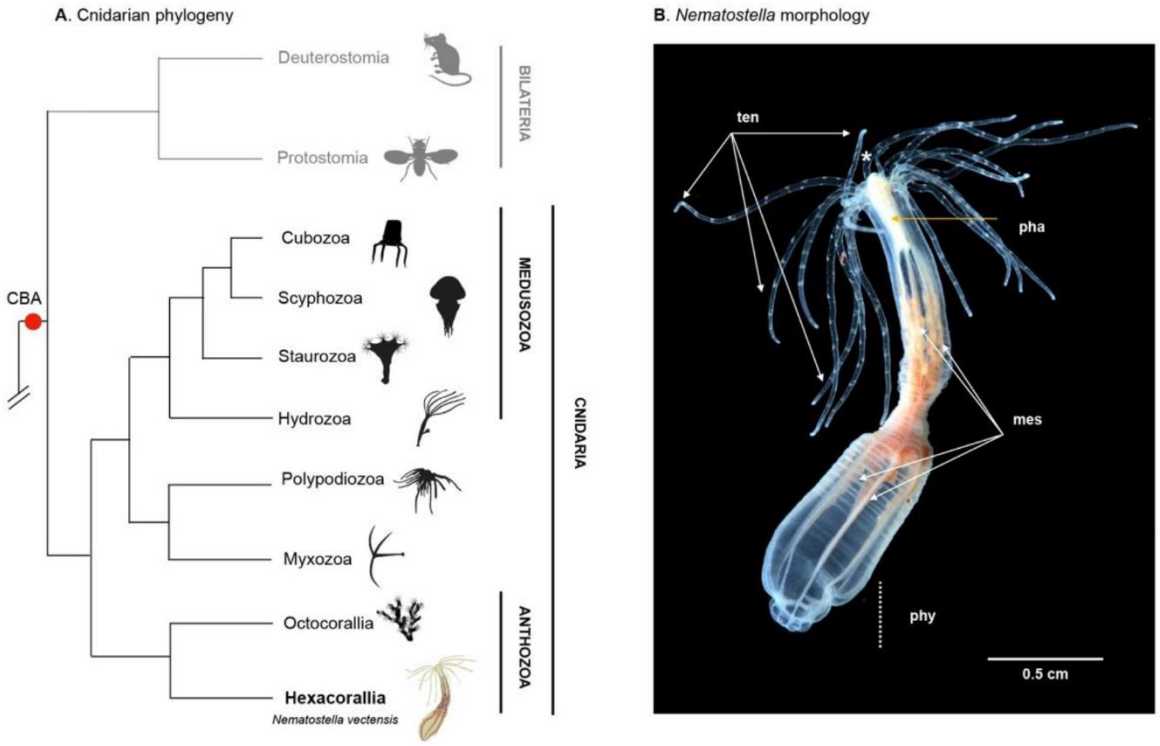

Figure 1-6 *Nematostella's phylogenetic position among the Cnidaria (A) and its adult appearance (B)* (Röttinger 2021). *Nematostella belongs to the phylum Cnidaria and locates within the Anthozoa and Hexacorallia. The adult polyp possesses a head region with tentacles and pharynx, a column region with the mesenteries, and a physal region. Ten=tentacles, pha=pharynx, mes=mesenteries, phy=physa. The star marks the mouth opening.*

In contrast to Bilateria, Cnidaria possess only two germ layers instead of three (Martindale, Pang, and Finnerty 2004). The outer epidermis is considered to be derived from the ectoderm, while the blind gut and the inner linings of the tentacles are comprised of endoderm. Both cell layers are connected via a largely acellular matrix, the mesogloea (Martindale et al. 2004; Tucker, Shibata, and Blankenship 2011). Within the cnidarians, they belong to the class of Anthozoa, in contrast to Medusozoa (Collins 2002; Medina et al. 2001). The most obvious difference between those two phylogenetic groups is the absence of a medusa stage in anthozoans (Collins 2002). With the medusa generally considered as the sexually reproducing life form in medusozoans, in anthozoans the polyp unifies the sexual and asexual life style (Technau and Steele 2011). The nervous system of cnidarians is considered to be a nerve net with regionalization in some species, however, this regionalization is not considered to be homologous to the centralized nervous system as it is present in bilaterians (Watanabe, Fujisawa, and Holstein 2009). Cnidarians also possess one of the most elaborate cellular secretion product, the nematocyte (Tardent

1995). Nematocytes contain cysts, which can be discharged upon triggering. These cysts are either specialized in stunning and killing prey by toxin piercing its bodies and releasing toxins, or in producing sticky tubules which are used for sticking to substrate and locomotion (Berking and Herrmann 2006).

Nematostella, like all cnidarians, possesses a very simple body plan. It is comprised of a head region, a body column and a foot region (Stefanik, Friedman, and Finnerty 2013) (**Figure 1-6** B). Its head normally carries 16 tentacles, which are fully retractable into the body column. If sexual reproduction is not induced regularly, they can grow more than 18 tentacles (Ikmi et al. 2020). The whole animal is translucent so that its pharynx and mesenteries, which stretch from pharynx into the foot region and divides the animal into eight radial segments, are clearly visible (Ikmi et al. 2020). The foot region carries a small pore on the polar end which can eject fluids from the body column (Amiel et al. 2015).

Although cnidarians are generally seen as radially symmetrical, many cnidarians exhibit subtle bilateral traits (Finnerty et al. 2004). So are the mouth opening, the pharynx and the mesenteries of *Nematostella* organized in such a way that it breaks the radial symmetry of the directive axis in favor of a bilateral symmetry (Berking 2007; Finnerty et al. 2004). This bilateral symmetry can also be observed on the level of gene expression: several pattern-forming genes like bone morphogenic protein (BMP) genes and homeobox (Hox) genes but also less obvious genes like red fluorescent protein (RFP) genes show an asymmetrical expression (Genikhovich et al. 2015; Ikmi and Gibson 2010).

The mesenteries of *Nematostella* and anthozoans generally are subdivided into a basal muscular, a median gonadal (or in non-gonadal regions a trophic) and a distal septal filament region (Steinmetz 2019). The tips of the septal filaments contain cnidocytes and zymogen cells, producing chitinase- and trypsin- like enzymes, with the extracellular digestion probably being contact-dependent (Steinmetz 2019). This part of the mesenteries is also comprised of the pharyngeal ectoderm. Intracellular digestion via phagocytosis is exhibited by the non-gonadal gastrodermal part of the mesenteries (Steinmetz 2019). The mesenteries are also the production site of nematosomes, which are small, multi-cellular free-floating bodies in the gastrovascular tract which are only found in *Nematostella* and other members of the *Edwardsiidae* family. Nematosomes can also sometimes be found resting on the inner lining of the body wall and are packed into the jelly of the egg packages laid by females upon sexual induction (Frank and Bleakney

2007; Hand and Uhlinger 1992). They are comprised of mostly cnidocytes, phagocytes, and cells equipped with two types of cilia which share morphological similarities to cnidocyte support cells (Babonis, Martindale, and Ryan 2016). Their biological role is not well understood, but is hypothesized to be involved in immobilization of prey, clearing of the gastrovascular cavity from foreign objects, and immune responses (Babonis et al. 2016; Williams 2007).

1.3.2 Natural habitat

Nematostella inhabits estuarine habitats like salt marshes and saline lagoons (Darling, Reitzel, and Finnerty 2004). It lives burrowed in the sediment, with just its head with the tentacle crown and small parts of the body column sticking out (Hand and Uhlinger 1994). It is widely distributed across the North American Atlantic coast, ranging from Nova Scotia to the Gulf of Mexico, and across the US American Pacific Coast and Canada, as well as the English southeastern coast (**Figure 1-7**) (Hand and Uhlinger 1994).

Figure 1-7 *Distribution of Nematostella vectensis along the North American (A) and the English (B) coast. Nematostella occurs on both, the Pacific and Atlantic coast of North America, as well as on the southeastern coast of England. Blue dots mark sites where Nematostella polyps could be found. Map from https://www.marlin.ac.uk/species/detail/1136, accessed on 13.10.2021.*

However, amplified fragment length polymorphism fingerprinting analysis implies that the populations along the Atlantic coast of North America are the only native populations of *Nematostella*, while the populations along the Pacific coast and in England were dispersed there, probably through anthropogenic influences (Reitzel et al. 2008). This is remarkable

as the first descriptions of *Nematostella* were published in 1935 by Stephenson on the Isle of Wight, pinpointing down its dispersal to the English coast prior to the 1930s (Stephenson, 1935).

Nematostella tolerates a wide range of pH, salinity and temperature, with pH ranging from <7 to >9, with salinities from 2 ‰ to 52 ‰ and with temperatures from -1.5°C to 28.5°C ,contributing to its wide distribution and vulnerability to dispersal, (Hand and Uhlinger 1994; Stefanik et al. 2013) .Temperature tolerance is even reported to go as high as 39°C (Reitzel et al. 2013). Although animals reach just 1-2 cm in the wild, they can grow up to several centimeters when cultured in the lab (Stefanik et al. 2013).

1.3.3 Reproduction and life cycle

Nematostella vectensis is a valuable cnidarian model organism since it is one of the few anthozoans which reproduces sexually under laboratory conditions (Fritzenwanker and Technau 2002). *Nematostella* is dioecious with no sign of sex reversal (Reitzel et al. 2007). Although the appearance of males and females is identical, sexes can be distinguished upon sexual reproduction when females release egg packages and males release sperm from their mouth opening (Hand and Uhlinger 1992). Upon fertilization, the *Nematostella* undergoes a complex life cycle with a larval stage, a metamorphosis and a juvenile stage, before the animal enters the sexual mature adult stage (**Figure 1-8**) (Hand and Uhlinger 1992).

Freshly spawned eggs are embedded into a gelatinous matrix which also contains nematosomes (Hand and Uhlinger 1992). Fertilization occurs externally. The zygote undergoes a series of radial and holoblastic cleavages before the blastula enters the gastrula stage with several invagination-evagination cycles (Fritzenwanker et al. 2007; Layden, Rentzsch, and Röttinger 2016). After 24 to 48 hours, planula larvae emerge from the egg jelly (Fritzenwanker and Technau 2002; Reitzel et al. 2007). The planula larva is free swimming and possesses an apical tuft on its future aboral end. During the next 5-10 days, the larva elongates and loses its apical tuft, before it finally settles to undergo a subtle metamorphosis and develops 2-4 tentacle buds on its future oral end, 2 mesenteries and a pharynx (Layden et al. 2016; Reitzel et al. 2007). During the development of the juvenile polyp into a sexual mature adult polyp, the juvenile will grow in size and will develop its

complete set of 16 tentacles, 8 mesenteries and an abundant number of nematosomes (Hand and Uhlinger 1992). The time in which the juvenile reaches the adult stage is nutrient- and temperature-dependent and can range from as little as 8 weeks, but is mostly reported as around 3 months (Darling et al. 2005; Röttinger 2021).

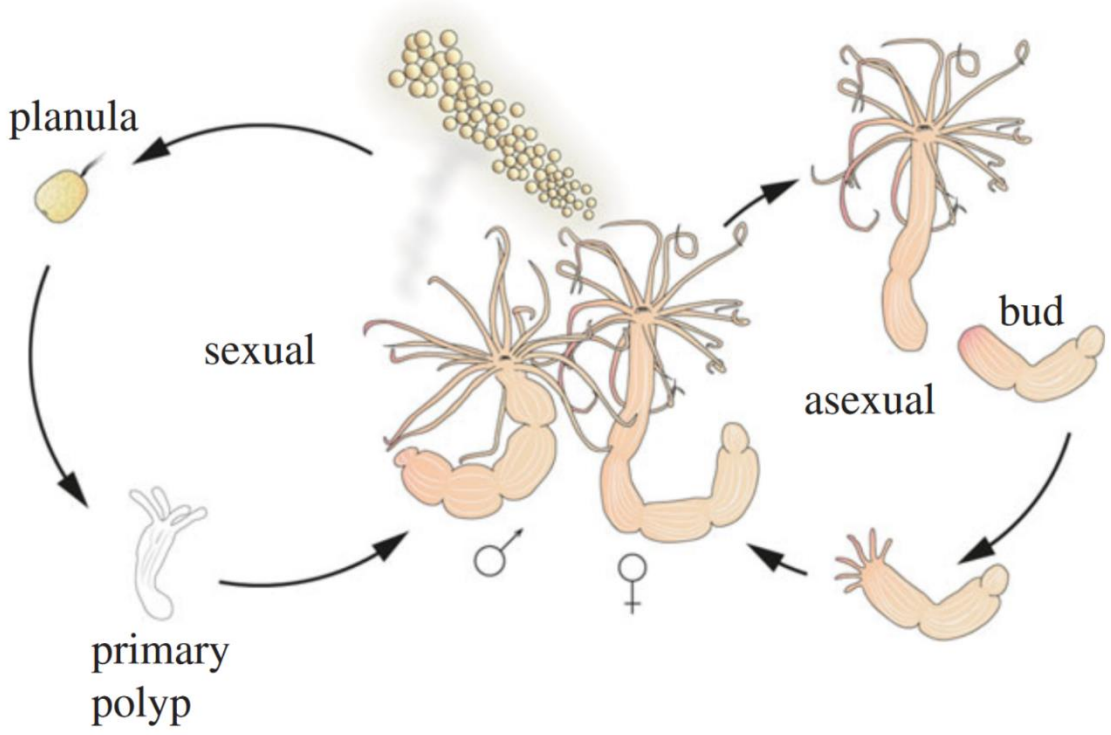

Figure 1-8 *Sexual und asexual life cycle of Nematostella vectensis* (Kelava, Rentzsch, and Technau 2015). *Upon induction of sexual reproduction, females will spawn egg masses while males will release sperm. After external fertilization, a planula larva will develop from the zygote. The planula larva will undergo metamorphosis to a primary polyp which then develops again into a sexual mature adult polyp. One form of asexual reproduction is the physal pinching, where a bud is pinched off of the physal region. The bud will regenerate the head region within a few days.*

Besides sexual reproduction, *Nematostella* can also reproduce asexually (**Figure 1-8**). The most observed form is by physal pinching. Hereby the foot region gets pinched off, which will regenerate a head region within just a few days (Darling et al. 2005). Another less frequent form is by polarity reversal, where the animal will develop a second crown of tentacles on its foot region. The animal will divide at its midpoint at least once and all parts will eventually regenerate a foot region (Darling et al. 2005; Hand and Uhlinger 1995). Another form of asexual reproduction stems from *Nematostella*'s enormous regeneration potential, where detached body parts can regenerate into fully functional whole polyps (Darling et al. 2005; Röttinger 2021). This regeneration potential can be triggered by

natural (predation) or artificial (bisection) influences, rendering it very suitable for e.g. regeneration research (Röttinger 2021).

1.3.4 *Nematostella* as model organism

Nematostella possesses several characteristics which make it so suitable as a model organism for a variety of research questions (Darling et al. 2005). Firstly, *Nematostella* is easy and cheap to culture with little requirements. They can be cultured in simple artificial salt water in numbers of thousands in very little space, with no need for water circulation or additional substrate (Hand and Uhlinger 1992; Stefanik et al. 2013). It readily undergoes its whole life cycle under lab conditions, with a generation time of 2-3 months (Fritzenwanker and Technau 2002; Hand and Uhlinger 1994; Stefanik et al. 2013). In addition, due to its fast regeneration time from just small pieces of tissue, clonal lines can be established in order to erase the background of genetic diversity (Genikhovich and Technau 2009; Röttinger 2021).

Another advantage of *Nematostella* as a model organism is its ecological context. As it is inhabiting estuarine habitats, samples from the wild are easily collectible with little to no equipment (Stefanik et al. 2013). It can be found along the Pacific and Atlantic coast of Northern America as well as the eastern coast of England, exhibiting a strong tolerance to a wide range of habitats, salinities and temperatures (Darling et al. 2004; Reitzel et al. 2008, 2013). This facilitates its culture and makes it suitable for research questions investigating mechanisms of local adaptation (Darling et al. 2005; Fraune, Forêt, and Reitzel 2016).

Its phylogenetic position at the base of the animal tree and as an outgroup to bilaterians make it suitable for evolutionary research questions (Dunn et al. 2008; Layden et al. 2016; Martindale et al. 2004). The genome was sequenced in 2007 and revealed an unexpected degree of complexity and conservation with bilaterian and vertebrate genomes on gene content and organization, but also genetic and epigenetic regulation (Putnam et al. 2007; Schwaiger et al. 2014). Recently, the genome was sequenced again, generating a chromosome-level genome (Zimmermann et al. 2020). Several transcriptomes are also available, including a single-cell transcriptome of adults and larvae and specific transcriptomes for regeneration and embryogenesis (Helm et al. 2013; Sebé-Pedrós et al.

2018; Tulin et al. 2013; Warner et al. 2018). Additionally, several other sequencing technologies like ChIP-seq and microarrays have been established, as well as data on microRNAs, genome methylations and histone modifications (Grimson et al. 2008; Layden, Boekhout, and Martindale 2012; Moran et al. 2013, 2014; Rottinger, Dahlin, and Martindale 2012; Schwaiger et al. 2014; Zemach et al. 2010). Based on this information, a diverse portfolio for injection-based functional studies was established, including protocols for gene manipulation by morpholinos, RNAi, CRISPR/Cas9, TALEN and inducible promoters (Ikmi et al. 2014; Renfer et al. 2010; Rentzsch et al. 2008).

For all these reasons is *Nematostella vectensis* one of the leading cnidarian model organisms for developmental, ecological, evolutionary and interdisciplinary research (Darling et al. 2005; Fraune et al. 2016; Genikhovich and Technau 2009; Layden et al. 2016; Röttinger 2021). It is a valuable addition to other cnidarian models like *Hydra*, *Aiptasia* or *Acropora* for its willingness and to predictably undergo its complete life cycle under laboratory conditions (Darling et al. 2005). For its enormous regeneration potential, it was also established as a model for regeneration (Layden et al. 2016; Röttinger 2021). More recently, *Nematostella* was also established as a model for phenotypic plasticity and local adaptation, especially in the interdisciplinary context of genomic, epigenetic and bacterial research (Fraune et al. 2016).

1.3.5 Bacterial colonization of the metaorganism *Nematostella*

The first review about *Nematostella vectensis* as an emerging model organism was published in 2005 (Darling et al. 2005). Research about *Nematostella*'s microbiome is an even younger field with its first publications published in 2015 (Har et al. 2015; Mortzfeld et al. 2016). Nonetheless, today *Nematostella* is on the verge of establishing itself as a model organism for microbiome research.

Nematostella possesses a microbiome that undergoes a specific succession during development (Mortzfeld et al. 2016). The microbiome is distinct for each of the three developmental stages until the polyp reaches adulthood (**Figure 1-9** A).

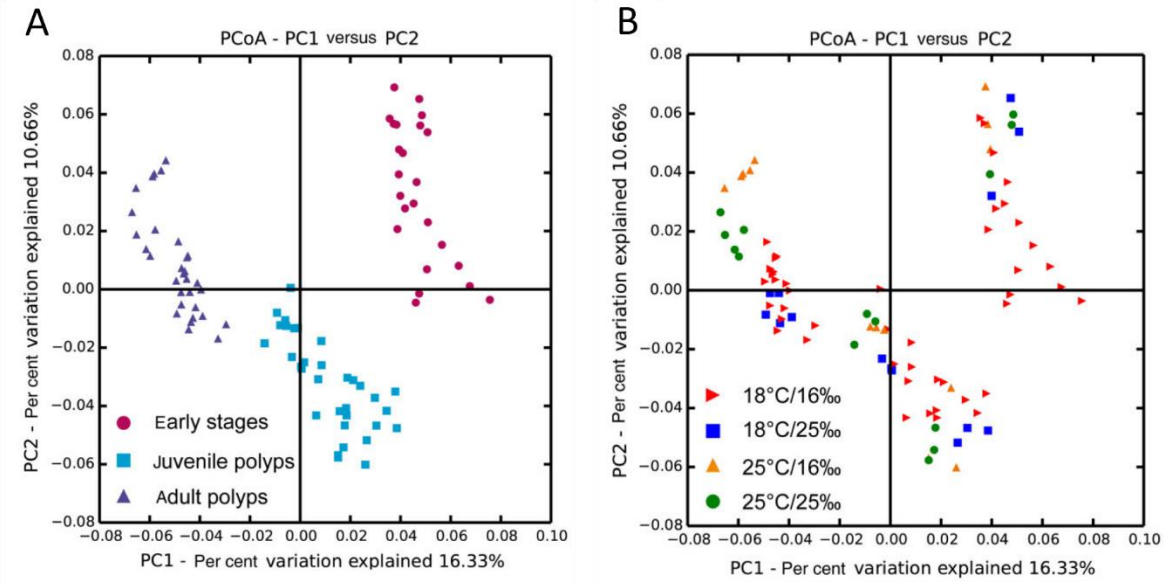

Figure 1-9 *The microbiome of Nematostella vectensis is specific for its developmental age* (Mortzfeld et al. 2016)*. (A) PCoA plot of the different microbial communities in early, juvenile and adult developmental stages. (B) PCoA plot of the microbiome depending on salinity and temperature.*

It is indicated that during sexual reproduction, bacteria are mostly transmitted maternally to the offspring, with a small fraction of transmission occurring paternally (Baldassarre et al. 2021). Horizontal transmission of bacteria during early life is also speculated as the alpha-diversity in planula larvae is enriched and specific bacteria don't seem to occur in adult polyps and gametes but in the medium and early life stages (Baldassarre et al. 2021). Besides *Nematostella*'s microbiome being highly specific for the developmental stage, it also loosely depends on salinity and temperature of the medium (**Figure 1-9**). It also changes along the gradient of the US-American east coast, with the changes persisting even if the animals were maintained in the lab for years prior to sampling (Mortzfeld et al. 2016). Also pollutants like phthalate and nitrate show a negative effect on the microbiome composition of *Nematostella*, but not on the evenness and richness of the microbiome (Klein et al. 2021). This study also shows a dependency of the microbiome on the media in which the animals are grown, however, they used unfiltered salt marsh water as a comparison to artificial sea water, therefore generating an influx of environmental bacteria, without showing if these bacteria could manifest themselves as steady colonizers. The microbiome is also highly variable on a much shorter timely scale than the whole developmental process. So do single bacterial OTUs vary strongly over a 24-hour period, in presence and absence of light (Leach, Carrier, and Reitzel 2019). Single bacterial taxa also

exhibit a gradual colonization of the body column. So do Spirochaetes almost exclusively colonize the head of the adult polyp with an almost absence in the rest of the body column and foot region (Bonacolta et al. 2021).

Because data on *Nematostella*'s microbiome and its succession over the course of the development are publicly available, these date were also used for theoretical frameworks (Mortzfeld et al. 2016). In one publication, data on *Nematostella*'s microbiome were searched for the presence of sequences of *Bdellovibrio* and like organisms (BALOs) (Johnke et al. 2019). BALOs are predatory bacteria which feed on gram negative bacteria. They found that BALOs are present in the microbiome of *Nematostella* and calculated that they have an elevating effect on the alpha-diversity of the community, but no effect on beta-diversity (Johnke et al. 2019).

In another publication, the theory of the neutral model was tested (Sieber et al. 2019). It is often assumed that a host can actively shape its bacterial community by its immune system or by providing a special niche. In contrast to that, a neutral model proposes that the microbial community structure within a host is the result of stochastic population dynamics, immigration and local extinction (Sieber et al. 2019). When a theoretical neutral expectation is fitted onto the microbiome of *Nematostella*, it results in a poor fit, indicating that *Nematostella*'s microbiome composition underlies selective pressures e.g. the host's immune system rather than neutral processes (Sieber et al. 2019) .

Besides these observatory and theoretical studies of the microbiome of *Nematostella*, there is also one functional study investigating the microbiome's role in thermal acclimation of the host (Baldassarre et al. 2022). Interestingly, the study could show that the microbiome of long-term acclimated animals could confer thermal tolerance if transplanted on non-acclimated animals. The microbiome conferred heat-tolerance to a non-acclimated animal if the donor animals were acclimated at a higher temperature, but the microbiome also conferred thermal susceptibility if the donor animals were acclimated at a lower temperature.

1.3.6 Immune system

The immune system and microbes were long perceived in a dualistic way, with the immune system as “good” and microbes as “bad”. This dualistic viewpoint framed bacteria as a cause of diseases and the immune system as the protector. In the 20th century, this viewpoint shifted and recognized the benefits of e.g. lactic acid-producing bacteria. This lead to the hypothesis that the immune system is not a “killer” but a force that is able to shape the microbiome and as a result also shapes the metaorganism (Eberl 2010).

The immune system is comprised of the innate immune system and the adaptive immune system. While the innate immune system is encoded by genes and acts rapidly against molecular patterns associated with pathogens and toxins, the adaptive immune system acts slowly because its response is encoded by gene elements which need to be rearranged and proliferated in specific cells (Chaplin 2010). Therefore, the innate immune system reacts relatively unspecifically against microbe-associated molecular patterns (MAMPs), while the adaptive immune system reacts with a high specificity against unique foreign structures (Chaplin 2010). The adaptive immune system is evolutionarily young and seems to be restricted to vertebrates, while innate immune mechanisms are found in even the most primitive life forms, as even unicellular organisms need to discriminate self from non-self (Buchmann 2014).

A central signaling pathway of the innate immune system is the Toll-like receptor (TLR) pathway. The Toll-like receptor itself is a pattern recognition receptor (PRR), which upon recognizing MAMPs activates a signaling cascade, which results in the activation of the transcription factor NF-kB, initiating immediate host defensive responses (Kawasaki and Kawai 2014). The Toll-like receptor recognizes MAMPs via its extracellular leucine-rich repeats (LRRs) and transduces the signal to MyD88 via its intracellular Toll/Interleukin-1 receptor (TIR) domain (Kawai and Akira 2010). Together with TLRs, the IL-1 receptors (IL-1Rs) form the TIR family of transmembrane proteins. IL-1 receptors possess the same intracellular domain as TLRs, the TIR domain, but instead of extracellular LRRs, they possess immunoglobulin-like (IL) domains (Martin et al. 2002). While components of the TLR pathway are already present in both phyla Porifera and Cnidaria, a bona fide TLR is missing in sponges, but not cnidarians. However, both cnidarians and sponges possess receptors with an intracellular TIR domain and extracellular IL-1R-like domains (Hentschel et al. 2012; Miller et al. 2007; Riesgo et al. 2014). Cnidarians possess a variety of TLR-like

and IL-1R-like receptors, with varying quantities of LRRs or IL-1R-like domains in its extracellular domain (Poole and Weis 2014). The vast complexity of TIR-only proteins, with no extracellular domains, especially in corals, opened the hypothesis that TIR-only proteins might be a way of cnidarians to fine scale differentiation between beneficial and pathogenic microbes (Poole and Weis 2014).

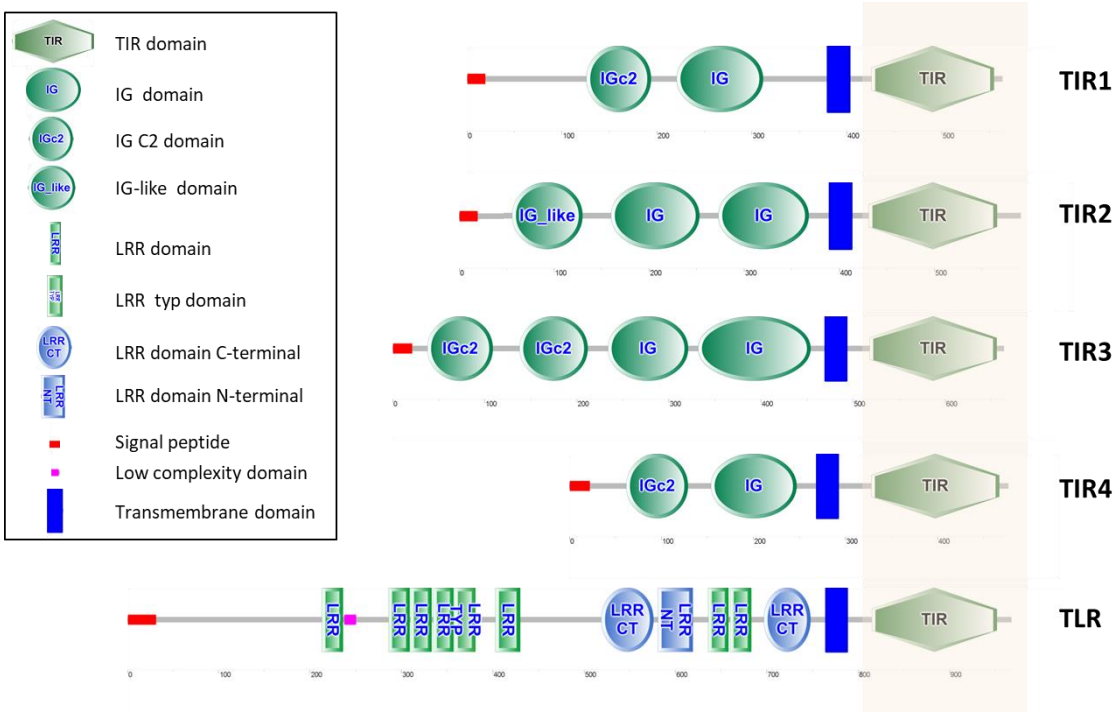

Figure 1-10 *Predicted TIR domain-containing receptors in the genome of Nematostella vectensis. It possesses four receptors with extracellular IL-1R-like domains (IG domains, TIR1 – TIR4) and one receptor with extracellular LRRs (TLR).*

For *Nematostella*, one classical TLR and four IL-1R-like receptors are described (**Figure 1-10**, MA H.Domin) (Miller et al. 2007). As sponges don't possess a classical TLR, the other IL-1R-like receptors in sponges and cnidarians pose an interesting candidate as effectors of the TLR signaling pathway. Functional studies to *Nematostella*'s immune system, however, are sparse. One study investigated *Nematostella*'s sole TLR, and showed its ability to activate NF-kB, at least in human cell cultures (Brennan et al. 2017). They could also show that NvTLR and NF-kB colocalize in a subset of nematocytes and that NvTLR is also expressed in nematosomes, strengthening the potential role of nematosomes in immunity (Chapter 1.3.1).

Aims

In order to understand the interplay of *Nematostella* and its bacteria, I addressed following tasks:

- Identify bacteria involved in positive, neutral, or negative bacteria-bacteria interactions within the community and test their ability to influence the whole bacterial community
- Track the recolonization pattern of gnotobiotic polyps with the bacterial communities of three different developmental stages of *Nematostella*
- Measure host's response upon recolonization with the three different developmental stages to identify host-mediated mechanisms to influence the community
- Calculate the metabolic potential of the microbiome over the course of the recolonization to identify potential metabolic drivers
- Test the ability of native bacterial strains typical for different developmental stages for their ability to recolonize adult polyps

2 Results

2.1 Bacterial Networks

2.1.1 Bacteria–Bacteria Co-occurrence Networks During Host Development

To infer potential bacteria–bacteria interactions in the bacterial community of N. *vectensis*, network links were inferred using SparCC methodology to the relative abundance of 508 OTUs over the whole ontogeny (Friedman and Alm 2012; Mortzfeld et al. 2016). Using bacterial abundance data, network correlations were inferred from: (1) all sampling time points together, leading to the representation of the most important interactions along the whole development of the animal and (2) the three developmental stages separately, which characterize the most relevant correlations during each developmental stage.

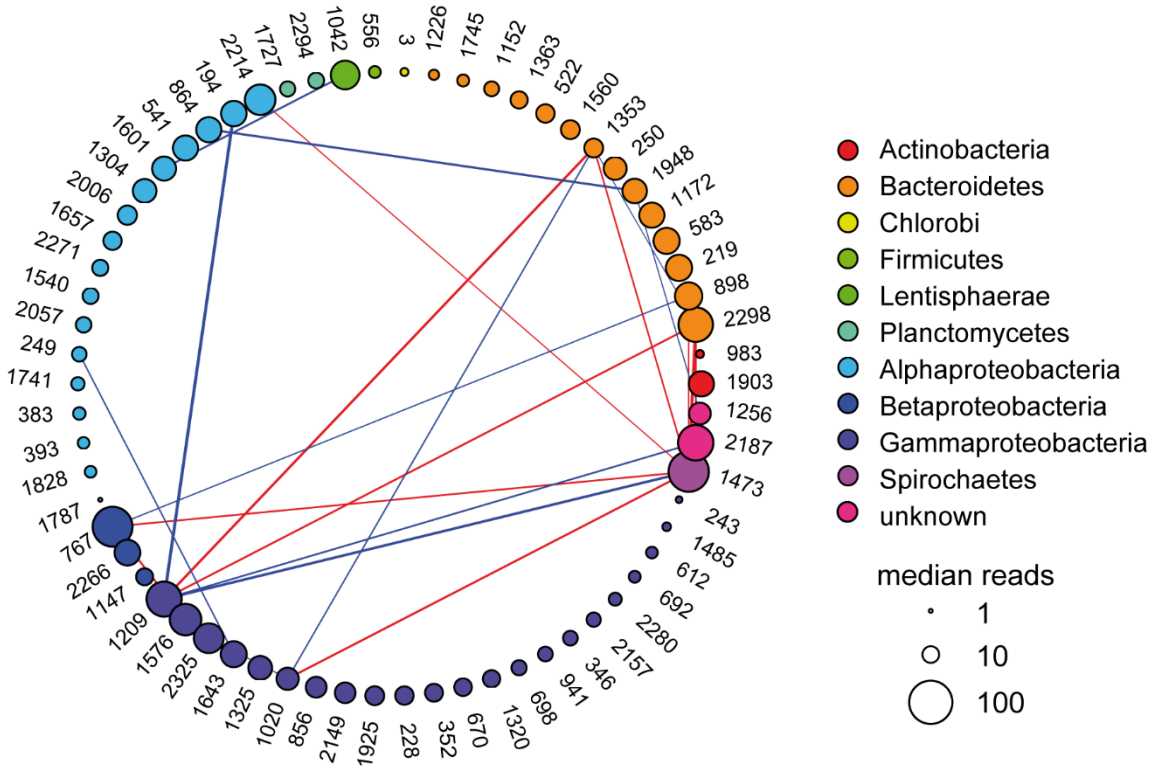

Figure 2-1 *Microbial co-occurrence network among OTUs during the whole development of N. vectensis. Nodes (N = 66) are the OTUs involved in at least one strong interaction during the whole development or the three developmental stages; their color reflects taxonomic affiliation. The size of the nodes is proportional to the log10 of the median reads (relative abundance of the OTUs) along the whole development. OTUs are arranged by taxonomy and relative abundance. Links represent the interactions (i.e., significant co-occurrences; pseudo p-value ≤ 0.05) with absolute correlation values above 0.5. Red links are negative interactions, while blue links stand for positive interactions; the thickness of the links is proportional to the strength of the interactions.*

For the construction of the co-occurrence networks, the strongest significant interactions (i.e., those with pseudo p-value ≤ 0.05 and an absolute correlation value larger than 0.5) in each of the datasets were selected. A list of 66 nodes (N = 66), representing 66 bacterial OTUs, was obtained from the union of all OTUs that were found at least once in one of the four datasets of the significant and strong correlations. Using these 66 nodes, the four co-occurrence networks were constructed. **Figure 2-1** is the co-occurrence network along the whole developmental process of *N. vectensis*.

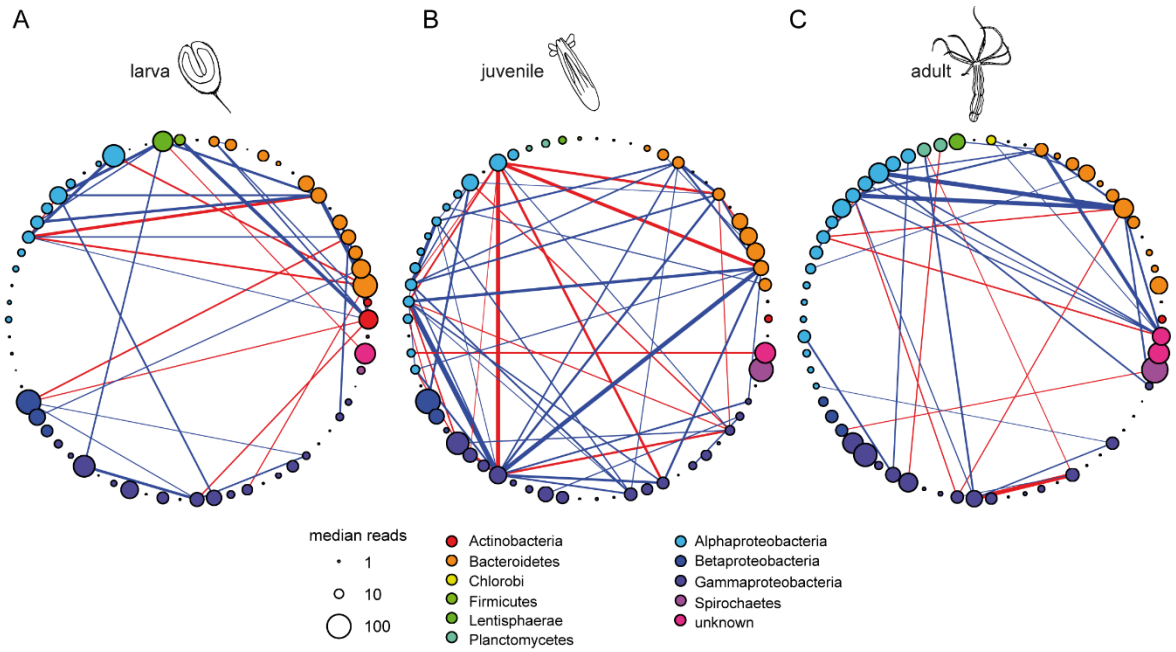

Figure 2-2 *Microbial co-occurrence networks for (A) larval stage, (B) juvenile stage, and (C) adult polyps of N. vectensis. Nodes (N = 66) are the same as in Figure 2-1 and Suppl. Figure 1, their order in the circular arrangement was preserved. OTU numbers are provided in Suppl. Figure 1. The colors inform about the taxonomic affiliation of the nodes. The size of the nodes is proportional to the relative abundance of the OTUs (measured as log10 of median reads) in each developmental stage. Links are significant correlations (pseudo p-value ≤ 0.05) with absolute values above 0.5; their color allows distinguishing among negative (red) and positive (blue) interactions, while the thickness is proportional to the strength.*

None of the constructed networks has more than 56 interactions (L = 56) or involves more than 29 OTUs (NC ≤ 29), resulting in a low density across all networks (**Table 2-1**). All networks have more positive than negative interactions (LP > LN), which is reflected in the mean correlation values calculated considering the total set of links (**Table 2-1**). All networks are composed of two or more subnetworks, but this could be a consequence of the chosen correlation cut-off rather than a biological property. The four networks together have 145 interactions and only one shared interaction between different

developmental stages (i.e., the interaction OTU1601–OTU1657 is present in both larval and adult stages).

Table 2-1 *Network descriptors used to characterize the properties of the correlation networks. Indices were calculated for both the whole development network (i.e., based on all correlations among OTUs, irrespective of the various stages of polyp growth) and the networks that refer to three developmental stages (i.e., larva, juvenile, and adult). All networks are composed of the same 66 OTUs (N = 66).*

Descriptors	**Whole development**	**Larvae**	**Juvenile**	**Adult**
Number of links (L)	22	35	56	37
Number of connected nodes (N_C)	20	25	29	29
Density of the network (D)	0.010	0.016	0.026	0.017
Number of positive links (L_P)	12	25	39	27
Number of negative links (L_N)	10	10	17	10
Proportion of positive links (%L_P)	0.545	0.714	0.696	0.730
Proportion of negative links (%L_N)	0.455	0.286	0.304	0.270
Mean of total correlations (m_t)	0.045	0.250	0.218	0.260
Mean of positive correlations (m_p)	0.535	0.569	0.559	0.559
Mean of negative correlations (m_n)	-0.544	-0.548	-0.565	-0.547
Number of subnetworks (n_{sub})	4	2	6	5
Mean degree ($\overline{d}$)	2.200	2.800	3.862	2.552
Maximum degree (d_{max})	7	8	14	7
OTUs with maximum degree	1473	1903	1643	1948, 1601, 1256

The co-occurrence network spanning the whole host development (**Figure 2-1**) has the lowest number of connected nodes (NC = 20; **Table 2-1**). Here, a spirochaete bacterium (OTU1473) has the highest degree of links indicating a potential role as organizer along the whole development of N. *vectensis* (*Suppl. Table 1* and **Figure 2-1**). Interestingly, when analysing the different developmental phases separately, the structure of the interactions (**Figure 2-2**) and the degree of the nodes (*Suppl. Table 1*) vary during animal development. Thus, the set of nodes with the highest degrees (i.e., OTUs with the higher number of direct links in the co-occurrence network; **Table 2-1**) is also modified, which reflects how the importance of the various phylogenetic groups changes through development. At the larval stage, the strongest correlations are mainly found between Actinobacteria, Bacteroidetes, Lentisphaerae, and Alphaproteobacteria (**Figure 2-2**A), but these links change during the onset of development. During the juvenile stage, Gammaproteobacteria

become greatly important, interacting mainly with Alphaproteobacteria and Bacteroidetes (**Figure 2-2**B). However, at the adult stage, almost all interactions are between Alphaproteobacteria, Bacteroidetes, and an unknown taxon (**Figure 2-2**C). While at the larval stage, the bacterium with the highest degree belongs to Actinobacteria (OTU1903), at the juvenile stage, it is replaced by a Gammaproteobacterium (OTU1643). At the adult stage, three different bacteria are the most connected: one bacterium from the Bacteroidetes (OTU1948), one from the Alphaproteobacteria (OTU1601), and one unknown bacterium (OTU1256; *Suppl. Table 1*). Interestingly, the network constructed from the bacterial data of juvenile animals shows the highest number of links (L = 56; **Table 2-1**). This suggests that in this developmental phase of the animal, the bacteria–bacteria interactions may be of greater importance for shaping the bacterial community composition than during the two other developmental phases.

2.1.2 Experimental Testing of Predicted Bacteria–Bacteria Interactions

In order to test the role of predicted bacteria–bacteria interactions in the assemblage of the juvenile microbiota in vivo, five bacterial strains were selected for recolonization experiments. The bacterial isolates representing OTU194 (*Ruegeria sp.*) and OTU1209 (*Vibrio sp.*) are characterized by mainly negative correlations and therefore may act as competitive bacteria. Both isolates belong to the group of most abundant colonizers in juvenile polyps (**Figure 2-2**, **Figure 2-3**), while in the bacterial community of larvae, they are underrepresented (Mortzfeld et al. 2016). In contrast, the isolate representing OTU670 (*Acinetobacter sp.*) exerts mainly positive correlations, thus seeming to be a cooperative bacterium (**Figure 2-3**).

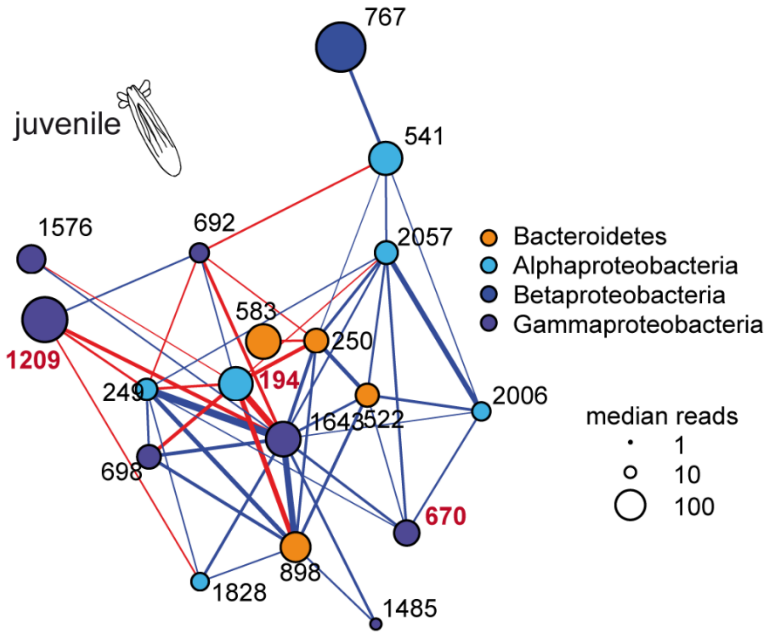

Figure 2-3 *Dominant microbial co-occurrence subnetwork in juvenile polyps. The colors inform about the taxonomic affiliation of the nodes. The size of the nodes is proportional to the relative abundance of the OTUs (measured as log10 of median reads) in juvenile polyps. Links are significant correlations (pseudo p-value ≤ 0.05) with absolute values above 0.5; their color allows distinguishing among negative (red) and positive (blue) interactions, while the thickness is proportional to the strength. OTUs with representative isolates available are labeled in red.*

Using these three bacterial isolates, it was tested if predicted bacteria–bacteria interactions influence the assemblage of the juvenile microbiota *in vivo*. Therefore, the experiments with antibiotic-treated juvenile polyps were conducted by recolonizing with: (1) larval bacteria; (2) juvenile bacteria; and (3) larval bacteria mixed with single bacterial isolates in excess (**Figure 2-4**).

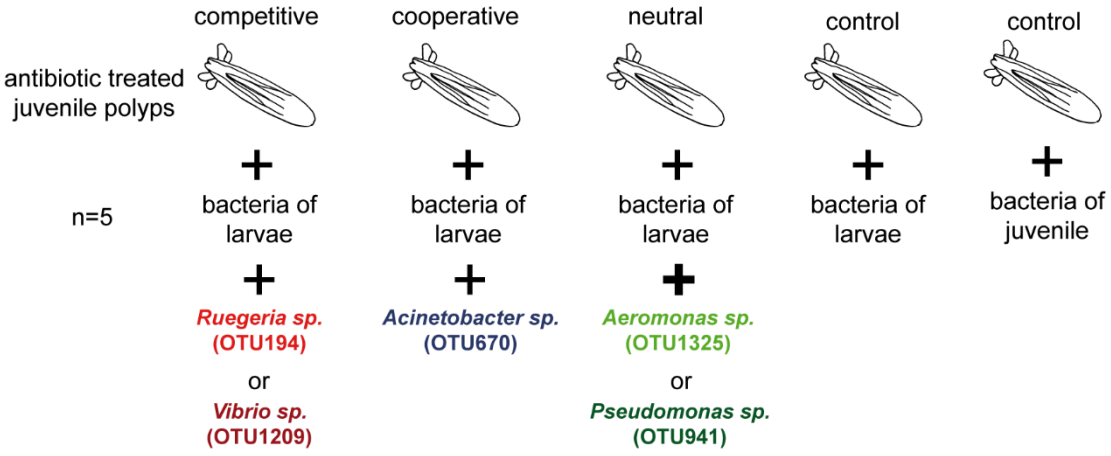

Figure 2-4 *Experimental setup for the recolonization experiments. For each treatment, juvenile polyps were treated with antibiotics and then recolonized with different bacterial inocula. For recolonizations with competitive, cooperative, or neutral bacteria, the selected OTUs were mixed with bacteria of larvae. For the two controls, antibiotic treated juveniles were recolonized with bacteria of larvae or juveniles alone.*

Two isolates without any correlations at the juvenile stage, OTU1325 (*Aeromonas* sp.) and OTU941 (*Pseudomonas* sp.), were selected as controls. The recolonization with larval bacteria was chosen as the tested bacterial isolates are not overrepresented in this bacterial community and this allows their overrepresentation in the recolonization experiments. All treatments were conducted with five independent replicates, sampled at 3- and 7-day post-recolonization (dpr) and analysed by 16S rRNA gene profiling.

Juvenile polyps which were inoculated with either juvenile (bJ) or larval bacteria (bL) showed a different community composition after 3dpr in comparison to the inocula and to each other (**Figure 2-5**A, ADONIS $R^2 = 0.95$, $p < 0.001$). After 7 days of recolonization, both bacterial communities shifted back in the direction of the native bacterial situation characterizing juvenile polyps. The animals recolonized with bacteria of juveniles resembled hereby the native situation significantly better than animals recolonized with bacteria from larvae (**Figure 2-5**B). Similar results were obtained when calculating weighted UniFrac distances instead of Bray-Curtis distances (*Suppl. Figure 2*). In contrast, the recolonized animals showed no difference in their bacterial alpha-diversity, even though they were recolonized with bacterial inocula that differed significantly in their alpha-diversity (**Figure 2-5**C).

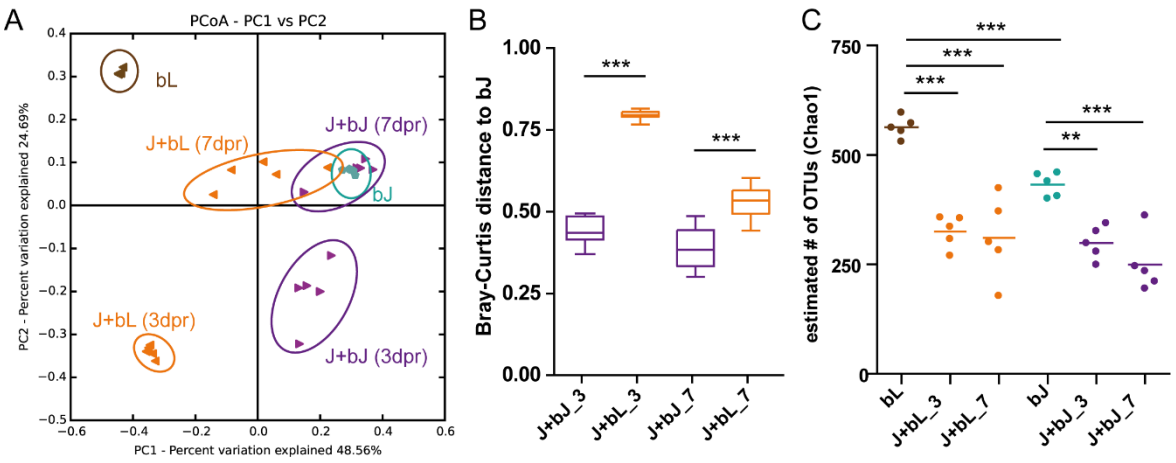

Figure 2-5 *Juvenile polyps recolonize differentially with larvae (bL) or juvenile bacteria (bJ). (A) Bacterial communities were clustered using PCoA of the Bray–Curtis distance matrix. The percent variation explained by the principal coordinates is indicated on the axes. bL, source bacteria of larvae; bJ, source bacteria of juvenile polyps; J+bL, bacterial community of polyps recolonized with bL after 3dpr and 7dpr; J+bJ, bacterial community of polyps recolonized with bJ after 3dpr and 7dpr. (B) Bray–Curtis distances to bJ after 3dpr and 7dpr. (C) Estimated number (Chao1) of OTUs of the source communities and recolonization communities. Statistical analysis was conducted using analysis of variance (ANOVA; **p < 0.01, ***p < 0.001).*

These results indicate that juvenile polyps can be recolonized with different source bacterial communities, but over time they develop back to the native juvenile community composition. However, only around 70% of the total bacterial diversity of juvenile polyps (bJ) could be restored within 7dpr (**Figure 2-5**C), independently of the alpha-diversity of the bacterial inoculum.

Before testing the effect of bacterial isolates on the composition assemblage in juvenile polyps, it was first checked if the overrepresented bacterial isolates are able to colonize the polyp. Over the course of the experiment, all five isolates remained overrepresented (*Suppl. Figure 3*). At 3dpr, the isolates were overrepresented between 3- and 27-fold (*Suppl. Figure 3B*). While both competitive bacteria (OTU194; *Ruegeria sp.* and OTU1209; *Vibrio sp.*) showed the highest initial colonization efficiency, one of the neutral isolates (OTU1325; *Aeromonas sp.*) recolonized with the lowest efficiency (*Suppl. Figure 3B*). At 7dpr, all bacterial isolates showed a similar overrepresentation of two to fivefold compared to the control (*Suppl. Figure 3C*). Therefore, it was possible to recolonize the juvenile polyps with an overrepresentation of bacterial isolates.

To test for the effect of bacterial isolates on bacterial community assemblage in juvenile polyps, the colonization dynamics with isolates were compared to the control colonization without isolates. At 3dpr, the community composition was significantly affected by the addition of all five different isolates compared to the control (*Suppl. Figure 4A*). Surprisingly all isolates, cooperative (OTU670; *Acinetobacter sp.*), competitive (OTU194; *Ruegeria sp.* and OTU1209; *Vibrio sp.*), or neutral (OTU1325; *Aeromonas sp.* and OTU941; *Pseudomonas sp.*), shifted the community composition in a similar pattern (**Figure 2-6**A). Additionally, the distances between juvenile bacteria and recolonized juvenile polyps became significantly smaller if bacterial isolates were added (*Suppl. Figure 4A*), indicating a slightly better reconstitution of the original juvenile microbiota in the presence of the isolates. Moreover, the competitive bacteria (OTU194; *Ruegeria sp*. and OTU1209; *Vibrio sp.*) caused a significantly greater alpha-diversity compared to the control; in contrast, cooperative and neutral isolates had no effect on the alpha-diversity of the bacterial community (**Figure 2-6**B).

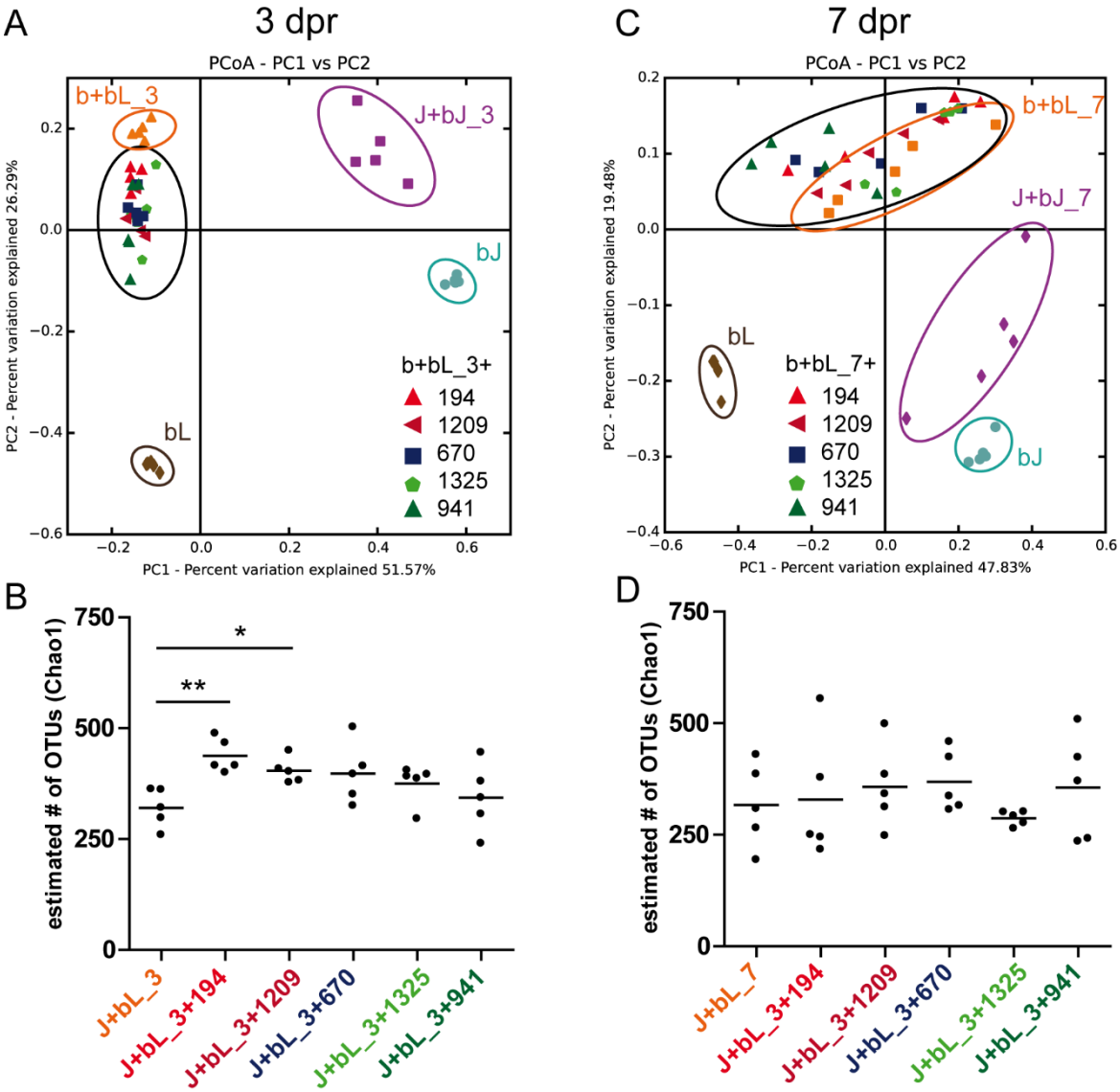

Figure 2-6 *Recolonization patterns in the presence of selected isolates. Bacterial communities at 3dpr (A) and 7dpr (C) were clustered using PCoA of the Bray–Curtis distance matrix. The percent variation explained by the principal coordinates is indicated at the axes. bL, source bacteria of larvae; bJ, source bacteria of juvenile polyps; J+bL, bacterial community of polyps recolonized with bL after 3dpr and 7dpr; J+bJ, bacterial community of polyps recolonized with bJ after 3dpr and 7dpr; b+bL+isolates, bacterial community of polyps recolonized with bL and one of the selected isolates. Estimated number (Chao1) of OTUs after 3dpr (B) and 7dpr (D). Statistical analysis was conducted using analysis of variance (ANOVA; $*p < 0.05$, $**p < 0.01$, n = 5).*

However, the effect of the isolates on the Bray–Curtis distances (**Figure 2-6**B and *Suppl. Figure 4B*) and the alpha-diversity (**Figure 2-6**D) vanished after 7dpr. Therefore, all bacteria caused only temporary shifts in the community composition and only competitive bacteria were able to induce a significant but temporary increase in alpha-diversity.

2.2 Bacterial recolonization experiments on host and on a neutral surface

2.2.1 Bacterial recolonization of adult *Nematostella* polyps is dependent on time

In order to understand the diversity of the microbial communities during development, I tracked the reassembly of the microbiome after removal of the native microbiome and recolonization of adult *Nematostella* polyps with three different bacterial inocula, respectively. The inocula were prepared by homogenizing whole tissue of larvae (6 days old, bL), juveniles (54 days old, bJ) and adult polyps (from long-term culture, bA). Recolonization was tracked over one month and samples were taken 2 days post recolonization (dpr), 7 dpr, 14 dpr and 28 dpr (**Figure 2-7**, **Figure 2-8**).

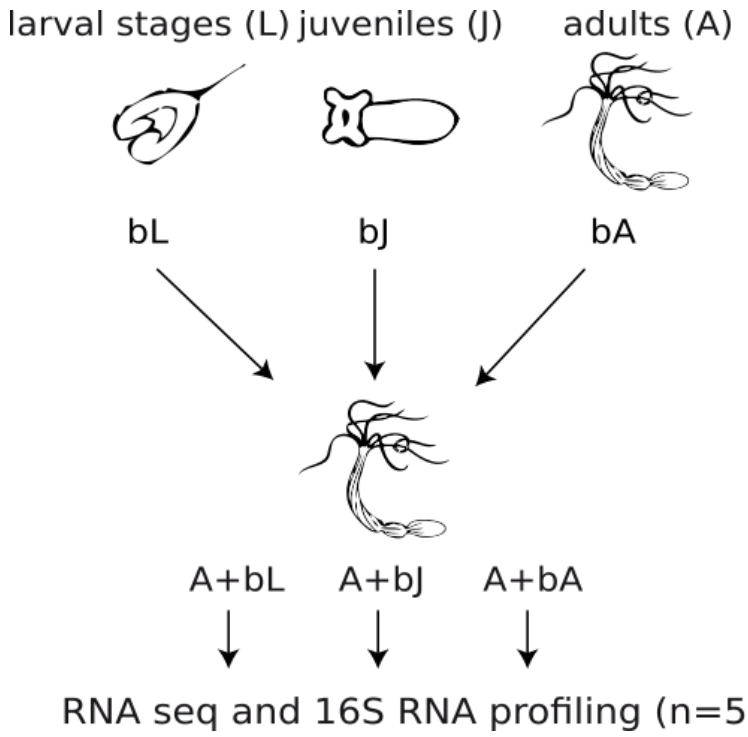

Figure 2-7 *Experimental design for the recolonization experiment. Bacterial inocula from the three different developmental stages were used to recolonize gnotobiotic adult polyps. Samples for RNSA seq were taken after two days of recolonization (dpr). Samples for 16S rRNA profiling were taken 2 dpr, 7 dpr, 14 dpr and 28 dpr. bL =bacteria of larvae, bJ = bacteria of juveniles, bA = bacteria of adults.*

As control, adult polyps with their native microbiome were kept in sterile NM and sampled at the same time points. Additionally, samples were taken 2 dpr for analysis of the host's transcriptomic response upon recolonization.

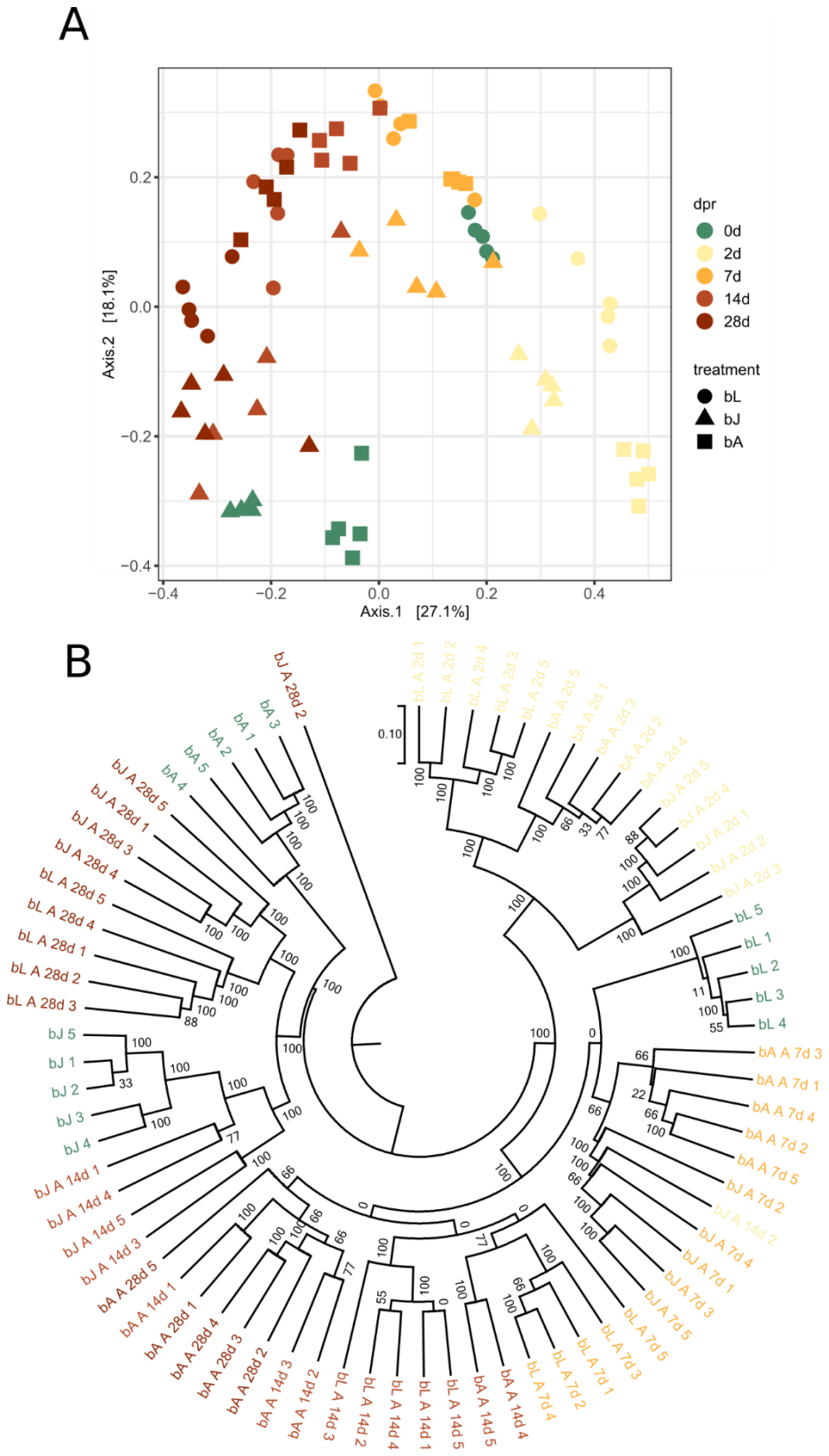

Figure 2-8 *PCoA plot of the bacterial recolonization of gnotobiotic adult Nematostella polyps over the course of one month. (A) bacterial composition of the three inocula (dark green) und after 2 days of recolonization (egg shell), after 7 dpr (orange), after 14 dpr (brown), and after 28 dpr (dark brown). Basis for the calculations was the Bray-Curtis dissimilarity. (B) UPGMA tree of the same samples and colored with the same color code, showing the similarities between samples.*

The analysis revealed that bacterial composition is mainly driven by time rather than by the bacterial source (**Figure 2-8**, **Table 2-2**). After 2 days, the bacterial communities of all three treatments shifted towards one another and continued to cluster together for the remainder of the experiment. However, the identity of the three treatments changed over the course of the experiment. After 2 days, the identity of the three communities from the different inocula clustered the closest to the bacterial community specific for larval stages. This becomes even more apparent 7 dpr. After 14 dpr however, the bacterial identities of the three treatments approached the bacterial community specific for juvenile stages, with 28 dpr getting even more close to the juvenile identity, while also shifting towards the adult community identity. This can also be illustrated with an UPGMA tree (**Figure 2-8**B) and with the Bray-Curtis distances (**Figure 2-9**).

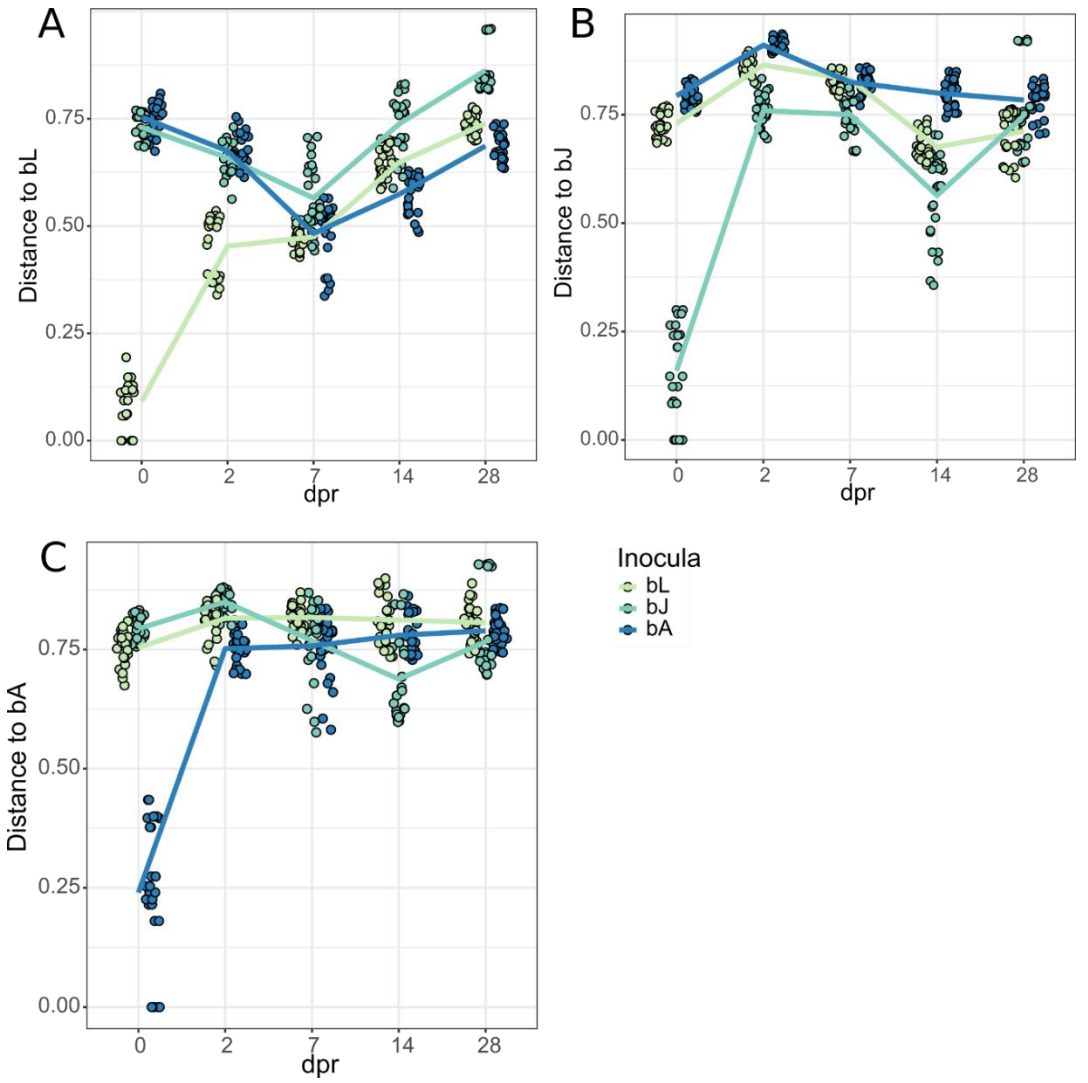

Figure 2-9 *Bray-Curtis Distances of the recolonization dynamics in comparison to (A) the larval inoculum, (B) the juvenile inoculum and (C) the adult inoculum.*

All three treatments show the lowest Bray-Curtis distances to the larval bacterial community 2 dpr and 7 dpr, while the lowest Bray-Curtis distance was measured to the juvenile bacterial community 14 dpr and 28 dpr. Although there was an approaching visible in the PCoA plots, there wasn't a measurable decrease of the Bray-Curtis distance of the three treatments to the adult bacterial community (**Figure 2-8**A, **Figure 2-9**C). However, there is an indication that on beta-diversity level, the recolonization dynamics show a succession from larval identity to juvenile identity and eventually towards adult identity. These results don't just hold true for the Bray-Curtis distances, but also five other metrices. The changes in beta-diversity are significant between the three different inocula and also between the different time points, showing an influence of time and inoculum on the recolonization progression also with different metrices (**Table 2-2**). The influence of time is however always stronger than the influence of the inoculum.

Table 2-2 *Statistical analysis for the significance of the effect of inoculum and time after recolonization. Both an adonis as well as an anosim was calculated for six different beta-diversity measures.*

Parameter	Metric	Adonis R^2	Adonis p	Anosim R	Anosim p
inocula	**Bray-Curtis**	0.15902	0.001***	0.2363	0.001***
	Jensen-Shannon Divergence	0.20891	0.001***	0.2576	0.001***
	Weighted Unifrac	0.13448	0.001***	0.1912	0.001***
	Unweighted Unifrac	0.16308	0.001***	0.3468	0.001***
	Jaccard	0.13066	0.001***	0.2363	0.001***
	Binary Jaccard	0.15872	0.001***	0.3612	0.001***
dpr	**Bray-Curtis**	0.40159	0.001***	0.5814	0.001***
	Jensen-Shannon Divergence	0.51878	0.001***	0.5831	0.001***
	Weighted Unifrac	0.42372	0.001***	0.6094	0.001***
	Unweighted Unifrac	0.18852	0.001***	0.2783	0.001***
	Jaccard	0.31023	0.001***	0.5814	0.001***
	Binary Jaccard	0.18240	0.001***	0.3044	0.001***

In addition to the beta-diversity, the recolonization dynamics were also followed on alpha-diversity level. On alpha-diversity level, a first drop during the first 7 days of recolonization was observed, before a recovery towards the chao1 measure of the adult community was visible (**Figure 2-10**).

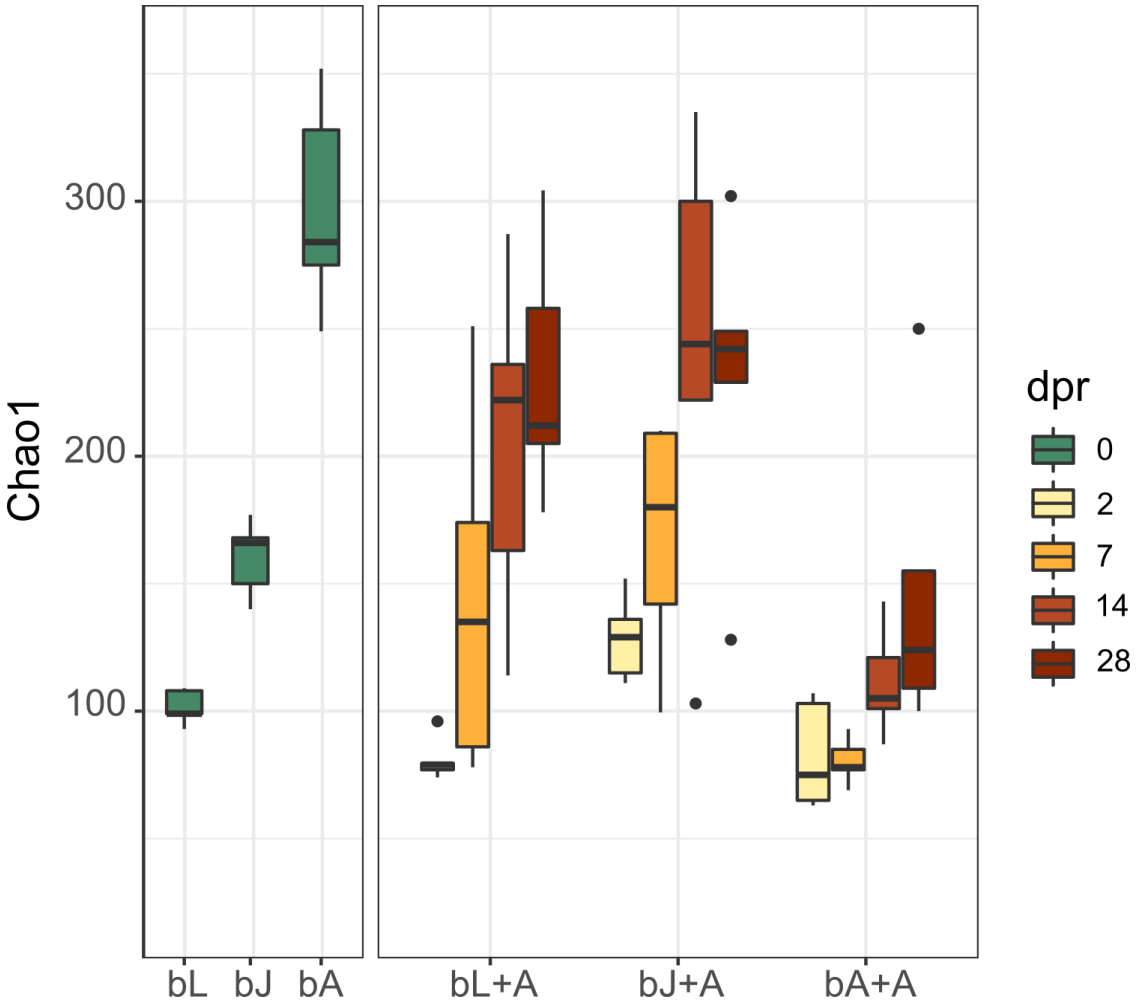

Figure 2-10 *alpha-diversity measured by Chao1 over the course of the experiment. Left: alpha-diversity of the three inocula. Right: alpha-diversity over the course of the recolonization, visually divided by inoculum.*

Interestingly, the adult polyps recolonized with the larval and juvenile bacterial community show the strongest recovery of alpha-diversity during recolonization, while adult polyps recolonized with the adult bacterial community show the strongest drop in alpha-diversity and the slowest recovery. After 28 days of recolonization, the alpha-diversity hasn't even recovered to the Chao1 level of the juvenile bacterial community. Compared to **Figure 2-8**, it also appears as if the polyps recolonized with the adult community moved the slowest towards the juvenile community and ultimately the adult community. This is surprising as

it would have been logical to assume that the adult bacteria could settle immediately on the adult gnotobiotic animals. However, the opposite was the case – the recolonizations with the adult bacteria show the slowest recovery and the lowest alpha- and beta-diversity.

Next, I checked if the bacterial abundances increased on the recolonized polyps, which could be an indication for bacterial growth. For this, I measured via qRT-PCR the proportion of host DNA to bacterial DNA with host- and bacterial-specific primers (**Figure 2-11**).

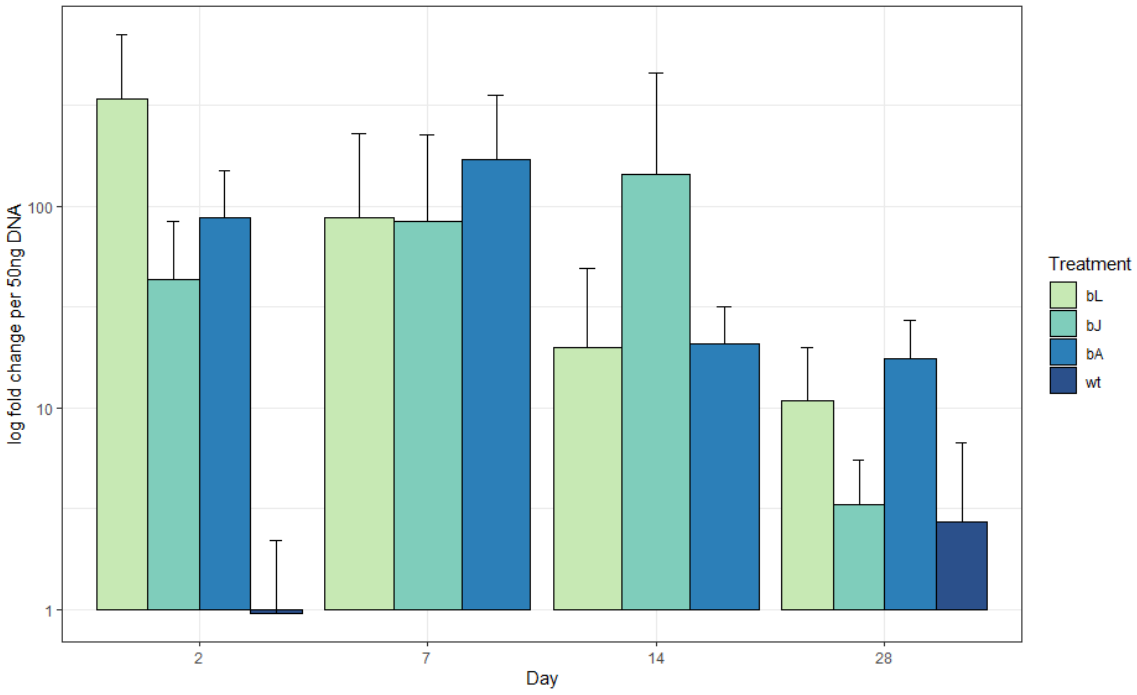

Figure 2-11 *Bacterial load over the course of the recolonization process. Shown is the log10 fold change per 50ng of DNA. Here, the amount of amplificate with the universal bacterial primers 27F-338R was normalized to host tissue with elongation factor a1 primers (EF1a). The deltaCT values were normalized to the 28 dpr value of wildtype samples.*

As a comparison, wildtype control animals were used, which were incubated in sterile medium during the course of the antibiotic treatment and the recolonization process. In comparison to the wildtype control animals, bacterial DNA was overrepresented during the whole duration of the recolonization. However, over time the level of bacterial DNA decreased towards the level of the wildtype controls. This indicates an adaptation of the bacterial load on the recolonized polyps to the bacterial load in wildtype animals.

2.2.2 Under sterile conditions, the microbiome of *Nematostella* changes under starved conditions

Although it could be seen in **Figure 2-8** that the bacterial communities of the three inocula seem to approach the adult bacterial community identity, the dynamics from 14 dpr to 28 dpr could also indicate a halt in community progression. Therefore, the data were reanalysed, this time adding the wildtype controls to the analysis. These are the animals from the long-term culture which were kept in sterile medium during the antibiotic treatment and the recolonization process. All animals weren't fed during the experiment, neither the wildtype animals nor the recolonized ones. In **Figure 2-12** it is visible that the microbiome of these wildtype animals also changed over time.

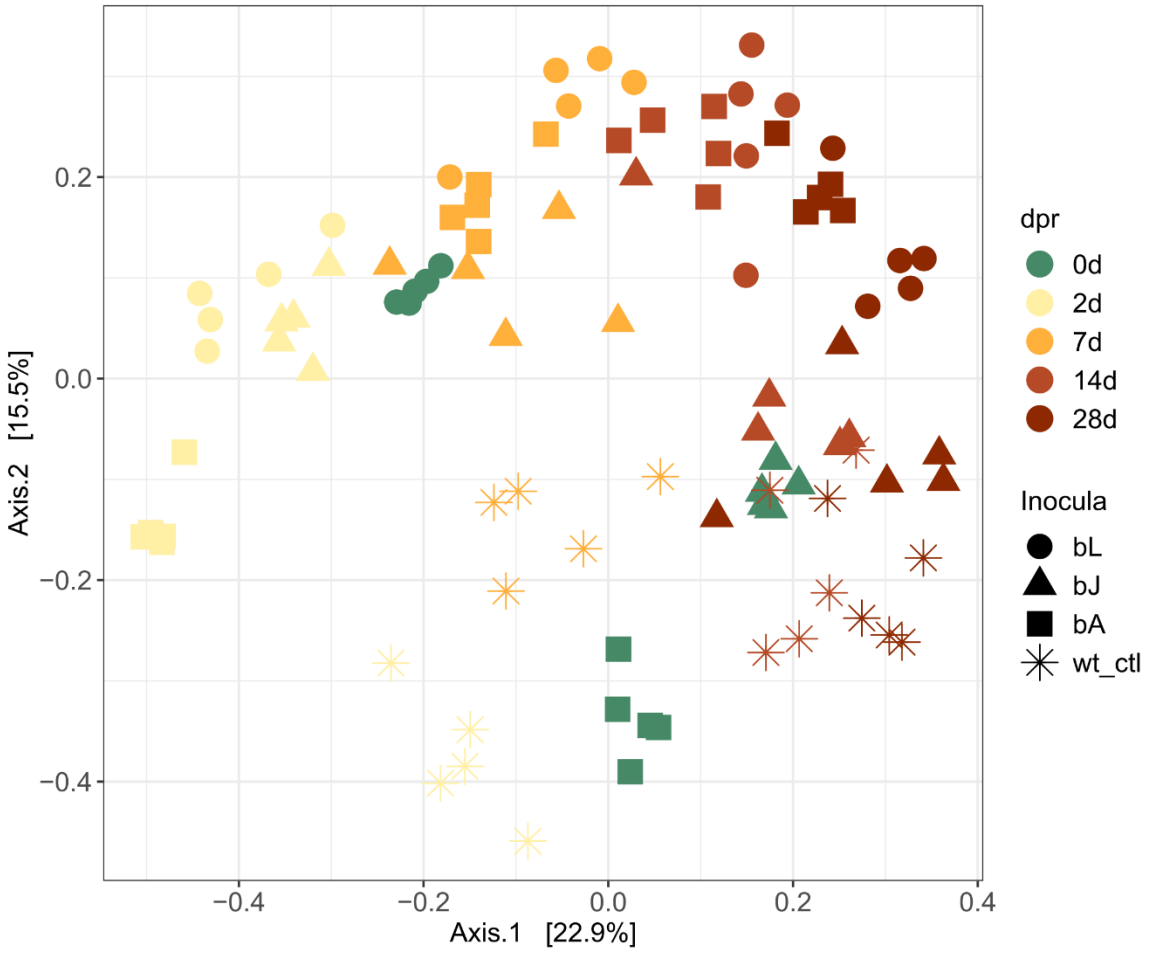

Figure 2-12 *PCoA plot of the effect of starvation on the recolonization dynamics. The wildtype control (wt_ctl) is comprised of animals taken from the standard lab culture, but were kept in sterile medium over the course of the time of the antibiotic treatment and the recolonization experiment. Basis for the calculations was the Bray-Curtis dissimilarity.*

The community identity of these wildtype animals scattered around the native identity of the adult polyps, which weren't kept unfed in sterile medium. Time seems to drive this change as the samples move from the right to the left of Axis.1. After 28 days of recolonization, the adults recolonized with juvenile bacteria seem to be congruent with the wildtype animals which remained in sterile medium for the same amount of time. I infer from that that the community identity of the recolonized animals can't reach the initial community identity of the adult inoculum because starvation also plays a role in the bacterial community composition of *Nematostella*.

2.2.3 Bacterial colonization of a neutral surface like silicone tubes is dependent on the inoculum

In order to disentangle the microbial recolonization effect from *Nematostella*'s transcriptomic response, I challenged a neutral surface with the three inocula. For this, I cut hollow silicone tubes with an inner diameter of 3 mm, an outer diameter of 5 mm and a wall thickness of 1 mm into pieces of approximately 1 cm length. This should imitate a polyp with an inner (gastrodermic) and an outer (ectodermic) surface. I sampled in shorter time intervals during the first week as I sampled for the recolonization of *Nematostella* polyps but tracked over the same time period of 28 days. The experimental setup was otherwise equivalent to the recolonization of adult polyps (Chapter 6.2.7). For sampling, I bisected the silicone tubes longitudinally to isolate gDNA from one half and dye the second half with crystal violet to track biofilm formation.

As in previous results, the three inocula again clustered differentially (**Figure 2-13**).

However, the recolonization succession differed from the one on *Nematostella* polyps observed in **Figure 2-8**. During recolonization of silicone tubes, the inoculum as well as the time shows influence on the recolonization dynamics (**Figure 2-13**).

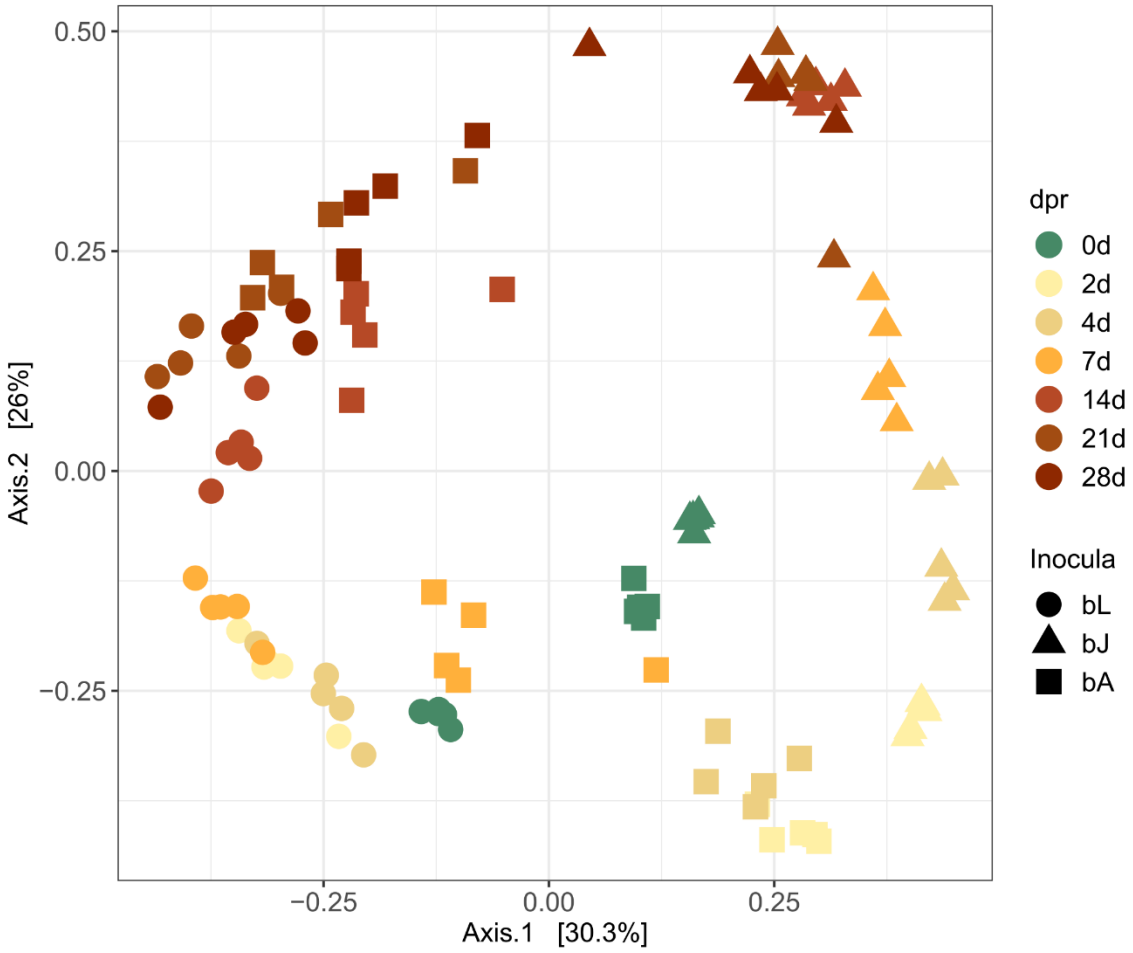

Figure 2-13 *PCoA plot of the recolonization of silicone tubes with inocula from three different developmental stages. For this experiment, instead of adult gnotobiotic polyps, approximately 1cm of silicone tube was inoculated with the three developmental-specific bacterial communities. The colonization was tracked over the course of 28 days. Basis for the calculations was the Bray-Curtis dissimilarity.*

The inocula were divided in the dimension plotted on Axis.1. The three inocula stayed distinctly separated over the course of the 28 days of recolonization with no mixing or approaching one another. However, the inocula isolated from adult polyps and from larvae clustered more closely to one another while the inoculum isolated from juveniles stayed isolated to both. The three different inocula showed the same shifts over time, where they first move down on Axis.2 before they all moved up on the same axis. Therefore, the dimension plotted on Axis.2 explains the effect of time on the recolonization, while the dimension plotted on Axis.1 explains the effect of the different bacterial sources.

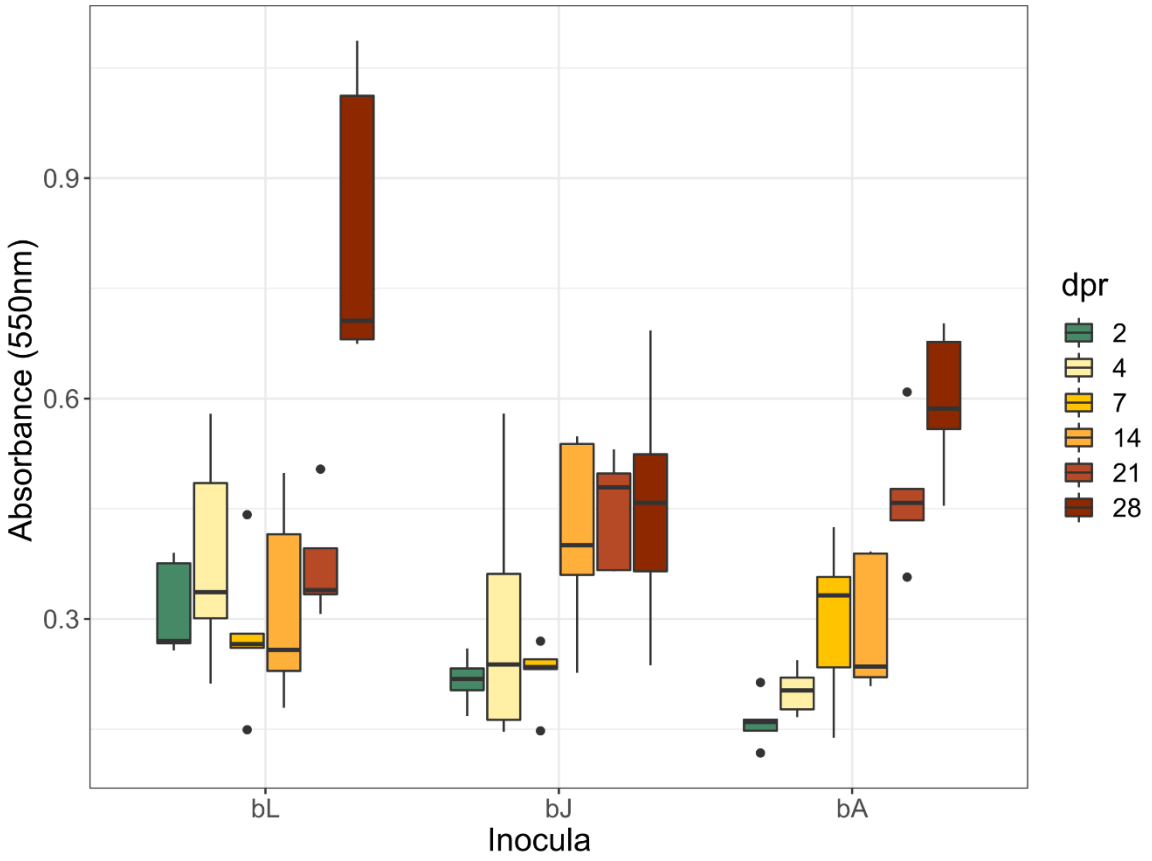

Figure 2-14 *Amount of biofilm on silicone tubes quantified by the intensity of crystal violet staining. The intensity was quantified by rising the Crystal Violet off of the silicone tubes and measuring the absorbance at 550 nm. Rise in biofilm formation between 2dpr and 28 dpr was significant in all three treatment groups (p<0.0001). Biofilm formation was just significantly different if bL is compared to bA (p<0.05).*

In addition to the 16S rRNA data, biofilm production on the silicone tubes was measured. For this, halves of the silicone tubes were first dyed with crystal violet, before it was washed and then diluted in ethanol. The intensity of crystal violet was then measured at 550 nm in a Tecan microplate reader (**Figure 2-14**).

Firstly, in all samples a biofilm formation could be observed. Therefore, bacteria seem to be able to also settle on a transcriptional inactive surface. The crystal violet intensity and therefore biofilm formation also rose significantly over time for all three inocula. However, just the silicone tubes recolonized with bacteria of larvae showed a significantly higher biofilm formation if compared to the silicone tubes recolonized with adult bacteria. So although the three inocula showed a different timely progression on beta-diversity level, the biofilm formation just showed a significantly different effect in regards of time, but just a subtle difference in biofilm amount across the three inocula.

2.2.4 *Nematostella* shows a strong transcriptomic response to bacterial recolonization

In order to elucidate the host short-term response to bacterial recolonization, RNA was sampled two days post recolonization (2 dpr). The samples of the three different inoculated animals were compared to one another and gnotobiotic controls. In total, 4103 genes were differentially regulated in comparison to gnotobiotic animals, representing almost 16% of the whole transcriptome with 25729 genes (**Figure 2-15**).

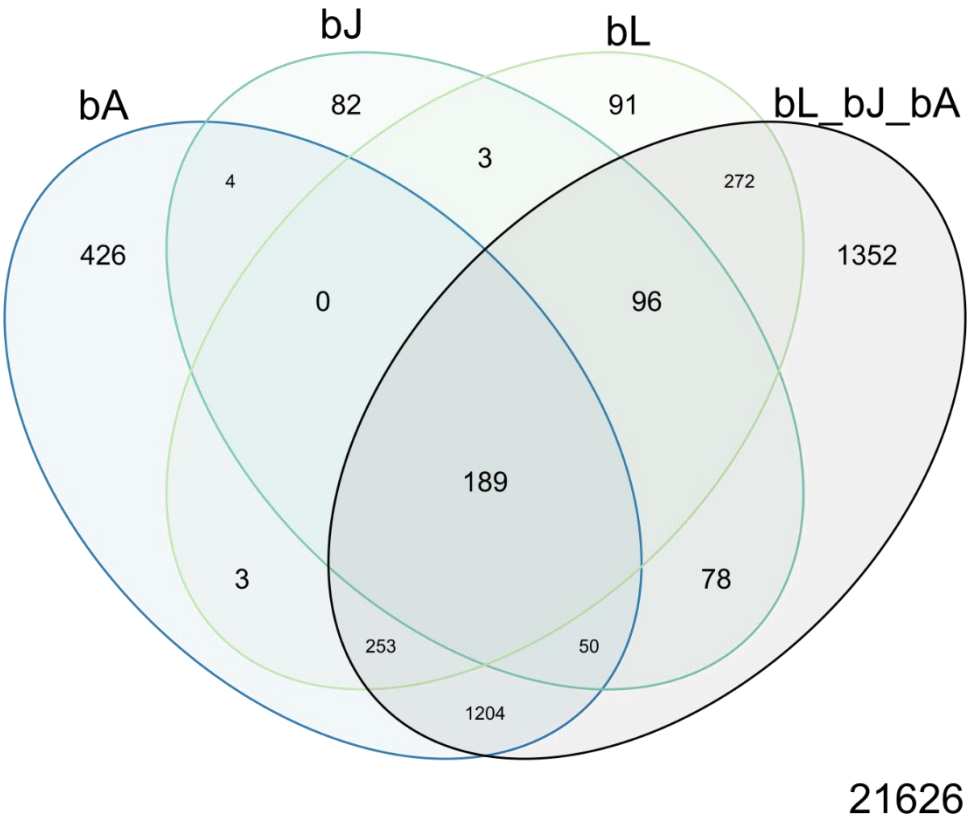

Figure 2-15 *Venn diagram of the differentially expressed genes 2 days post recolonization. To enhance the statistical power, the three comparisons of bL, bJ and bA vs GF were pooled and separately calculated again against GF. This way, 1352 additional genes were found which are differentially regulated in all three recolonizations. Calculations were done by Dr. Jan Taubenheim.*

The response to the recolonization of the three developmental-specific inocula was highly specific. Interestingly, the highest transcriptomic response was exhibited by the adult polyps which were inoculated with adult bacteria with 426 genes. This is in line with the

observations during the beta-diversity development, as the adult inoculum shows the highest distance to the larval inoculum, but showed the biggest drop of distance upon recolonization (**Figure 2-8**, **Figure 2-9**). Therefore, the adult inoculum undergoes the biggest restructuring upon recolonization and also triggers the highest transcriptomic response in the host. The polyps also respond to the adult inoculum with the upregulation of the single TLR gene present in *Nematostella* (log2FC -0.41, padj < 0.05) (Brennan et al. 2017). The polyps recolonized with larval and juvenile bacteria just showed 91 and 82 differentially regulated genes, respectively. The common response of the polyps towards recolonization with bacteria in general with 189 genes was also not as strong as the response to recolonization with adult bacteria alone. However, with enhancement of the statistical power, 1352 more genes were found which react to bacterial recolonization in general, rendering this the strongest response.

Looking at the KEGG clusters of the differentially regulated genes, several clusters are regulated (**Figure 2-16**).

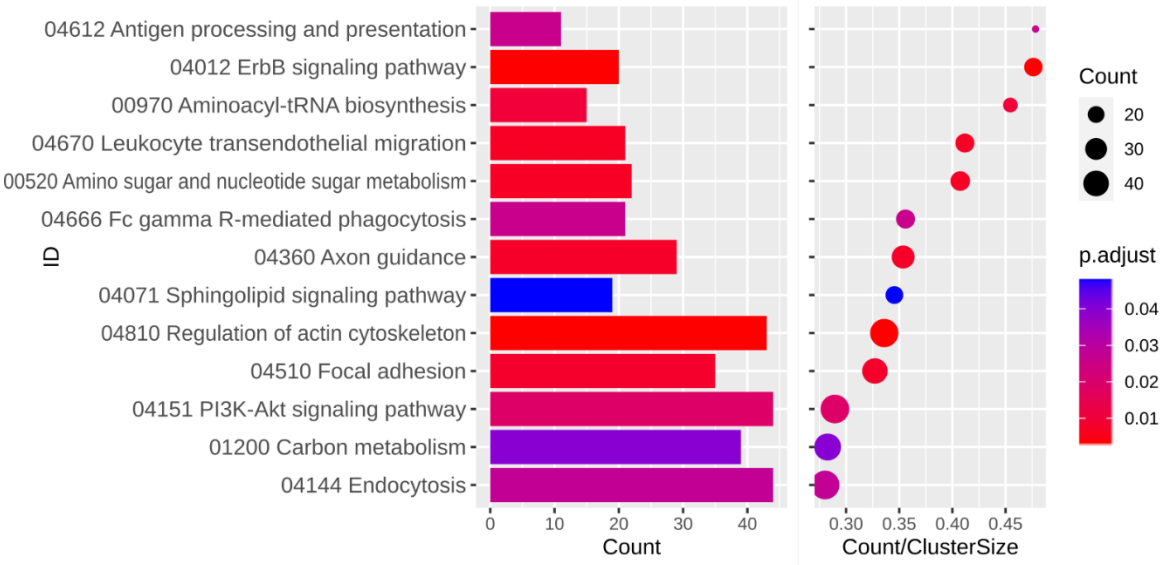

Figure 2-16 *Regulation of KEGG clusters of differentially regulated genes upon recolonization versus the gnotobiotic treatment. The barplots show the counts of the single KEGG clusters while the dots show the ratio between count and cluster size with the dot size showing the amount of counts. Calculations were done by Dr. Jan Taubenheim.*

Particularly high numbers of counts are exhibited by clusters belonging to cell regulation like the regulation of the actin cytoskeleton, focal adhesion, the PI3K-Akt signaling pathway and endocytosis. One enriched KEGG cluster not directly involved in cell regulation is carbon metabolism. If the ratio of counts to cluster size is calculated, other clusters

become apparent, like clusters involving the immune response like antigen processing and presentation, or leukocyte transendothelial migration. But also here, cell regulatory pathways like the ErbB signaling pathway protein translation are showing an upregulation. Next, I looked more closely into single regulated genes instead of gene clusters. The 20 top upregulated genes which react to all three bacterial inocula can be found in **Table 2-3**, showing the gene ID, its log2 fold change and the p-value. If known, the Top BLASTP hit of the ncbi database is also stated.

Table 2-3 *Top 20 upregulated genes upon recolonization with bacteria, independent of the inoculum. The upregulation is shown as the Log2 fold change (Log2FC). The p-value is smaller than 5.204e-11 for all of these 20 genes and therefore not separately stated. Calculations were done by Dr. Jan Taubenheim.*

Top	Gene ID	Log2 fc	Top blastp hit
1	NVE6003	2.722	-
2	NVE1384	2.617	-
3	NVE23862	2.597	-
4	NVE4826	2.574	Phthiocerol synthesis polyketide synthase type I
5	NVE23912	2.502	Sorting nexin-12
6	NVE24772	2.390	Phthiocerol synthesis polyketide synthase type I
7	NVE123	2.387	Stromal membrane-associated protein 2
8	NVE22726	2.377	Caskin-1
9	NVE8785	2.230	-
10	NVE23583	2.216	-
11	NVE16014	2.151	-
12	NVE4825	2.134	Highly reducing polyketide synthase sdnO
13	NVE11847	2.113	Carbamoyl-phosphate synthase
14	NVE6997	2.108	von Willebrand factor A domain-containing protein 7
15	NVE8298	2.076	Failed axon connections homolog
16	NVE4304	2.039	-
17	NVE14301	2.036	Chitin synthase 1
18	NVE1302	2.035	-
19	NVE17842	2.035	-
20	NVE8085	1.988	Hepatic leukemia factor

The Log2 fold change of the highest regulated gene is with 2.72 relatively low and therefore shows a generally low regulation of the genes. However, considering the amount of differentially regulated genes, the animals seem to react to the bacterial recolonization with a weak regulation of a big variety of genes instead of with a strong regulation of just

a few genes. Almost half of the genes could not be assigned to any known proteins and just showed hits to hypothetical proteins or unknown proteins from other organisms if blasted. Here, genes belonging to the clusters from **Figure 2-16** is just apparent in the regulation of NVE23912, NVE123 and NVE 22726, which are involved in intracellular trafficking, in NVE14301, a chitin synthase involved in carbon metabolism, and in NVE6997, which is involved in immunity. Other hits include lipid metabolism (NVE4826, NVE24772), axonal development (NVE8298) and DNA binding (NVE8085).

2.2.5 Bacteria show a distinct recolonization success on adult polyps depending on their abundance during specific developmental time points

During recolonization with bacterial inocula isolated from three different developmental life stages of *Nematostella*, the source of the inocula did not appear to have a decisive influence on the subsequent dynamics of recolonization. Instead, it seemed like the bacterial had to "reset" to a starting point that resembled the larval bacterial community before the bacterial communities of the three bacterial inocula could move towards an adult identity. This led me to the hypothesis that bacteria specific for larval developmental stages possess a higher potential for recolonization of a gnotobiotic animal than bacteria specific for adult developmental stages. For this, I recolonized gnotobiotic adult polyps with single bacterial strains that were isolated from *Nematostella*. I chose the bacteria for their appearance during the recolonization experiment, regardless of their appearance during ontogeny. If they occurred predominantly in early recolonization, they were defined as early-appearing bacteria. If the bacteria occurred predominantly during late recolonization, they were defined as late-appearing bacteria. Gnotobiotic polyps were recolonized with single bacterial strains and homogenized and spread on MB plates two days after recolonization (**Figure 2-17**).

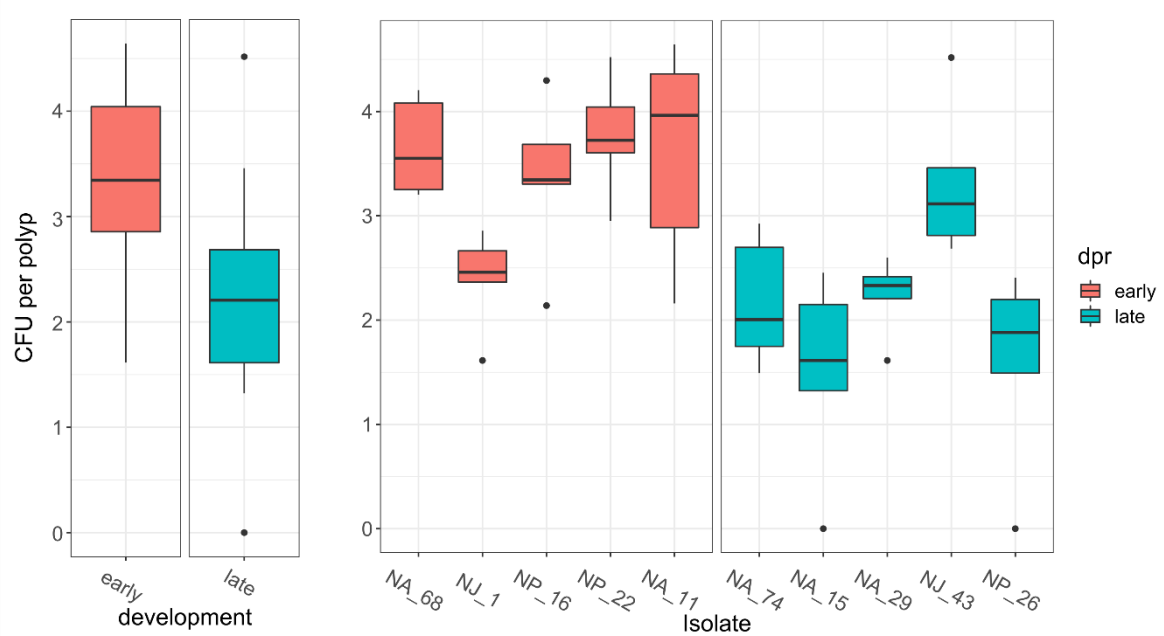

Figure 2-17 *Mono-associations for early (red) and late (blue) colonizers. On the left, the CFUs for all early and all late colonizers are pooled. On the right, The CFU counts are shown separately for each bacterial strain. Bacteria were classified as early or late colonizers according to their appearance during early or late recolonization. Polyps were recolonized for seven days before plating out and colonies were counted after 3 days of incubation (n=5). CFUs are shown on a log10 scale. The recolonization of early-appearing bacteria is significantly higher than the recolonization of late-appearing bacteria (Kruskal Wallis rank sum test, chi-squared = 16.528, df = 1, p-value < 0.0001).*

Polyps recolonized with bacterial isolates which appear early during development generally show a higher bacterial load after 7 days of recolonization than polyps recolonize with late-appearing bacteria. This generally hints towards a mechanism which facilitates the first colonization events for early-appearing bacteria or inhibits the direct settling of late-appearing bacteria. This mechanism could either be bacteria-bacteria-specific or it could be bacteria-host-specific. As the late-appearing bacteria are mostly bacteria that show a higher abundance in adult stages, it is unlikely that the adult host actively selects against those strains. However, for both scenarios, the metabolic potential of early- and late-appearing bacteria could shed light on the requirements of these bacteria to their environment.

2.3 Bacteria-Bacteria interactions during the recolonization process

2.3.1 Modelled bacterial metabolic potential is changing over the course of the recolonization process

In order to evaluate if and how the metabolic potential of the bacteria influence the community dynamics, potential metabolic pathways were calculated across the whole recolonization process. For this, the relative bacterial abundance data were combined with genomic data inferred from genomes sequenced directly from bacteria isolated from several developmental stages of *Nematostella*, or from genomes found in the NCBI database. The corresponding bacteria showed an at least 97% identity on 16S rRNA level to bacteria occurring over the course of the recolonization time frame. A complete list of the bacterial genomes can be found in the Appendix (*Suppl. Table 2*).

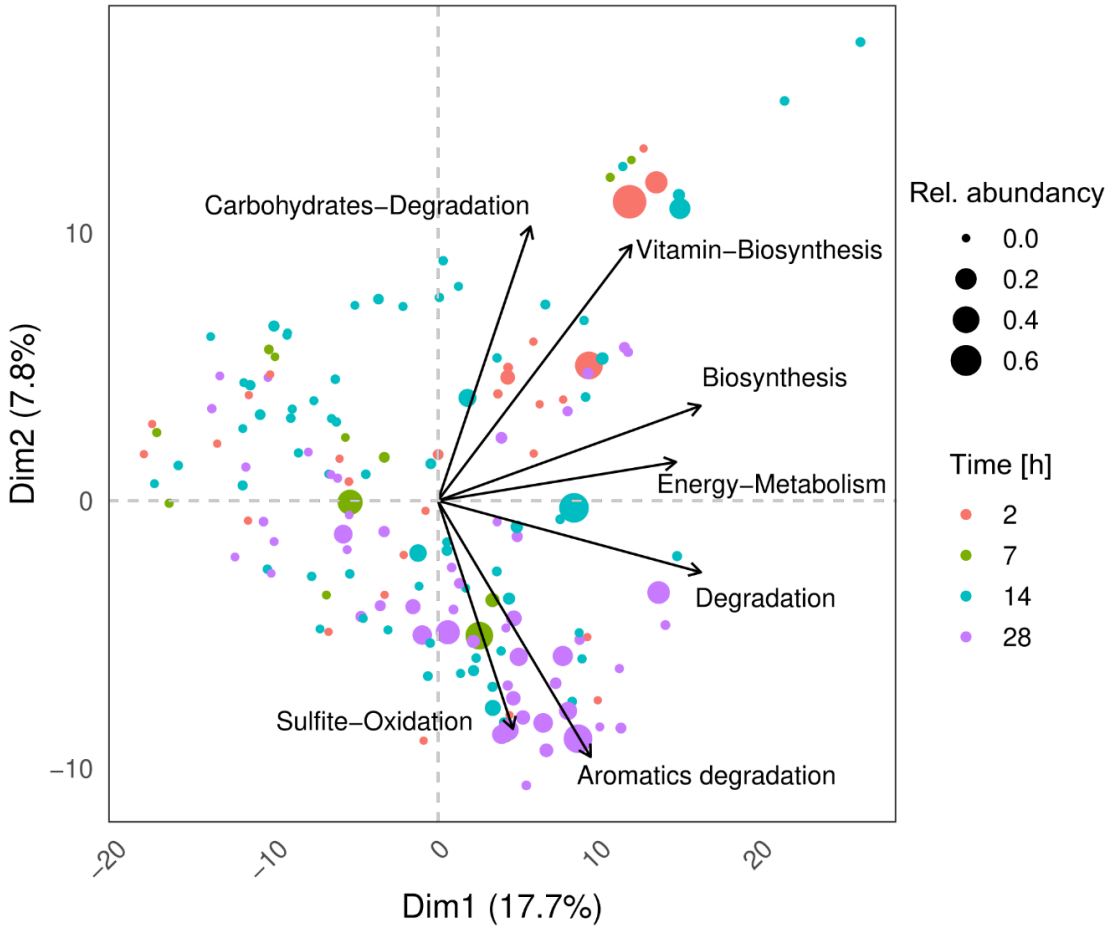

Figure 2-18 *Principal component analysis (PCA) of the distribution of metabolic subsystems predicted to be present in bacterial isolates by metabolic pathway analysis. Each dot represents one bacterium. Dot size codes for the relative abundance, dot color codes for the time point when the bacterium shows the highest relative abundance. The arrows indicate the subsystem, which correlates the strongest with principal components. Calculations were done by Dr. Johannes Zimmermann, Institute for Experimental Medicine, Kiel.*

The metabolic potential present in the recolonizing bacteria hereby showed a distinct temporal pattern (**Figure 2-18**). During early recolonization (2-7 dpr), carbohydrate degradation and vitamin biosynthesis are enriched, while during late recolonization (14-28 dpr) sulphite oxidation and aromatics degradation are prevalent. As *Nematostella* possesses a mucus layer and a glycocalyx which are composed of a carbohydrate-rich matrix, carbohydrate degradation was looked into more specifically as a driver of early recolonization.

2.3.2 Chitin as a possible driver of the recolonization dynamics

Looking more closely into the potential of carbohydrate degradation during early colonization, chitin degradation stood out as a carbohydrate that showed an enrichment 2 dpr in the recolonizations with all three inocula (**Figure 2-19**).

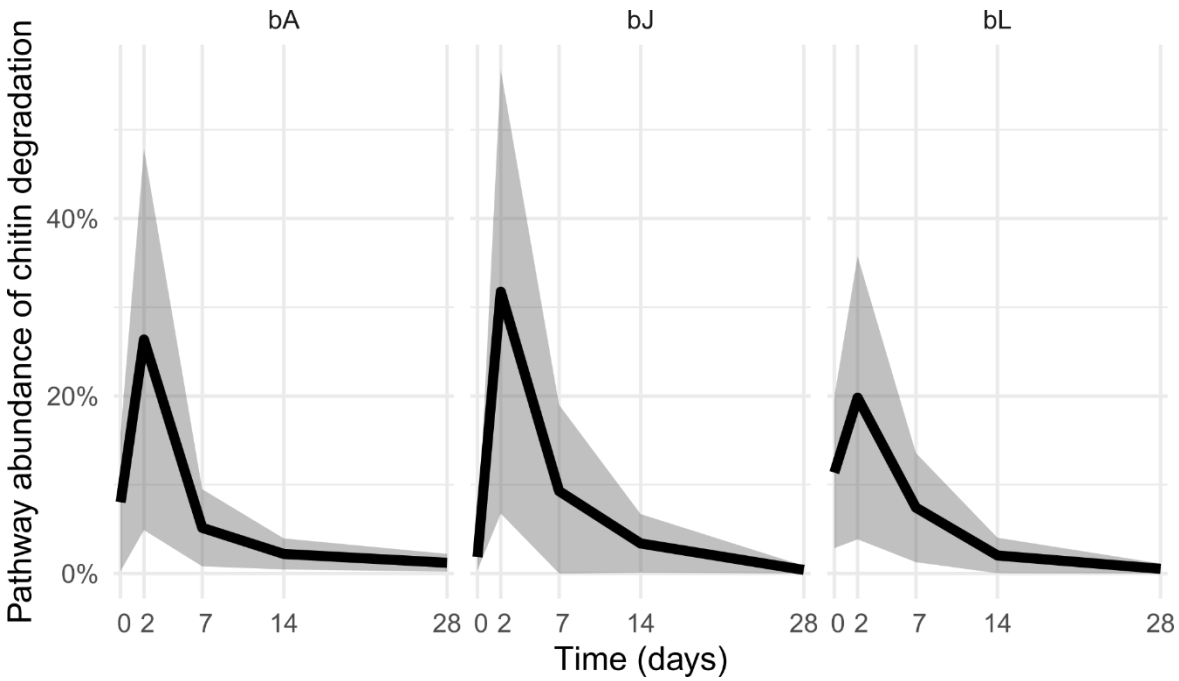

Figure 2-19 *Predicted pathway abundance of chitin degradation based on the genome data of the bacterial isolates and their abundance over the course of the recolonization black = mean, grey = standard deviation. Calculations were done by Dr. Johannes Zimmermann, Institute for Experimental Medicine, Kiel.*

The pathway abundance of chitin degradation is enriched by 30-40% in the recolonizations with all three inocula during early recolonization. Therefore, the model suggests that early

colonization is driven by chitin degradation by the colonizing bacteria, independent of the inoculum.

Because these calculations are based on the metabolic potential of the bacteria and not their actual metabolic activity, bacterial colonizers of *Nematostella* were checked for their actual chitin degradation capability. For this, tissue homogenates of adult polyps and of larvae, and single bacterial strains isolated from *Nematostella* were spread on agar plates enriched with chitin flakes. As chitin is not water-soluble, it produces murky agar plates. Chitin degradation results in a clearing of the agar. In **Figure 2-20** this clearing can be observed for an exemplary single bacterial strain (A) and for the larval tissue homogenates (B).

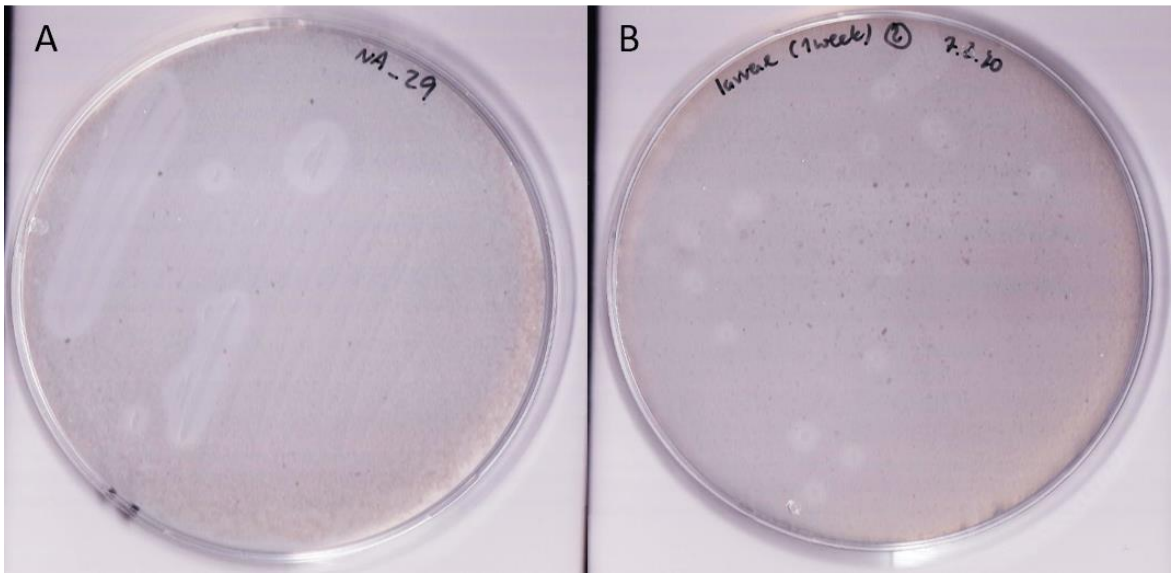

Figure 2-20 *Chitin degradation of (A) a single bacterial isolate and (B) a complex tissue homogenate of Nematostella larvae that were one week old.*

Independent of if the bacterial strain was streaked out separately or if whole tissue homogenates were plated, bacterial growth could be observed on these plates as well as a clear halo around the colonies. This shows the bacterial ability to grow on and to digest chitin under the given circumstances.

Several other bacterial strains isolated from different developmental stages of *Nematostella* were checked for their ability to degrade chitin. Especially strains predicted to be able to degrade chitin from their metabolic potential were checked. All tested bacterial strains which were either predicted to degrade chitin or exhibited chitin

degradation without prior prediction can be found in **Table 2-4**. A complete list of all tested strains can be found in the Appendix (*Suppl. Table 3*).

Table 2-4 *Chitin degradation of single bacterial isolates of Nematostella.*

Genome ID	Cryo ID	Species	Predicted	Chitin Degrading	early/late
G21603	NA_2	*V. alginolyticus*		x	late
G21623	NA_62	*V. alginolyticus*		x	late
G21624	NA_65	*V. alginolyticus*		x	late
G21639	NA_29	*V. alginolyticus*		x	early
G21641	NA_33	*V. alginolyticus*		x	late
G21644	NJ_12	*V. alginolyticus*		x	late
G21621	NA_54	*V. alginolyticus*		x	late
G21615	NP_8	*V. alginolyticus*	x	x	late
G21600	NA_12	*Aeromonas hydrophila*		x	adult/rare
G21616	NA_15	*Sulfitobacter sp*	x	x	late
G21653	A_MB_4	*Ruegeria pelagia*	x		juv/rare
G21606	NA_7	*V. pomeroyi*	x		late
G21625	NA_68	*V. shilonii*	x		early
G21612	NP_3	*V. diazotrophicus*	x		late

Chitin degradation potential was exhibited by a wide variety of *Vibrio alginolyticus* strains, although its potential was just predicted for a single strain. Just two other tested strains were able to degrade chitin under the given circumstances, one *Aeromonas* and one *Sulfitobacter* species. For other predicted bacterial strains, the chitin degradation potential could not be verified.

In order to find candidates for an interplay between host and bacteria, which may drive the recolonization dynamics seen when gnotobiotic animals are inoculated with the three development-specific bacterial communities, metabolically enriched pathways in bacteria were compared to differentially regulated genes in the host's transcriptome.

Interestingly, one of the top 20 upregulated genes upon bacterial challenge was chitin synthase 1 (NVE14301, **Table 2-3**, **Figure 2-21**B). Besides chitin synthase 1, *Nematostella*

possesses a second chitin synthase, which didn't show a differential regulation, independent of inoculum (NVE8515, **Figure 2-21**A).

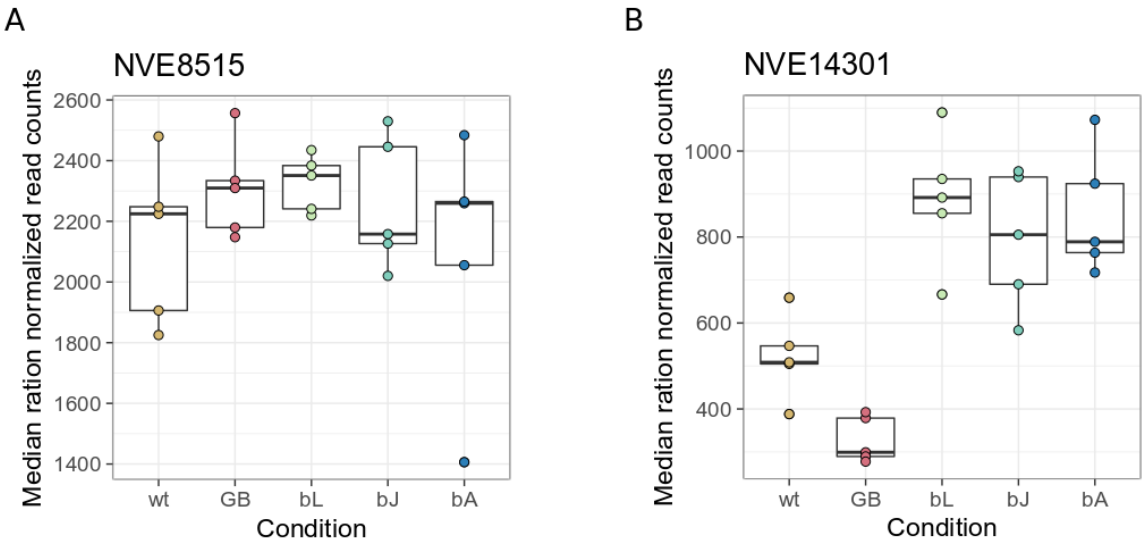

Figure 2-21 *Expression of the two chitin synthases (A) NVE8515 and (B) NVE14301 in wildtype (wt), gnotobiotic (GB) and recolonized adult polyps. While NVE8515 is not differentially expressed, NVE14301 is significantly upregulated during recolonization in comparison to GB animals. In wildtype animals, expression is slightly elevated in comparison to GB animals.*

As the transcriptome results just show the transcription of a gene into mRNA, I next stained the protein product of the chitin synthase, without discriminating between the two synthases. For this, whole polyps were first fixed in paraformaldehyde (PFA), before they were stained with a fluorescently labelled probe coupled to a chitin-binding domain (CBD), which was gifted by the Moerschbacher group from the Westfälische Wilhelms-University in Münster. After staining, the whole polyps were observed under the confocal system Fluoview 3000 from Olympus. Staining could only be observed within the tentacles, seemingly in nematocytes (**Figure 2-22**A, B).

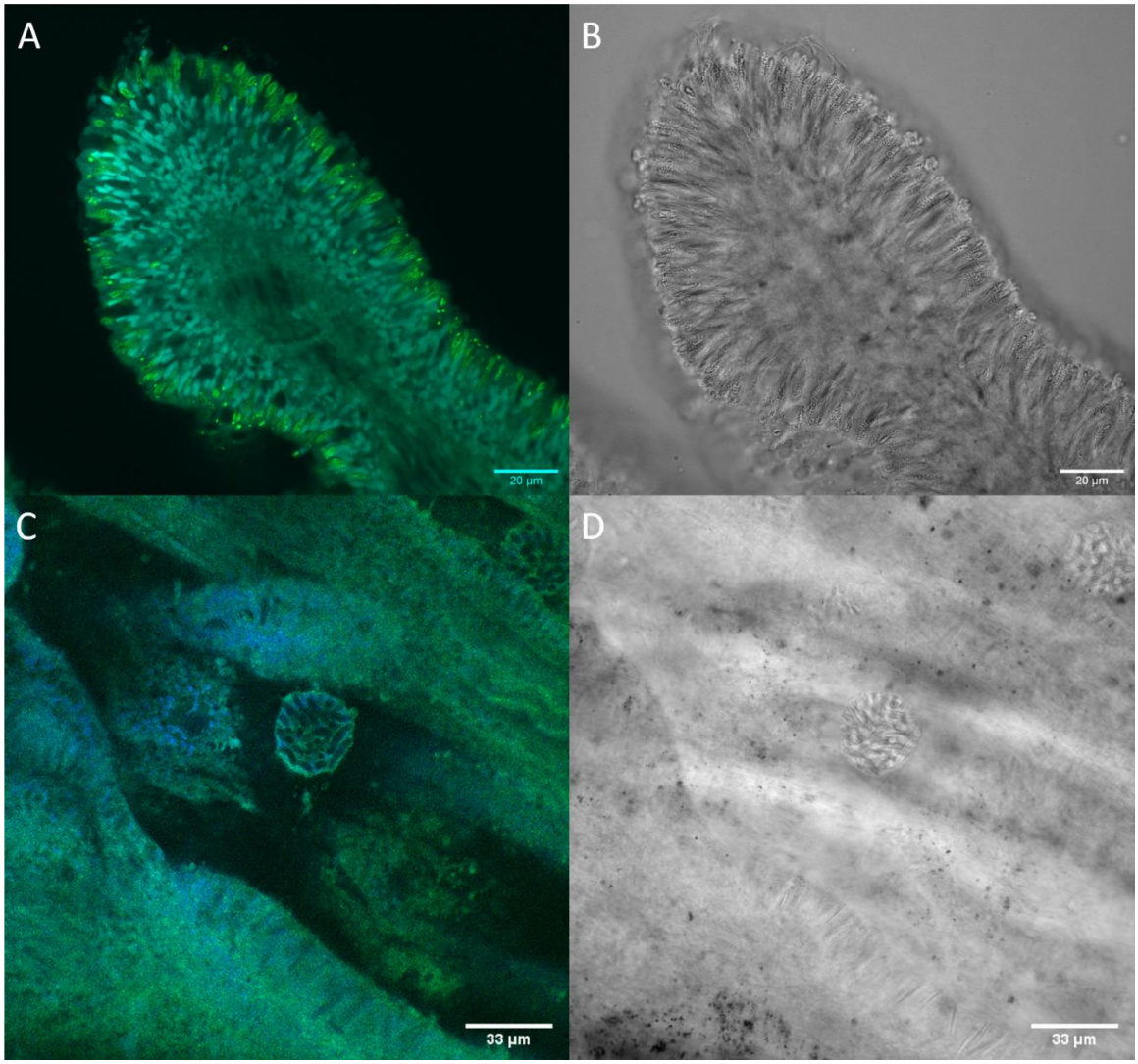

Figure 2-22 *Staining with a fluorescently labelled probe binding to chitin. (A, B) Tip of a tentacle stained with Hoechst and a fluorescent probe specific for chitin. (C, D) Free-floating single nematosome inside of the body column stained with a fluorescent probe specific for chitin. (A, C) under fluorescent light. Blue: Hoechst. Green: GFP coupled to a chitin-binding domain (kind gift of the Moerschbacher group, WWU Münster). (B, D) Same structures in bright field.*

This shows that *Nematostella* not just possesses genes for a chitin synthase but that *Nematostella* is actually capable of producing chitin. For the localization, the staining is limited to a subset of nematocytes. The staining could just be observed in the nematocytes located in the tentacles, but not in nematocytes in the body column or nematosomes (**Figure 2-22** C, D), probably representing spirocytes with a staining of the tubules inside of the cyst (Zenkert et al. 2011).

3 Discussion

3.1 Bacterial co-occurrence networks show highly dynamic bacterial interactions

Co-occurrence networks were constructed to quantify the importance of specific bacteria based on community-level interactions (Faust and Raes 2012). The goal was to focus on the co-occurrence networks to infer the ecological role of the bacteria (i.e., cooperation and competition) and identify the hubs (i.e., bacteria with many direct connections of the same sign). The reestablishment of the whole bacterial community in the presence of cooperative, competitive, or neutral bacteria was tested with in vivo recolonization experiments. The bacteria with strongest predicted interactions changed the community composition during the early recolonization steps of *N. vectensis*, but only the communities inoculated with competitive bacteria exhibited a significant but temporary increase in alpha-diversity. Our study shows that co-occurrence network inference can be used to retrieve ecologically relevant interactions.

The network approach allows identifying the most important bacteria by their potential role in the community rather than solely relying on their relative abundance (e.g., (Jordán et al. 2015)). In our work, the degree of the nodes (OTUs) was used to study the direct effects of the bacteria in the community (Scotti and Jordán 2010), under the assumption that co-occurrence networks can be informative of ecological processes. While at large phylogenetic levels, the abundance can still be a good descriptor of the microbial community associated to N. *vectensis* (Mortzfeld et al. 2016), the most abundant OTUs are not always those displaying the higher number of links (see **Figure 2-1**; **Figure 2-2**). Network analysis suggested potentially important bacteria and enabled designing in vivo experiments to test whether the predicted interactions are ecologically relevant.

Generalized Lotka–Volterra equations were previously applied to predict interactions in microbial communities, and the validity of model results was confirmed by culture experiments (Mounier et al. 2008). However, studies based on dynamical modelling routinely involve only a small number of species, and the validation of network inference (e.g., based on 16S rRNA sequencing data) with culture experiments is in its infancy (Faust and Raes 2012). The novelty of our study stems from the ability to culture single bacterial

isolates, representing certain OTUs, which allows experimental testing of their ecological roles predicted by analysis of co-occurrence networks.

The microbial networks, inferred using the bacterial data from larvae, juvenile, and adult polyps, demonstrate that bacterial interactions during host development are highly dynamic. On the one hand, aspects determining changes in the bacterial networks might be linked to physiological and immunological factors of the host that are remodelled during development as shown during metamorphosis in amphibians (Faszewski et al. 2008; Rollins-Smith 1998) and insects (Vigneron et al. 2014). Especially, effector molecules of the innate immune system like AMPs (Sören Franzenburg et al. 2013; Login et al. 2011; Mukherjee et al. 2014; Salzman et al. 2010) or the provision of selective nutrients by the host (Ley, Peterson, and Gordon 2006) may directly influence the bacterial interactions. In addition, the specific composition of complex carbohydrates on the boundary between epithelium and environment may have a huge impact on individual bacterial fitness and interactions between bacterial species (Kashyap et al. 2013; Pickard et al. 2014). On the other hand, observed changes within the bacterial interactions could be explained by successions driven by ecological bacterial interactions alone. Studying the succession of plant colonization of new habitats was part of ecological research for a long time already, but recently this approach also gained popularity to study successional patterns of microbial communities (Fierer et al. 2010). It was shown that microbial community successions in a host are accompanied by changes in the metabolic potential, adapting to environmental changes like diet (Koenig et al. 2011), but are also predictable after infection and recovery (David et al. 2014b). However, the changes in microbial succession and metabolic potential also occur in the absence of a host, leaving these successions exclusively to ecological interactions between bacteria alone (Datta et al. 2016).

3.2 The microbiome of *Nematostella* is stable and resilient against overgrowth of single members

In the experiment, we show that the early recolonization dynamics depend on the initial bacterial inoculum, but after 7dpr all recolonizations result in a similar bacterial community composition (**Figure 2-5**, **Figure 2-6**). Three days after recolonization, the community composition observed for all treatments (i.e., those inoculated with

cooperative, competitive, or neutral OTUs) was significantly different from both the native larval (bL) and the native juvenile (bJ) bacteria (**Figure 2-6**). Nevertheless, 7dpr all treatments resembled more the native microbiota of juveniles than the larval source used to assemble the communities (**Figure 2-5**). This process was more efficient when juveniles were recolonized with juvenile microbiota rather than with bacteria extracted from larvae. Even when starting from different initial conditions, all recolonization treatments that included isolates followed recolonization paths that were similar to that of native larval bacteria. Recolonization with competitive, cooperative, or neutral bacteria always developed toward attaining the native juvenile bacterial state, thus showing the resilience of the system to perturbations. One explanation, why even neutral bacteria showed an effect on the assembly of the community, could be that the neutral bacteria were chosen based on network inference (e.g., the decision of considering strong correlations as those with absolute values above the 0.5 threshold, or the use of the SparCC algorithm for correlation detection). Although neutral bacteria do not present strong correlations in the larval and juvenile networks, they still have the potential to influence the community during initial establishment of the community or the later development of the host (**Figure 2-2**).

The convergence of all communities toward the native juvenile bacterial state shows that the initial composition is crucial for the stability of the system. The tested communities in our experiment showed resilience irrespective of the interaction strategy of the OTUs added in excess. Although the interaction mode of overrepresented OTUs does not alter the long-term equilibrium of the community, the competitors are the only OTUs challenging the stability of the system. As described in the literature (Coyte et al. 2015; Czárán, Hoekstra, and Pagie 2002), the addition of competitive OTUs significantly increased community diversity, even though such an effect was transient.

Competitive interactions between members of the bacterial community are expected to increase community diversity (Coyte et al. 2015; Czárán et al. 2002), spatial structure (Hyun et al. 2008), stability (Kelsic et al. 2015), and functioning (Wei et al. 2015). After 7dpr, all communities have transited to a more stable composition, as the number of OTUs is almost the same among treatments (**Figure 2-6**) and overrepresented OTUs declined. In our recolonization experiment, mainly the spatial structure got abrogated by the antibiotic treatment and homogenization of the inocula. While with our experiment, we cannot

assess the spatial structure or the functioning of the community, we can clearly see that only competitive bacteria increase community diversity, which is predicted by ecological theory (Coyte et al. 2015). The temporal increase in alpha-diversity could be explained by the fact that during the initial phase, the spatial structure of the bacterial community is not yet re-established. In this initial phase bacteria can exert contact-dependent competition, which is particularly relevant in the treatments with overrepresented competitive bacteria, leading those communities to higher diversity. With the reestablishment of spatial structure, contact-dependent competition might be less pronounced. This is often described in literature as a real-life game of "rock-paper-scissors" (Kerr et al. 2002; Reichenbach, Mobilia, and Frey 2007), in which coexistence of competing communities is ensured by local interaction and dispersal (van Nouhuys and Hanski 2005).

Neither the larval nor the juvenile bacterial communities are the final state of the system. Both are transient configurations from which the adult stable community develops (Fieth et al. 2016; Mortzfeld et al. 2016). Although stability has been described in marine ecosystems for microbial communities associated to various host taxa (Hester et al. 2016; Schmitt et al. 2012), there are examples (i.e., microbiota communities of corals) that do not present high resilience to perturbations (Pogoreutz et al. 2018; Rosenberg et al. 2009). Previous research has shown that environmental perturbations trigger slight changes in the composition of N. *vectensis* microbiota (Mortzfeld et al. 2016), but these effects were minor compared to the ones associated to the host development. Therefore, it is possible that the bacterial community associated to N. *vectensis* is able to buffer internal shifts such as the overrepresentation of single members of the community, as was simulated with our experiment.

Our study cannot exclude that host–bacteria interactions played a role in the succession of the microbial community, like the innate immune system (Franzenburg et al. 2012; Sören Franzenburg et al. 2013), spatial restriction (Hyun et al. 2008; Welch et al. 2017), or diet (David et al. 2014a). Therefore, further investigations are needed to understand whether bacteria–bacteria interactions, host–bacteria interactions, or both modulate the resilience of the bacterial community. In the same way, we cannot discard that working with the strongest inferred correlations could mask some network properties (e.g., network connectivity and degree of each node) of particular relevance when choosing an

OTU to implement an experiment. With the increasing number of isolates, exploration of other network properties or centrality measurements might be possible, and we could even gain the capacity to study only a few interactions at a time in a synthetic community approach (Bodenhausen et al. 2014).

3.3 The initial recolonization steps are controlled by the host

The establishment and succession of the species-specific microbiome plays a crucial role in early development and disturbances during these early time points are linked to susceptibility to several diseases (Arrieta et al. 2014). In order to understand the processes involved in the community assembly of *Nematostella vectensis*, a broad approach was taken by stripping adult polyps of their microbiome and recolonizing them with bacteria from their different developmental stages. Additionally, silicone tubes were inoculated with the same bacteria from the different developmental stages in order to elucidate potential host effects, and to identify priority effects and other indirect effects.

The recolonization of adult *Nematostella* polyps seemed to proceed independently of the inoculum. During early recolonization (2-7 dpr), the bacterial identity of the three treatments approached one another and resembled the identity of the larval inoculum. After 14 dpr, the distance of three treatments increased to the larval inoculum and approached the identity of the juvenile inoculum. After 28 dpr, the identity of the three treatments did not quite reach the adult inoculum. However, that could be a starvation effect, as it approached the starved adult wildtype control. Therefore, all three treatments undergo the same bacterial succession during recolonization, which resembles the ontogenetic colonization pattern during natural development (**Figure 2-8**; **Figure 2-12**).

Therefore, the results show that the host is interacting with the three different microbiomes in such a way to restore an adult-specific microbiome. This is supported by the RNAseq results, which show a differential response to all three bacterial inocula (**Figure 2-15**), indicating an inoculum-specific restructuring of the bacterial community towards an adult-like community. As the highest number of genes are regulated upon challenge with the adult community, this also indicates the highest restructuring effort of this inoculum to reset the community to a larval one. The involvement of the host in this restructuring of the communities is undeniable when looking at the recolonization of a neutral surface

with the same three inocula as here all three inocula stay distinct from one another (**Figure 2-13**). However, there is also a variety of genes which are generally regulated upon bacterial inoculation and probably represent genes which are generally involved in the selection of bacterial colonizers and can therefore represent genes involved in general host-bacteria interactions, which can be direct or indirect.

3.3.1 Direct host-microbe interactions shape the early recolonization pattern

Direct host-microbe interactions include selective pressures applied by the host upon challenge with specific bacteria belonging to e.g. immunity or cell renewal (Rawls et al. 2006).

One of the mechanisms mediated by the host directly influencing the microbiome is the expression of different pattern-recognition receptors (PRRs). PRRs like TLRs (Toll-like receptors), NLRs (NOD-like receptors), CTLRs (C-type lectin receptors), PGRPs (peptidoglycan recognition proteins), scavenger receptors and GPCRs (G protein-coupled receptors) all can recognize microbe-associated molecular patterns (MAMPs) like flagellin, LPS (lipopolysaccharides), peptidoglycans and other glycans, while some can even discriminate between pathogens and commensals (Dierking and Pita 2020). In Cnidarians, TLRs and other TIR-domain containing receptors are conserved and functionally characterized as receptors involved in pathogen recognition (Bosch et al. 2009; Brennan et al. 2017; Poole and Weis 2014; Williams et al. 2018). In *Nematostella*, a single TLR is known and its function was verified as a receptor involved in immunity via NF-kB signal transduction, in pathogen detection, and in development (Brennan et al. 2017). This one TLR gene could also be found in the transcriptome data as a regulated gene upon recolonization with the adult microbiome in comparison to the gnotobiotic control.

Another mechanism of interaction between a host and its microbiome is the production of AMPs by the host. AMPs are often expressed on epithelial surfaces in order to enhance the functionality of the barrier function of epithelia (Zasloff 2002). They can either be constitutively expressed or are effector proteins of e.g. the TLR pathway (Cunliffe and Mahida 2004). They do not only play a role in the defence against pathogens but are also important for the maintenance of the species-specific microbiome (Bosch 2012; Franzenburg et al. 2013). Several *Hydra* species not only show a species-specific bacterial

colonization but also a species-specific expression of AMPs stemming from the arminin family. It was shown that arminins are involved in the selection of the species-specific microbiome (Franzenburg et al. 2013).

Another possibility for direct host-microbe interaction lies in the modification of quorum sensing (QS). Classically, quorum sensing is used as a mean of communication within bacterial species to regulate processes like e.g. virulence, competence motility and biofilm formation by sensing cell population density (Miller and Bassler 2003). However, QS can also be used as a mean of interspecies and even interkingdom communication (Wu and Luo 2021). Especially in the context of the gut, bacteria can use QS signals to induce host cell apoptosis or to regulate immune mediator secretion. However, the communication can also work the other way around, with the host producing QS signals itself, or by interfering with the bacteria-bacteria communication by modifying QS signals (Wu and Luo 2021). In *Hydra* it is shown that Hydra modifies 3-oxo-homoserine lactones via an oxidoreductase, influencing the gene expression of its main bacterial colonizer *Curvibacter* sp. and its colonization efficiency (Pietschke et al. 2017).

The transcriptomic response of the host towards the bacterial recolonization was observed two days post recolonization. Besides a specific response of each inoculum of the three different developmental stages, the host also exhibited a strong common response upon recolonization. As the recolonization of a neutral surface does not result in an assimilation of the three inocula, this underlines the importance of the direct transcriptomic effect of the host during early recolonization. One explanation for this initial reset of the three inocula during early recolonization could be a host-driven restructuring towards a “foundation guild”, which is necessary to create the adult-specific microbiome. A guild in macro-ecology is a functional group, which members exhibit similar functions within a community tend to show co-abundance patterns, but the term was already applied to microbial communities as well (Wu et al. 2021). In this recolonization experiment, this initial guild could be selected by the host through the upregulation of chitin-related genes, so that it can modify the habitat through chitin degradation to open the habitat for subsequent and adult-specific bacteria.

3.3.2 Indirect host mechanisms that shape early recolonization

The dynamics during early recolonization cannot exclusively be explained by direct host-microbe interactions. This is indicated by the mono-association experiments, which show a higher success of colonization for early-appearing bacteria than late-appearing bacteria, although late-appearing bacteria are more abundant in adult polyps and therefore should be specialized in colonizing adult polyps. As *Nematostella* probably does not actively select against adult-specific bacteria during early recolonization, another indirect host-microbe mechanism seems likely. Indirect host-microbe interactions can be very diverse and therefore hard to identify.

Firstly, the interaction can be in the form that the bacteria are selecting their habitat by selecting for the substrate provided by the host. In a study with marine bacteria and chitin beads it was shown that bacterial communities undergo rapid successions when colonizing chitin beads (Datta et al. 2016). They divide the colonization process into three phases, each phase is characterized by specific taxa and a specific capability. The first phase is characterized by taxa being able to attach to chitin, the second phase by taxa that are able to metabolize chitin and by a rapid dispersal ability, and the third phase is characterized by an inability to metabolize chitin but an ability to metabolize other carbon sources most likely provided by the taxa from the second phase. So here the bacterial colonization and succession is not driven by a direct interaction but by the energy sources, e.g. carbon-rich products like chitin, which the host provides. As *Nematostella* also shows an upregulation of a chitin synthase during early recolonization and is shown to actually produce chitin, this might be a host-microbe interaction that shapes the microbial succession during early recolonization.

Related to this indirect interaction of providing a certain energy source, metabolic interactions can also be a form of indirect interaction as here the interaction is mediated by a metabolic substrate instead of being a directed interaction triggered by the presence or absence of one of the interaction partners. One famous example of a metabolic interaction between a host and a microbe is the aphid-*Buchnera* symbiotic relationship. In this system, the plant sap-feeding lifestyle of aphids leaves them deficient of essential amino-acids, resulting in retarded growth and sterility. They compensate this deficiency through maintaining an endosymbiotic relationship with *Buchnera sp*., which they provide with non-essential amino acids. In return, *Buchnera* is providing essential amino acids and

other nutrients to the aphid (Buchner 1965; Douglas 1998). Similarly to this metabolic interaction in insect symbiosis, the gut microbiome is tightly regulated by exhibiting a certain metabolic microenvironment within the gut, characterized by a pH gradient, varying speed of the lumenal flow, production if immunoglobulin A and antimicrobial compounds, and targeted provision of certain nutrients (Walter and Ley 2011). So is the bacterial colonization and microbiome structure in the gut controlled by e.g. the provision of glycans or the limitation of nutrients and of electron acceptors to force anaerobic fermentation (Koropatkin, Cameron, and Martens 2012; Reese et al. 2018; Winter, Lopez, and Bäumler 2013). Glycans can either be taken up by the host or can stem from host mucosal secretions, which can be fermented by the microbiome to short chain fatty acids (SCFAs) (Koropatkin et al. 2012). These SCFAs play an important role in maintaining colonic T_{reg} cell homeostasis and therefore inhibiting intestinal inflammation and maintaining gut homeostasis (Litvak, Byndloss, and Bäumler 2018; Smith et al. 2013).

One promising candidate for a metabolic substrate in the metaorganism *Nematostella* could be represented by chitin. Complex carbohydrates are shown in microbial systems to be the primary energy source which drives a subsequent community restructuring by creating a specific metabolic microenvironment. In this publication of Chng et al., they show an enrichment of metabolic pathways during microbiome recovery belonging to carbohydrate degradation and energy metabolism, conforming to the findings of the metabolic pathway analysis for the recolonization on *Nematostella* (**Figure 2-18**) (Chng et al. 2020). In *Nematostella*'s case, chitin could function as primary carbohydrate source, as chitin degradation pathways are enriched and the gene of one chitin synthase of *Nematostella* is upregulated (**Figure 2-20**; **Figure 2-21**). Chitin could be the driving force of a metabolic cascade that determines a succession of bacteria specialized in the degradation of chitin metabolites as it is shown with marine bacteria and chitin beads (Datta et al. 2016).

Nutrient limitation likewise is an important mechanism to maintain gut homeostasis as nutrient limitations can define ecological niches which can just be occupied by specialists, promoting competition (Pereira and Berry 2017). It is e.g. shown that mammalian hosts limit dietary nitrogen within their guts by absorption before it can be utilized by the bacteria, and that the limitation of dietary nitrogen for microbes is even beneficial for the host (Holmes et al. 2017; Reese et al. 2018). For microbes, in order to coexist, it is also

important how they are spatially distributed, as with spatial distance, they can avoid direct competition like substrate competition or direct harm reduction (Deines, Hammerschmidt, and Bosch 2020b). Another important factor are rare microbes which are hypothesized to be important for the more abundant microbiome members to realize their specific niche (Deines, Hammerschmidt, and Bosch 2020a).

The recolonization dynamics therefore could also represent a process in which the microbial members find and occupy their specific niches, while avoiding or promoting other members of the community. This happens without a direct influence of the host on the microbiome, but indirectly by providing a habitat on which the microbes can settle. The mono-association results also hint towards a mechanism, in which certain bacteria can't settle unless they are promoted by other bacteria as adult-specific bacteria can't readily settle on the adult polyp (**Figure 2-17**). However, there seem to be no priority effects in *Nematostella* like e.g. in human birth (Sprockett, Fukami, and Relman 2018). Priority effects come into play when the order of arrival of species influences the following colonization patterns (Drake 1991). In humans, the delivery of a baby via C-section instead of vaginally disrupts the transmission of maternal bacterial strains and promotes the colonization of opportunistic pathogens (Shao et al. 2019). In *Nematostella* however, the composition of the bacterial inoculum is not the crucial factor for the bacterial succession. Instead, the bacterial inoculum is reshaped into a larval-specific microbiome during early recolonization, before it is reshaped into an adult-specific microbiome during late recolonization, independent of the developmental stage from which the inoculum was isolated. This indicates that the order of arrival of bacterial species is not important but that specific bacteria from the inocula are selected like e.g. the provision of chitin by the host.

3.4 The bacterial succession during late recolonization is influenced by bacteria-bacteria interactions

While the early recolonization seems to be defined by mainly direct and indirect host-microbe interactions, the late recolonization seems to be orchestrated by bacteria-bacteria interactions. I come to this conclusion because the recolonization experiments with the silicone tubes which were recolonized three developmental stage-specific

bacterial communities showed that each bacterial community underwent a distinct recolonization pattern (**Figure 2-13**). However, in the recolonization experiments with adult polyps, all three communities underwent the same recolonization pattern with an initial "reset" and then the recapitulation of the ontogenetic colonization pattern (**Figure 2-8**). This initial "resetting" step seems to be controlled by the host, but the subsequent recolonization is controlled by bacteria-bacteria interactions.

Mortzfeld et al. stated that the bacterial colonization of *Nematostella* is dependent on its developmental age (Mortzfeld et al. 2016). However, as in my recolonization experiments the bacterial communities still underwent this ontogenetic pattern without the developmental background and in a much faster time scale (1 month in the recolonization experiment versus 6 months during development), the conclusions Mortzfeld et al. drew from their observations seem to be false. The colonization pattern during the development of *Nematostella* is not caused by the ontogeny but is only correlative.

During recolonization on adult polyps, the bacterial communities shift from a larval to a juvenile community identity, before it approaches the adult community without actually reaching it (**Figure 2-8**). This could be due to the limited time of the experiment of one month or because of the loss of single bacterial strains as indicated in the alpha-diversity measure (**Figure 2-10**). However, looking at the wildtype controls which were sampled in the same time frame, it shows that the beta-diversity of the wildtype controls also varies over time and cluster closely to the 28 day post-recolonization time point of the recolonized samples (**Figure 2-12**). As the experiments were conducted without feeding, this might pose a starvation effect. As the recolonized samples and the wildtype controls seem to linger or approach the bacterial community composition of the juvenile inoculum, it can be hypothesized that the starvation triggers a "rejuvenation" of the microbiome. In a study comparing the microbiome of undernourished children and the microbiome of fed children, it was shown that malnutrition (here, undernutrition) of children is correlated with an immature microbiome compared with their nourished counterparts (Subramanian et al. 2014). The immature microbiome in turn causes growth impairments which can be rescued via transplantation of the microbiome of healthy children (Blanton et al. 2016; Roswall et al. 2021). In the context of *Nematostella*, this could mean that the starvation period of one month during the experiment, the undernutrition leads to an "immature" or juvenile microbial identity.

In transplantation experiments in mice, the microbiome could be rejuvenated on beta-diversity level. The transplanted microbiome could be sourced either from a young or an old microbiome and could be transplanted by fecal microbiome transplantation into old mice and resulted in both cases not only in a rejuvenation of the microbiome, but also in the rejuvenation of cognitive brain functions (Boehme et al. 2021). Concluding from this it is logical to assume that in *Nematostella*, also when recolonizing with an adult-like microbiome, the microbiome appears rejuvenated.

Recently the neutral theory was applied on metaorganisms, competing with the assumption that the metaorganism is an actively shaped symbiotic unit (Sieber et al. 2019). Instead, the neutral theory assumes that a community can just form or develop through a continuous cycle of immigration, births and deaths, disregarding differences between species and their response to their environment (Sloan et al. 2006). Applying the neutral theory on *Nematostella* reveals that the colonization of *Nematostella* deviates from full neutrality, but showing a trend towards a higher fit to a neutral model during later life, although statistically this is not significant (Sieber et al. 2019). This indicates a mechanism forming the later recolonization that goes beyond simple stochastic processes like dispersal predicted by the neutral model. This fits my results, in which I show that the bacterial recolonization is not a stochastic process as the recolonization of silicone tubes is distinct from the recolonization of adult polyps. During the recolonization of adult polyps, non-neutral processes like host-bacteria interactions and bacteria-bacteria interactions shape the succession of the bacterial community.

Although there are no studies to my knowledge where developing wildtype groups are compared to germfree-but-recolonized counterparts, there are several longitudinal studies showing the impact of disturbances during early or later life and how these disturbances can influence the host (Laforest-Lapointe and Arrieta 2017). One study shows that after disturbances like antibiotic admission, recolonization with a pair of keystone species can facilitate the successful recovery of microbial abundance, microbial diversity and reconstruction of the pre-antibiotic microbiome (Chng et al. 2020). Although for *Nematostella*, I removed the microbiome instead of disturbing it, and recolonized with complex microbiomes instead of with single bacterial isolates, this study can give insight in the mechanisms behind the recolonization dynamics and the role of synergistic effects within the microbiome.

3.4.1 Chitin as a driving force of recolonization

As one of the most upregulated genes upon recolonization is a chitin synthase, this gene poses a promising candidate for a mechanism which influences recolonization by providing a substrate which can be utilized by early colonizers, and which metabolic degradation products are essential for the establishment and maintenance of an adult-specific microbiome.

Chitin is long known as an important substance in the marine context as an important source of carbon and nitrogen (Souza et al. 2011). Generally, nutrients in aquatic systems are often aggregated in form of particulate organic matter (POM), which with a particle size of >500 µm are also called marine snow (Simon et al. 2002). POM on the one hand ensures cycling of nutrients from the water surface to the floor, but are also the place for the formation of microenvironments (Simon et al. 1990). Marine snow creates a microenvironment especially for microbes, which form complex communities on its surface undergoing distinct population dynamics (Thiele et al. 2015). As marine sediments only contain traces of chitin, it must be that chitin in marine snow is metabolized before the snow can reach the ocean floor (Souza et al. 2011). It was shown that especially *Vibrio* strains possess a complex machinery to sense and adhere to chitin oligosaccharides, which not only influences the degradation of chitin but also induces natural competence in *Vibrio* (Bassler, Gibbons, and Roseman 1989; Meibom et al. 2005; Meiborn et al. 2004). Chitin or chitin oligomers therefore can be seen as colonization signal for *Vibrio* strains, which is a mechanism that can also be utilized by eukaryotic organisms. For example, the squid *Euprymna scolopes* uses chitobiose as a colonization signal to attract *Vibrio fischeri* to utilize the *Vibrio*-produced bioluminescence for camouflage, forming a close symbiosis.

Besides playing a role as a colonization signal, chitin is also a driver of bacterial communities, and that not only in the marine context. Chitin acts as modulator of the gut microbiome as well, where it promotes the growth of specific bacteria and improves metabolic syndrome in high-fat-diet-fed mice and by reversing dysbiosis by improving a disturbed glucose metabolism (Zheng, Cheng, et al. 2018; Zheng, Yuan, et al. 2018). Chitin also acts as a modulator of the immune responses and the physiological gut architecture by promoting beneficial bacterial communities (Udayangani et al. 2017). Chitin therefore

is also an important driver of the microbial community within a metaorganism. When looking into the chitinolytic potential of host-associated communities, it is shown that the general chitinolytic community structure is surprisingly diverse, indicating a versatile chitin degradation potential (Raimundo et al. 2021). This study also shows an indication of chitin cross-feeding in the host-associated microbiomes, in which some bacteria like *Vibrio* and *Aquimarina* catabolize the polymer while other bacteria like *Alphaproteobacteria* species feed on the hydrolysis products (Raimundo et al. 2021). That cross-feeding on chitin is a possibility for microbial communities is also shown with marine bacteria and chitin beads (Datta et al. 2016). Here, the cross-feeding involves a specific bacterial succession which is characterized by the chitinolytic potential. In my experiments, I could verify the ability of some native bacterial strains of *Nematostella* to degrade complex chitin, laying the basis for the possibility of cross-feeding on chitin (**Figure 2-20**, **Table 2-4**). As I could not verify chitin degradation for every bacterium predicted in the metabolic potential calculations, it should be noted that I just tested their degradation capability of deacylated shrimp chitin but not other chitin degradation products. Also pH and presence or absence of specific ions could influence the chitin degradation capability of the bacterial strains. Therefore, I can't deny the chitin degradation potential of the predicted bacteria, they just can't degrade chitin under the given circumstances.

Upon recolonization of *Nematostella*, one of the most upregulated genes is a gene for a chitin synthase. Calculating the metabolic potential of the microbiome of *Nematostella* during recolonization, early recolonization is characterized by chitin degradation. Therefore, it stands to reason that chitin is a driver of early recolonization in *Nematostella*, causing cross-feeding events and an accompanying succession in the microbiome, before a balance between production and degradation is achieved in form the adult-specific microbiome. Chitin is mainly expressed in the spirocysts of *Nematostella*, which are mainly located in the tentacles (Zenkert et al. 2011). Therefore, they probably are used for capturing prey by wrapping around it. However, one other study could localize three chitin synthase genes in *Nematostella*, which are differentially expressed during development and within the body, one of which is mostly expressed in spirocysts (Vandepas 2018). However, chitin seemed to be present all along the body column both in ecto- and endodermal tissue, providing a perfect basis for the colonization by chitin-degrading bacteria and forming niches for cross-feeding and co-habitating bacteria.

4 Conclusion

To conclude, I identified several potential mechanisms which are influencing the bacterial community assembly and succession during recolonization. Generally, there seem to be two successional driving forces. Early recolonization is mainly driven by host-bacteria interactions, while late recolonization is dominated by bacteria-bacteria interactions (**Figure 4-1**).

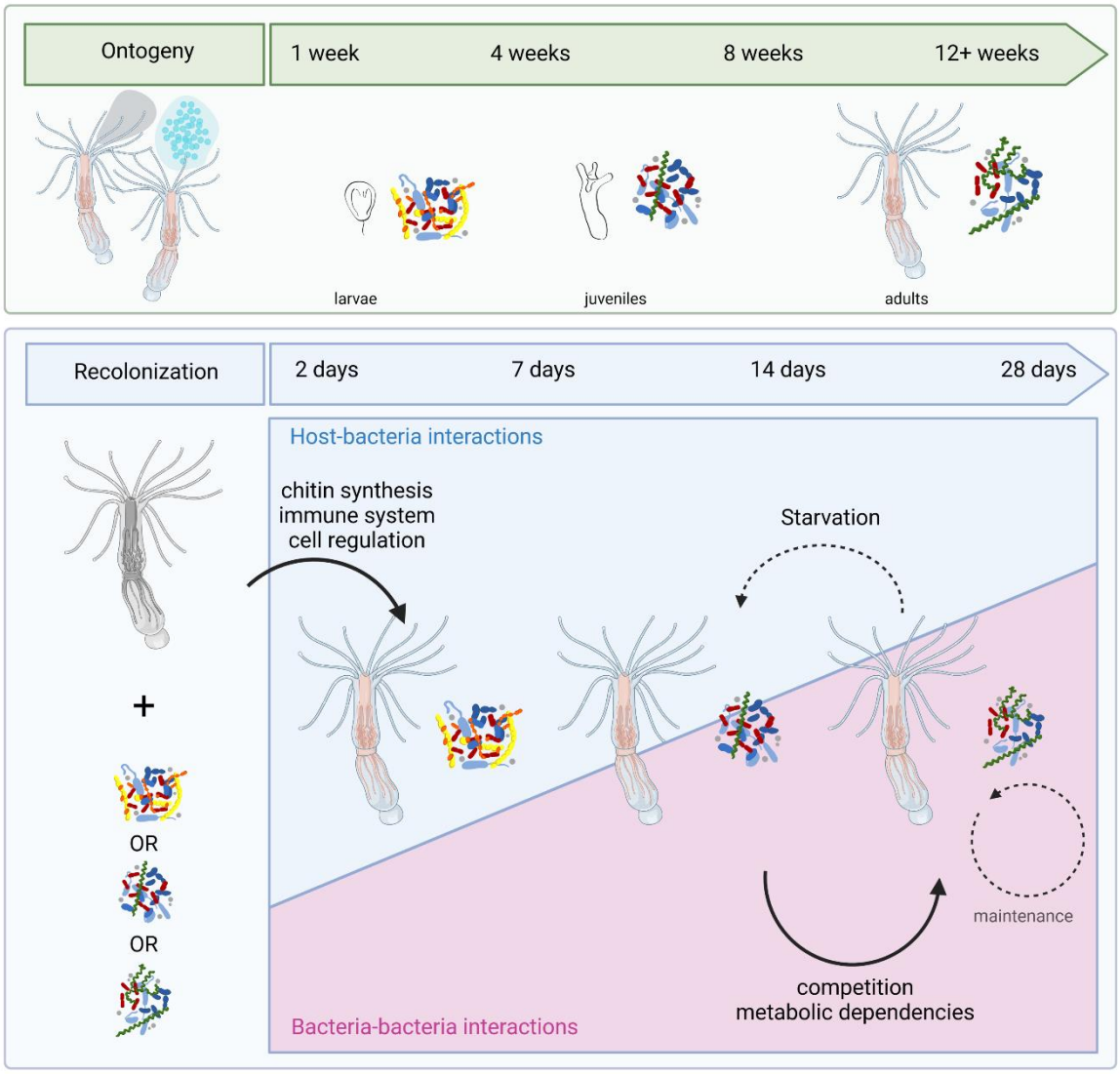

Figure 4-1 *Comparison of the bacterial succession during ontogeny and during recolonization. Larvae possess a microbiome which is distinct from its parents. Over the next few weeks, it develops into a juvenile polyp, which is accompanied by a succession of the microbiome. Upon reaching adulthood, the microbiome changes into an adult-specific form which is maintained through life if no disturbances occur. Upon recolonization of an adult polyp that was stripped of its microbiome with the three development-specific bacterial communities, all three communities get reshaped into a larval-like community (2 dpr). These changes are mediated by host-bacteria interactions like the provision of chitin by the host, the host's immune system and its cell cycle. Subsequently, the larval-like microbiome changes into a juvenile-like microbiome before it approaches the adult-like microbiome (28 dpr). During later recolonization, bacteria-bacteria interactions replace host-bacteria interactions as the driving force of the succession. Especially metabolic dependencies within the bacterial community and competition drive the succession towards an adult community and its maintenance. Starvation is a host-dependent mechanism which can rejuvenate the adult microbiome. Image created in BioRender.*

In order to come to this conclusion, I identified bacteria involved in positive, neutral, or negative bacteria-bacteria interactions within the community and tested their ability to influence the whole bacterial community. Surprisingly, the competitive bacteria were able to shortly elevate the alpha-diversity, but the community proved resilient enough to counteract this short-term effect. I also tracked the recolonization pattern of gnotobiotic polyps with the bacterial communities of three different developmental stages of *Nematostella.* Additionally, I measured the host's transcriptomic response to the recolonization and calculated the metabolic potential during recolonization. The bacterial succession during recolonization was very similar for all three communities of the three developmental stages. During early recolonization all three communities resembled a larval-specific microbiome. The community quickly shifted towards a juvenile-specific microbiome before it approached an adult-like community again. The shift towards an adult-like community during late recolonization underlines again the resilience of the community against changes, even if the source community had a drastically different composition than the adult microbiome. As soon as the resilient state of the adult microbiome is reached, also starvation can only minorly influence the microbiome by shifting it towards a juvenile-like community.

Recolonization of silicone tubes and polyps with the three development-specific communities show different succession patterns. On silicone tubes the three distinct bacterial communities stayed separated and did not approach a similar state, while the early recolonization polyps showed an approximating of the three different communities to the larval-like state. This points towards a host-controlled response controlling the initial colonizers. This point is underlines by looking at the transcriptomic response during early recolonization: The host shows a strong common response to all three bacterial communities involving the immune system and cell cycle control. Additionally, it shows the strongest response to its own native microbiome. This is also the developmental stage microbiome, which is restructured the most during recolonization in order to resemble the larval-like community. Therefore, I hypothesized that the host actively controls this initial step of selecting the bacterial species which act as foundation species. The subsequent restructuring into an adult-like microbiome however is controlled by the microbiome via e.g. metabolic dependencies. This hypothesis is supported by the mono-association

experiments and the metabolic potential calculations. The mono-associations show that bacteria specific for the adult developmental stage can't recolonize adult polyps as efficiently as early-appearing bacteria, although they are most abundant in adults. The metabolic potential calculations showed a variety and a succession of metabolic dependencies during recolonization, being a promising candidate for the explanation of this curious recolonization pattern of adult-specific bacteria on adult polyps. With a chitin synthase being upregulated in the host and chitin degradation being enriched in the microbiome during early recolonization, chitin makes a promising candidate for the community succession. Host-produced chitin could pose as a substrate for early-appearing bacteria, while chitin degradation products could act as substrate for late-appearing bacteria.

Summing up, chitin is a well-known molecule involved in immune barrier function and in bacterial signalling, and therefore, it is a promising candidate to research bacterial interactions (Nakashima et al. 2018; Raimundo et al. 2021). Further analyses will reveal the exact role and precise localization of chitin in *Nematostella*, as well as its role and of its metabolites as a host-controlled mechanism in (re)colonization.

Additionally, as microbiomes are very complex to analyse, minimal microbiomes are a promising reductionist tool to understand bacterial interactions in a microbiome (Clavel, Lagkouvardos, and Stecher 2017; Shetty et al. 2022). Recolonization with bacterial pairs in di-association and with a minimal microbiome will further clarify bacteria-bacteria interactions and their implications in bacterial assembly.

5 Material

5.1 Organisms

Investigated organism	*Nematostella vectensis*
Prey organism	*Artemia salina*
Electro-competent bacteria	*E.coli*
Nematostella-associated bacteria	A-MB-5, A-LB-1, P-R2A-1, A-LB-4, JB_053_A2-LB-5, NA_68, NJ_1, NP_16, NP_22, NA_11, NA_74, NA_15, NA_29, NJ_43, NP_26

5.2 Chemicals

Acetic Acid	Roth
Agar-Agar	Roth
Agarose	Roth
Ammonium chloride (NH_4Cl)	Roth
Ampicillin	Sigma, Roth
Beta-Mercaptoethanol	Roth
Bovine Serum Albumine (BSA)	Roth
Chitin	Roth
Crystal Violet	Sigma
Dimethylsolfoxid (DMSO)	Roth, VWR
Disodium phosphate (Na_2HPO_4)	Roth
DNA Loading Dye (6x)	Promega
dNTPs (10mM)	Thermo Fisher Scientific
EDTA	Sigma
Ethanol	Roth
Glucose	Merck
Glycerol	Roth
HCl (37%)	Merck
Hoechst	Thermo Fisher Scientific
Isopropanol	Roth
L-Cysteine	Roth
Magnesium chloride (MgCl2)	Merck
Magnesium sulfate (MgSO4)	Merck
Marine bouillon	Roth
Monopotassium phosphate (KH_2PO_4)	Roth
Mowiol	Roth
Neomycin sulfate	Roth
Paraformaldehyde	Roth
Potassium chloride (KCl)	Chemsolute
R2A Agar	Roth
R2A Broth	Neogen
Rifampicin	Roth, Duchefa
Sea salt (Red Sea Salt)	Red Sea

Sodium chloride (NaCl)	Roth
Sodium hydroxide (NaOH)	AppliChem
Spectinomycin	Roth, TCI
Streptomycin sulfate	Roth, J+K
Tris base	Roth
Tris HCl	Roth
Triton X-100	
Tryptone	Roth
Yeast extract	Roth

5.3 Media and buffers

Artemia Medium	31.8 g sea salt. ad 1 L Millipore H_2O
LB Medium	10 g NaCl, 10 g tryptone, 5 g yeast extract, ad 1 L Millipore H_2O
LB plates	1 L LB Medium, 15 g Agar Agar
MB Medium	40.1 g Marine bouillon, ad 1 L Millipore H_2O
MB Plates	1 L Marine bouillon Medium, 15 g Agar-Agar
mPBS buffer	26.3 g NaCl, 0,2 g KCL, 1,42 g Na_2HPO_4, 0,27 g KH_2PO_4, ad 1 L Millipore H_2O [pH 7.4]
Nematostella Medium	18.4 g sea salt, ad 1 L Millipore H_2O
R2A Medium	3.1 g R2A Broth, ad 1 L Millipore H_2O
R2A plates	18.1 g R2A Agar, ad 1 L Millipore H_2O
TAE Buffer (50x)	242 g Tris base, 57.1 mL acetic acid, 100 mL 0.5 M EDTA, ad. 1 L Millipore H2O [pH 8.0]

5.4 Kits

DNeasy Blood & Tissue Kit	Qiagen
Qubit RNA BR Assay Kit	Thermo Fisher Scientific
RNeasy Plant Kit	Qiagen

5.5 Enzymes

DNase	Qiagen
GoTaq® DNA Polymerase	Promega
Proteinase K	Qiagen
Phusion® Hot Start II DNA Polymerase	Thermo Scientific

5.6 DNA size ladders

GeneRuler™ DNA Ladder Mix	Thermo Scientific

5.7 Oligonucleotides

Name	Sequence (5’ -> 3’)	T_m [°C]
1492R	GGHTACCTTGTTACGACTT	53.1
Nv_EF1a_942_F	GTAGGCCGTGTTGAGACTG	58.8
Nv_EF1a_1222_R	CACGCTTGATATCCTTCACAG	58.8
27F	AGAGTTTGATCCTGGCTCAG	57.3
338R	TGCTGCCTCCCGTAGGAGT	61.0

5.8 Devices

5.8.1 Centrifuges

Centrifuge 5415 D	Eppendorf
Centrifuge 5417 R	Eppendorf
Centrifuge 5420	Eppendorf
Centrifuge 5425 R	Eppendorf
Z 366 K	Hermle
Mini Spin	Eppendorf
Multifuge 3 S-R	Heraeus Instruments
Multi-Spin MSC-6000	Kisker Biotech

5.8.2 Fluorometer

NanoDrop® ND-1000	Thermo Scientific
Implen NP90	Implen

5.8.3 Gel electrophoresis chambers

Separation system B1A	Owl Separation Systems
Separation system B2	Owl Separation Systems
Separation system D3	peqLab

5.8.4 Incubators/shakers

Certomat Incubator	B. Braun
HIS25 (Mini Shaking Incubator)	Grant Boekel
KS10 (Rotation Shaker)	Edmund Bühler
New Brunswick Innova 42	Eppendorf
REAX 2000 (Vortex Shaker)	Heidolph
Thermomixer compact	Eppendorf
ThermoStat plus	Eppendorf

5.8.5 Microscopy

MS 5 Binocular	Leica
SZX 16 Binocular	Olympus
Fluoview FV3000	Olympus

5.8.6 PCR thermocyclers

peqStar 2x	peqLab
Primus 25	MWG-Biotech
Primus 96 advanced	peqLab
Primus plus	MWG-Biotech
QuantStudio 3	Applied Biosystems
Real-Time Cycler 7300	Applied Biosystems
SimpliAmp	Applied Biosystems

5.8.7 UV and blue/green LED devices

FAS-Digi PRO	Nippon
Gel-Doc™ XR+	Bio-Rad
UV-table Chroma 43	Vetter GmbH
UV-Stratalinker® 1800	Stratagene

5.8.8 Other devices

1205 MP Weighing scale	Sartorius
Accumet AE150	Fisher Scientific
ECD01E (Climate Chamber)	Snijders Scientific
Electrophoresis Power Supply Consort EL 231	peqLab
Kern 770 Weighing scale	Kern
LaminAir® HB 2448 Clean bench	Heraeus instruments
Microplate reader Tecan 10M	Tecan
Milli-Q Academic System	Millipore
MSC-Advantage	Thermo Fisher
Omni THQ Homogenizer	Omni International
PCB Weighing Scale	Kern
pH 211 pH-Meter	Hanna Instruments
Qubit Fluoremeter	Thermo Fisher Scientific
SBA 33 Weighing Scale	Scaltec
Scanlaf Mars	Labogene

5.9 URLs

BioRender	https://biorender.com/
Compagen	http://www.compagen.org/
DOE Joint Genome Institute	http://www.jgi.doe.gov/
Marine Biological Association	https://www.marlin.ac.uk/species/detail/1136
NCBI	http://www.ncbi.nlm.nih.gov/
SMART	http://smart.embl-heidelberg.de/
UniProt	http://www.uniprot.org/

5.10 Software

BioEdit 7.2.5

DNAMAN 4.15

FigTree 1.4.4

ImageJ 1.52

Inkscape 0.92

Oracle VM Virtual Box 6.0

R 3.5

R 4

QIIME 1.9

QIIME 2

QuantStudio Design & Analysis Software v1.5.1

6 Methods

6.1 Cultivation

6.1.1 Cultivation of *Nematostella*

All cultures were F1 offspring of the laboratory culture of CH2XCH6 individuals collected from the Rhode River in Maryland, USA (Hand and Uhlinger 1992; Miller et al. 2007). All cultures were kept under constant, artificial conditions in absence of substrate and light at 18°C. The cultures were kept in artificial sea water with a salinity of 16 ‰ created with Red Sea Salt® and Millipore water or distilled water. Animals were fed at least twice a week with freshly hatched Artemia salina nauplii larvae and washed once a week to remove biofilm and accumulated waste.

To create offspring, male and female cultures were kept in separated culture dishes and induced with a shift of temperature to 25°C and exposure to light for 10 hours. Freshly spawned eggs were fertilized with freshly spawned sperm. If necessary, egg packages were dissolved with a 4% L-cysteine solution (pH 7.4) in NM for 20 minutes on an orbital shaker. The dejellied eggs were washed several times with fresh NM to remove any residual L-cysteine. Development of eggs occurred at 18°C. Primary polyps were fed with homogenized *Artemia salina* nauplii larvae until they were big enough to feed on whole Artemia larvae (after around 5 weeks of development). If fed with homogenized *Artemia* larvae, cultures were washed the next day to avoid rotting events.

6.1.2 Cultivation of *Nematostella*-associated bacteria

Bacteria were isolated from different developmental life stages of *Nematostella* by homogenizing the polyps or larvae and spreading them on agar plates prepared with LB-medium, MB-medium, R2A-medium or counting agar. After incubation at 4°C, 18°C or 37°C, bacteria were picked, sequenced and a cryostock or glycerol stock (25%) was prepared. Bacteria were spread on the respective plates to revitalize them and single colonies were used for liquid cultures. Bacteria were always tested for their ability to grow on MB before experiments. If not stated otherwise, all bacteria used in this thesis were grown on MB at 18°C for experiments. OTU1325 (*Aeromonas* sp.) and OTU941 (*Pseudomonas* sp.) were grown in LB medium, and OTU670 (*Acinetobacter* sp.) in R2A medium.

6.2 Standard laboratory methods

6.2.1 Polymerase Chain Reaction

With a Polymerase Chain Reaction (PCR), specific DNA fragments can be amplified with sequence-specific primers and subsequently visualized with an agarose gel or sequenced with e.g. Sanger Sequencing.

PCR was used as sterility check after antibiotic treatment of *Nematostella* polyps. For that, gDNA was extracted (see Chapter 6.2.5 and 756.2.6) and used as template for a PCR with the 16S rRNA-specific primers 27F/338R. Following PCR program was used:

Table 6-1 *Program for a PCR sterility check after antibiotic treatment.*

Step	Temperature [°C]	Time [min]
Initial denaturation	95	3
Amplification (30x)		
Denaturation	95	0.5
Annealing	55	0.5
Elongation	72	0.5
Final elongation	72	5

If bacterial identity should be confirmed, gDNA was extracted from pure bacteria cultures and a PCR with the 16S rRNA-specific primers 27F/1492R was performed with the same program as in **Table 6-1** but with an elongation time of 1.5 minutes and with 35 amplification cycles.

PCR was also used as colony check after ligation and transformation (see Chapter **Error! R eference source not found.** and **Error! Reference source not found.**). For this kind of PCR, the success of the ligation is assessed by checking the correct size of the bands of the desired insert. For this PCR, the plasmid-specific primers (for pGEM™-T they are called Sp6/T7) are used and following protocol is run:

Table 6-2 *Program for a PCR colony check after ligation and transformation. Elongation time depends on the expected size of the insert. For the Taq polymerase, elongation is calculated with 1 min/1kbp.*

Step	Temperature [°C]	Time [min]
Initial denaturation	95	3
Amplification (35x)		
Denaturation	95	0.5
Annealing	55	0.5
Elongation	72	depends
Final elongation	72	5

The elongation time depends on the expected size of the insert. If the Taq polymerase is used, elongation time is calculated with one minute for every 1000 base pairs (bp).

6.2.2 Quantitative Real Time PCR (qRT PCR)

With a quantitative Real Time PCR (qRT PCR) the expression of genes can be relatively quantified. This is achieved by measuring the fluorescence intensity of a fluorescent dye that intercalates into double-stranded DNA. The fluorescence intensity increases with the amount of PCR product. Here, qRT PCR was used to check the proportion of bacterial DNA to *Nematostella* DNA during recolonization. The gene targeted for bacterial DNA was the 16S rRNA gene, while the gene targeted for *Nematostella* DNA was elongation factor 1alpha (EF1alpha). The expression level was calculated with the comparative ΔΔCT method (Schefe et al. n.d.). For qRT-PCR, the GoTaq qPCR Master Mix (Promega) in MicroAmp® 0.2 mL optical strips (Applied Biosystems) and a QuantStudio 3 qPCR system (Applied Biosystems) was used according to the manufacturer's protocol with the following running protocol:

Table 6-3 Program for a qRT-PCR targeting EF1a of Nematostella and the V1/V2 region of bacteria. Data was collected during the third step pf stage 2.

Stage	Temperature [°C]	Time
1	95	2 min
2 (40x)	95	15 sec
	95	30 sec
	60	30 sec
3	95	15 sec
	60	30 sec
	95	15 sec

6.2.3 Agarose gel electrophoresis

In order to separate DNA or RNA bands after e.g. PCR, an agarose gel electrophoresis was conducted. For this, agarose in a concentration of 1% was prepared in TAE buffer by boiling it until dissolved. Dying of bands was done by either adding peqGreen or Midori Xtra into the agarose solution before casting the gel. Bands were visualized with either UV light or by a blue/green LED Transilluminator (Nippon). To estimate size, the marker GeneRuler™ DNA Ladder Mix (Thermo Fisher) was applied on the gel together with the samples.

6.2.4 Total RNA extraction

Total RNA was extracted from whole adult polyps with the RNeasy Plant Mini Kit (Qiagen). For this, whole animals were sampled and immediately frozen in liquid nitrogen. Animals were either stored at -80°C until RNA isolation or directly processed. For this, frozen animals were transferred into a mortar on ice filled with a few mL of liquid nitrogen. With a precooled pestle, animals were pulverized. The pulverized animal was transferred into a 15 mL falcon with perforated lid to allow evaporation of liquid nitrogen. As soon as all nitrogen was evaporated but the pulverized animal was not thawed, 450 µL buffer RLT with 5 µL beta-mercaptoethanol was added to the falcon. Afterwards, the lysated tissue was added to the QIAshredder spin column and further extraction occurred according to the manufacturer's protocol with an on-column DNase digest with DNase I from Qiagen. RNA was eluted into 30 µL RNase-free water, reapplied to the column and eluted once more. RNA concentration was measured with a Nanodrop ND-1000. RNA was stored at -80°C until further processing.

6.2.5 gDNA extraction

Genomic DNA (gDNA) was isolated from whole larvae, polyps or from bacterial cultures for checking the sterility, 16S rRNA sequencing or Sanger sequencing. For this, whole polyps were homogenized with an immersion blender and centrifuged at 4°C and 20.000 xg for 20 minutes. The supernatant was discarded and the pellet either directly processed or stored at -20°C until extraction. Larvae or bacterial pellets don't need homogenization before freezing or extraction. Extraction occurred with the DNeasy Blood & Tissue Kit

(Qiagen) according to the manufacturer's protocol for extraction from animal tissue. gDNA was eluted in 50 µL buffer AE and frozen at -20°C until use.

6.2.6 Setup for sterile *Nematostella*

In order to obtain sterile adult *Nematostella* polyps, the protocol for sterile *Hydra* polyps was adapted (Franzenburg et al. 2012). Polyps were incubated in a cocktail of five different antibiotics in NM for two or four weeks before they were let to recover in sterile medium for three days. The cocktail of antibiotics consists of ampicillin, neomycin, spectinomycin, streptomycin and rifampicin in a final concentration of 50 µg/mL each. Animals were either pooled in a 50 mL volume at 10-12 animals each for antibiotic treatment, or pooled in a 12-well plate with 4 mL volume with 2 animals each. The antibiotic medium was exchanged either every two days (50 mL volume) or every day (12-well plate). The vessel was exchanged every second day. Animals were starved during antibiotic treatment. After two weeks of treatment, animals were checked for their sterility. For this, at least one polyp per vessel was homogenized and half of the animal was spread on MB plates to control for bacterial growth, while gDNA was extracted from the other half (see Chapter 6.2.5). The extracted gDNA was used as template for a PCR with the 16S rRNA primers 27F/338 to check for an amplicon for bacterial DNA (see Chapter 6.2.1). Before animals were used for experiments, they were incubated in sterile, antibiotic-free NM for 3-4 days to flush out residual antibiotics in the body column.

6.2.7 Recolonization of juvenile polyps with complex microbiome complemented with single strains

The bacterial load of larvae and juveniles was estimated by colony forming units (CFUs) of larvae and juveniles. Larvae (6 days old) and juveniles (8–10 tentacle stages) were homogenized and spread on MB plates. The plates were incubated at 18°C for 3 days before counting colonies. One smashed larva resulted in ∼200 colonies grown on MB plates and one smashed juvenile spread on an MB plate yielded ∼2,000 colonies. To ensure successful recolonization, the polyps were exposed to double the amount of their native microbiota (e.g., ∼4,000 colonies per juvenile). The bacterial isolates were grown to an OD600 of 0.2, spread out on MB plates, and counted in order to calculate the cell number.

Prior to recolonization, the juvenile polyps were treated with antibiotics for 4 weeks and remained in sterile antibiotic-free medium for 4 days before recolonization. The animals were starved during the whole experiment. For each recolonization treatment and replicate, 10 juvenile polyps were put into a 2 mL Eppendorf tube and filled up with 2 mL of one of the following solutions: (1) native larval bacteria; (2) native juvenile bacteria; or (3) a mix of native larval bacteria and one single bacterial isolate in overrepresentation. Complex bacterial mixtures were obtained by smashing whole larvae or juvenile polyps in sterile NM. The homogenates were centrifuged and the pellet washed twice in sterile NM. Samples were collected for the three types of treatments at two time points. Five replicates per treatment and time point were used and each replicate consisted of five pooled animals.

The juveniles were recolonized with a mix of native larval bacteria together with single isolates with the aim of adding the single isolates in a 1:3 ratio of larval bacteria to single isolates. By sequencing the 16S rRNA genes of inocula, we estimated the overrepresentation of all isolates. Although it was not possible to obtain any mix of larval bacteria and bacterial isolates with the 1:3 target ratio, the five selected OTUs were still overrepresented at the start of each treatment, i.e., at least 10-fold their initial abundance in the control. The fold change of each isolate was estimated by comparing the sequencing reads of control (bL) to treatment.

6.2.8 Recolonization with complex microbiome

For recolonization with a complex microbiome, a protocol for conventionalized recolonized *Hydra* polyps was adapted (Fraune et al. 2015). Animals were sampled at 2 dpr, 7 dpr, 14 dpr and 28 dpr and therefore four gnotobiotic polyps per treatment were pooled into one 50 mL vessels. The complex microbiomes were prepared from whole-body tissues of larvae, juvenile polyps and adult polyps, respectively. For this, one adult sterile polyp was recolonized with one whole homogenized adult polyp from the long-term cultures. For recolonization with a juvenile and larval microbiome, approximately 0.1 mL of juvenile polyps or larvae were homogenized per four polyps and replicate. Larvae were 6 days old, juvenile polyps were 54 days old. The experiment was conducted in five independent replicates. Recolonization was allowed for 24 hours, before the medium was

exchanged in order to remove tissue debris and non-associated bacteria. Another 24 hours later, the first time point, 2 dpr, was collected. For this, one polyp per vessel was removed and washed three times with sterile NM. For gDNA extraction, the animal was homogenized with an immersion blender and 1/50 was spread on MB plates. The rest was pelleted at 4°C and 20.000 xg for 20 minutes and frozen until extraction. For total RNA extraction, whole polyps were frozen in liquid nitrogen and stored at -80°C until extraction. Due to problems with the RNA extraction, the experiment needed to be repeated for sampling for RNA extraction.

If silicone tubes instead of living *Nematostella* polyps were to be recolonized, hollow silicone tubes with an inner diameter of 3 mm and outer diameter of 5 mm and a wall thickness of 1 mm were cut into approximately 1 cm length. Samples were taken 2, 4, 7, 14, 21 and 28 dpr. The experimental setup was otherwise equivalent to the recolonization of adult polyps For sampling, I bisected the silicone tubes longitudinally to isolate gDNA from one half and dye the second half with Crystal Violet to track biofilm formation.

6.2.9 Recolonization with single bacterial strains

For recolonization with single bacterial strains, adult polyps were first treated with antibiotic to obtain gnotobiotic polyps. Bacteria for mono-association were chosen for their succession pattern during recolonization. Bacteria were grown in an overnight culture before fresh medium was inoculated with the overnight culture and regrown to an OD600 of 0.1. Each polyp was recolonized with a calculated OD of 0.001 (approximately 50000 cells) of a single bacterial strain. Recolonization was performed in five independent replicates. After 24 hours, the medium was exchanged with fresh sterile NM. After seven days of recolonization, samples were taken and animals were washed three times, homogenized with an immersion blender and plated on MB plates in 3 different concentrations. Colonies were counted 3 days after plating and incubation at 18°C.

6.2.10 Analysis of biofilm formation

In order to visualize and quantify biofilm built on recolonized silicone tubes, the tube was divided longitudinally with a sterile scalpel. One half was used for 16S rRNA sequencing The other half was used for the analysis of biofilm formation. The tube was washed twice

with MilliQ, before it was incubated in 1mL of 0.1% crystal violet solution for 15 minutes. Crystal violet was removed and tubes were washed three times with MilliQ, before tubes were let dry over night. The next day, crystal violet was removed from the tubes with 500µL of 95% ethonal with slight agitation for 10-15 minutes. Afterwards, the absorbance at 550nm was measured with the Tecan Spark 10M.

6.2.11 Chitin Staining

For staining, whole adult polyps first were fixed in 4% paraformaldehyde (PFA) in mPBS for 1 h at 4°C on a roller, before they were washed three times in 0.1% Triton X-100 in mPBS for 15 minutes each at 4°C on a roller. Animals were blocked in 2% BSA in mPBS for 2 h and again washed three times in 2% BSA and 0.1% Triton X-100 in mPBS. Animals were stained overnight at 4°C in 5% BSA and 0.1mg/mL of a probe consisting of a chitin-binding domain coupled to GFP. After staining, 2µg/mL of Hoechst was added and incubated for another 15 min. Animals were then washed five times in 0.1% Triton X-100 in mPBS for 10 minutes each. Animals then were embedded in Mowiol with DABCO and slides were dried overnight. Stained polyps were observed under the Olympus Fluoview FV3000 confocal microscope.

6.3 Preparation for and Analysis of Microbiome Sequencing

6.3.1 Inference of Bacteria–Bacteria Co-occurrence Networks

Network links were inferred using correlation analysis among 508 OTUs representing the relative bacterial abundance in N. *vectensis* (Mortzfeld et al. 2016). SparCC methodology was chosen as the inference method because it was explicitly designed for compositional (i.e., based on relative information) and sparse (with a small amount of non-zero values compared to the maximum possible) data, two key features displayed by the sequencing data used in our study (Friedman and Alm 2012). As the amount of significant correlations (pseudo p-value ≤ 0.05) was large, only the strongest correlations were considered for network construction and analysis (i.e., strong correlations are those exceeding 0.5 in absolute value).

SparCC methodology assigns a pseudo *p*-value to each correlation through a bootstrap approach. The pseudo *p*-value represents the proportion of times a correlation from

permutated datasets is at least as extreme as the observed "real". To calculate the pseudo *p*-values, 1,000 permutated datasets with a two-sided distribution were used.

The links in the co-occurrence networks can be either negative or positive. The value assigned to the interactions (i.e., interaction strength) ranges between -1 and +1, and the sign can provide proxies on the type of interaction (e.g., positive correlations can stand for cooperative activities, while negative correlations can indicate competition (Shade et al. 2012)). The number of nodes (the size of the network, which corresponds to the total number of OTUs; *N*), the number of links (the total number of significant correlations exceeding 0.5 in absolute value; *L*), the number of connected nodes (the OTUs with at least one interaction; N_C), the density [the ratio between *L* and the maximum number of links that an undirected network can have: $L_{max} = N\ (N - 1)/2$; $D = L/L_{max}$], the numbers and proportions of positive (L_P, $\%L_P$) and negative (L_N, $\%L_N$) links, the mean correlation values based on total (m_t), positive (m_p), or negative (m_n) interactions, and the number of subnetworks (networks composed by isolated subsets of *N*, where the nodes of each subnetwork show no connections outside the subset; n_{sub}) were taken as network descriptors. The degree (*d*) of the nodes was used as an indicator of centrality to identify the most important OTUs in the network (Wasserman and Faust 1994). Thus, an OTU *i* was considered to be important when it had a high degree (d_i is large if the node *i* is directly linked to several OTUs) and most connections of the same sign (i.e., to discriminate among cooperators or competitors). Also the mean ($\bar{d}$) and the maximum (d_{max}) degrees of the networks were calculated as global descriptors starting from single node values.

6.3.2 Genome Sequencing, Assembly and Annotation

Genomic DNA was isolated from single bacterial cultures with the Genomic DNA Purification Kit (Promega) using the protocol for gram positive bacteria. Libraries were prepared with the Nextera DNA Flex Kit (Illumina) and sequencing occurred on an Illumina NextSeq 1500. Read length was 2*150bp to approximately 60-80X coverage per genome. Genomic paired-end reads were first trimmed with TrimGalore to remove the remaining adapter sequences and reads shorter than 75 base pairs (Krueger 2021). Cleaned reads then were assembled into draft genomes with Spades and all-default settings (Bankevich

et al. 2012). Finally, gene models were annotated for each draft assembly using Prokka and its built-in reference database (Seemann 2014).

6.3.3 Metabolic pathway analysis

Because qiime2 creates the abundance table according to exact sequence variants (ESVs) and not operational taxonomic units (OTUs) on a specific identity percentage anymore, we manually clustered the ESVs into OTUS with 97% identity with cd-hit-est with a word size of 10 (Fu et al. 2012; W and A 2006). The output sequences were called clusters instead of ESV or OTU.

Metabolic pathway analysis on 97% clusters was performed by Dr. Johannes Zimmermann from the Institute for Experimental Medicine, CAU Kiel.

With metabolic pathway analysis, bacterial metabolic capacities were inferred as well as the potential pathway abundances over time were compared. Metabolic pathways were predicted by using gapseq (Zimmermann, Kaleta, and Waschina 2021). As input, the assembled genomes sequenced directly from *Nematostella* bacterial symbionts were used, as well as bacterial genomes published with NCBI which showed 97% identity to *Nematostella* bacterial. gapseq was run with default parameters (bitscore threshold of 200) with pathway definitions derived from MetaCyc (Caspi et al. 2018). Abricate was used to infer other bacterial traits, which were potentially relevant in host interactions and the virulence factor database VFDB (Chen et al. 2016; Seemann 2020). For each timepoint, bacterial source and replicate the relative bacterial abundance was calculated. With the relative bacterial abundance data and the genomic capacities, the potential pathway abundances were calculated. For each potential pathway the sum of relative abundances from all bacteria were determined, which were predicted to possess the corresponding pathway. From this, the relative cumulative pathway abundances were obtained, from which changes in metabolic capacities could be compared over time.

6.3.4 Library prep, Sequencing method for 16S

For sequencing, the hypervariable regions V1 -V2 of the bacterial 16S rRNA gene were amplified. The forward primer (5’-AATGATACGGCGACCACCGAGATCTACAC XXXXXXXX TATGGTAATTGT AGAGTTTGATCCTGGCTCAG-3’) contained the Illumina Adaptor p5 and the

reverse primer (5'-CAAGCAGAAGACGGCATACGAGAT XXXXXXXX AGTCAGTCAGCC TGCTGCCTCCCGTAGGAGT-3') contained p7. Both primers contain a unique 8 base index to tag each PCR product, here indicated with XXXXXXXX. The PCR was performed with 100 ng of template DNA (measured with Qubit) in a 25 µL PCR reaction. For amplification, the Phusion Hot Start II DNA Polymerase (Finnzymes, Espoo, Finland) was used. DNA was diluted with certified DNA-free PCR water (JT Baker). The cycling conditions were as followed: (98C – 30 s, 30 [98C – 9 s, 55C – 60 s, 72C –90 s], 72C – 10 min. Products were controlled on a 1.5% agarose gel. The concentration of the amplicons was estimated using a Gel DocTM XRC System coupled with Image LabTM Software (BioRad, Hercules, CA, United States). As internal standard, 3 µL of O'GeneRulerTM 100 bp Plus DNA Ladder (Thermo Fisher Scientific, Inc., Waltham, MA, United States) was applied to the gel for band intensity measurement. The samples of individual gels were pooled to obtain approximately equimolar subpools, judged by band intensity and the measurement with the Qubit dsDNA br Assay Kit (Thermo Fisher Scientific). Subpools again were mixed equimolarly and stored at -20°C until sequencing. Sequencing itself was performed on the Illumina MiSeq platform with v3 chemistry (Rausch et al., 2016). The raw data for the recolonization of juveniles are deposited at the Sequence Read Archive (SRA) under the project ID PRJNA433067.

6.3.5 16S rRNA data analysis with QIIME1.9

The sequence analysis for the recolonization of juveniles was conducted using the QIIME 1.9.0 package (Caporaso et al. 2010). Paired end reads were assembled using SeqPrep. Chimeric sequences were identified with Chimera Slayer (Haas et al. 2011). OTU picking was performed using the pick_open_reference_otus.py protocol with at least 97% identity per OTU and annotation was conducted with the UCLUST algorithm (RRID:SCR_011921; (RC 2010)) against the GreenGenes database v13.8 (RRID:SCR_002830; (DeSantis et al. 2006)) implemented in QIIME. OTUs with less than 50 reads were removed from the dataset to avoid false positive OTUs that may originate from sequencing errors (Faith et al. 2013). The number of reads was normalized to 10,000 reads for the analysis. Alpha-diversity was calculated with the Chao1 metric implemented in QIIME using ten replicates of rarefication per sample. Beta-diversity was depicted in a PCoA by 100 jackknifed

replicates using Bray–Curtis and weighted UniFrac metrics. For statistical analysis of clustering the method ADONIS was used.

6.3.6 16S rRNA data analysis with QIIME2

Analysis of the 16S rRNA Sequencing was performed for recolonization of adult polyps with QIIME2 (Bolyen et al. 2018; Caporaso et al. 2010). For this, samples were quality filtered with DADA2 and taxonomically classified with the q2-feature-classifier plugin for qiime2 with the Greengenes 13_8 97% OTU data set as reference (Bokulich et al. 2018; Callahan et al. 2016; DeSantis et al. 2006). Downstream analysis was performed with the R package phyloseq (McMurdie and Holmes 2013). Data were visualized with the R package ggplot2 (Wickham 2009). Statistical analysis was performed with the R package vegan (Oksanen et al. 2020).

6.4 Preparation and Analysis of RNA Sequencing

6.4.1 Quality Assessment, Depletion of rRNA, Library prep, Sequencing method

RNA quality was assessed on a 1.5% agarose gel for RNA degradation and on with the Qubit RNA BR (Broad-Range) Assay Kit (Thermo Fisher Scientific) for concentration and quality. RNA libraries were constructed with the TruSeq stranded mRNA (incl. p-A enrichment) protocol and were sequenced on a HiSeq4000 with a 2x75bp data yield and a paired-end mode.

6.4.2 RNA data analysis with DeSeq2

RNA data analysis was performed by Dr. Jan Taubenheim. First, the RNA-sequencing reads were trimmed for their adapters and for quality using trimmomatic in paired end mode using the following options: ILLUMINACLIP:{adapter.fasta}:2:30:10 LEADING:3 TRAILING:3 SLIDINGWINDOW:4:20 MINLEN:36 (Bolger, Lohse, and Usadel 2014). As mapping reference, the Vienna reference *Nematostella* transcriptome was used using the Bowtie2 software with default parameters (Fredman et al. 2020; Langmead and Salzberg 2012). The resulting sam files needed to be converted to bam format, for which the samtools suite was used (Li et al. 2009). The Salmon software package using default parameters and the -l ISR option was used for estimation of the read counts per transcript (Patro et al. 2017).

Differential analysis of the count data were performed using the R package DESeq2 (Love, Huber, and Anders 2014). Differential gene estimation was performed by first performing a log-fold change shrinkage and then tested for difference with a Wald-p-test (betaPrior = TRUE). Genes were considered differentially regulated if the adjusted p-value was lower than alpha = 0.05, irregardless of fold change.

7 References

Grimson, Srivastava M, Fahey B, Woodcroft BJ, Chiang HR, King N, Degnan BM, Rokhsar DS, and Bartel DP. 2008. “Early Origins and Evolution of MicroRNAs and Piwi-Interacting RNAs in Animals.” *Nature* 455(7217):1193–97.

Amiel, Aldine, Hereroa Johnston, Karine Nedoncelle, Jacob Warner, Solène Ferreira, Eric Röttinger, Aldine R. Amiel, Hereroa T. Johnston, Karine Nedoncelle, Jacob F. Warner, Solène Ferreira, and Eric Röttinger. 2015. “Characterization of Morphological and Cellular Events Underlying Oral Regeneration in the Sea Anemone, Nematostella Vectensis.” *International Journal of Molecular Sciences* 16(12):28449–71.

Arrieta, Marie Claire, Leah T. Stiemsma, Nelly Amenyogbe, Eric Brown, and Brett Finlay. 2014. “The Intestinal Microbiome in Early Life: Health and Disease.” *Frontiers in Immunology* 5(AUG):427.

Babonis, Leslie S., Mark Q. Martindale, and Joseph F. Ryan. 2016. “Do Novel Genes Drive Morphological Novelty? An Investigation of the Nematosomes in the Sea Anemone Nematostella Vectensis.” *BMC Evolutionary Biology* 16(1).

Bäckhed, Fredrik, Hao Ding, Ting Wang, Lora V. Hooper, Young Koh Gou, Andras Nagy, Clay F. Semenkovich, and Jeffrey I. Gordon. 2004. “The Gut Microbiota as an Environmental Factor That Regulates Fat Storage.” *Proceedings of the National Academy of Sciences of the United States of America* 101(44):15718–23.

Baldassarre, Laura, Shani Levy, Rinat Bar-Shalom, Laura Steindler, Tamar Lotan, and Sebastian Fraune. 2021. “Contribution of Maternal and Paternal Transmission to Bacterial Colonization in Nematostella Vectensis.” *Frontiers in Microbiology* 12:2892.

Baldassarre, Laura, Hua Ying, Adam M. Reitzel, Sören Franzenburg, and Sebastian Fraune. 2022. “Microbiota Mediated Plasticity Promotes Thermal Adaptation in the Sea Anemone Nematostella Vectensis.” *Nature Communications 2022 13:1* 13(1):1–13.

Bang, Corinna, Tal Dagan, Peter Deines, Nicole Dubilier, Wolfgang J. Duschl, Sebastian Fraune, Ute Hentschel, Heribert Hirt, Nils Hülter, Tim Lachnit, Devani Picazo, Lucia Pita, Claudia Pogoreutz, Nils Rädecker, Maged M. Saad, Ruth A. Schmitz, Hinrich Schulenburg, Christian R. Voolstra, Nancy Weiland-Bräuer, Maren Ziegler, and Thomas C. G. Bosch. 2018. “Metaorganisms in Extreme Environments: Do Microbes Play a Role in Organismal Adaptation?” *Zoology* 127:1–19.

Bankevich, Anton, Sergey Nurk, Dmitry Antipov, Alexey A. Gurevich, Mikhail Dvorkin, Alexander S. Kulikov, Valery M. Lesin, Sergey I. Nikolenko, Son Pham, Andrey D. Prjibelski, Alexey V. Pyshkin, Alexander V. Sirotkin, Nikolay Vyahhi, Glenn Tesler, Max A. Alekseyev, and Pavel A. Pevzner. 2012. “SPAdes: A New Genome Assembly Algorithm and Its Applications to Single-

Cell Sequencing." *Journal of Computational Biology* 19(5):455–77.

Baquero, F. and C. Nombela. 2012. "The Microbiome as a Human Organ." *Clinical Microbiology and Infection* 18(SUPPL. 4):2–4.

Bassler, Bonnie, Patrick Gibbons, and Saul Roseman. 1989. "Chemotaxis to Chitin Oligosaccharides by Vibrio Furnissii, a Chitinivorous Marine Bacterium." *Biochemical and Biophysical Research Communications* 161(3):1172–76.

Bauer, Maria A., Katharina Kainz, Didac Carmona-Gutierrez, and Frank Madeo. 2018. "Microbial Wars: Competition in Ecological Niches and within the Microbiome." *Microbial Cell* 5(5):215–19.

Berking, Stefan. 2007. "Generation of Bilateral Symmetry in Anthozoa: A Model." *Journal of Theoretical Biology* 246(3):477–90.

Berking, Stefan and Klaus Herrmann. 2006. "Formation and Discharge of Nematocysts Is Controlled by a Proton Gradient across the Cyst Membrane." *Helgoland Marine Research* 60(3):180–88.

Blanton, Laura V., Mark R. Charbonneau, Tarek Salih, Michael J. Barratt, Siddarth Venkatesh, Olga Ilkaveya, Sathish Subramanian, Mark J. Manary, Indi Trehan, Josh M. Jorgensen, Yue Mei Fan, Bernard Henrissat, Semen A. Leyn, Dmitry A. Rodionov, Andrei L. Osterman, Kenneth M. Maleta, Christopher B. Newgard, Per Ashorn, Kathryn G. Dewey, and Jeffrey I. Gordon. 2016. "Gut Bacteria That Prevent Growth Impairments Transmitted by Microbiota from Malnourished Children." *Science* 351(6275).

Bodenhausen, Natacha, Miriam Bortfeld-Miller, Martin Ackermann, and Julia A. Vorholt. 2014. "A Synthetic Community Approach Reveals Plant Genotypes Affecting the Phyllosphere Microbiota." *PLoS Genetics* 10(4).

Boehme, Marcus, Katherine E. Guzzetta, Thomaz F. S. Bastiaanssen, Marcel van de Wouw, Gerard M. Moloney, Andreu Gual-Grau, Simon Spichak, Loreto Olavarría-Ramírez, Patrick Fitzgerald, Enrique Morillas, Nathaniel L. Ritz, Minal Jaggar, Caitlin S. M. Cowan, Fiona Crispie, Francisco Donoso, Evelyn Halitzki, Marta C. Neto, Marzia Sichetti, Anna V. Golubeva, Rachel S. Fitzgerald, Marcus J. Claesson, Paul D. Cotter, Olivia F. O'Leary, Timothy G. Dinan, and John F. Cryan. 2021. "Microbiota from Young Mice Counteracts Selective Age-Associated Behavioral Deficits." *Nature Aging 2021 1:8* 1(8):666–76.

Bokulich, Nicholas A., Jai Ram Rideout, Matthew Dillon, Evan Bolyen, Benjamin D. Kaehler, Gavin A. Huttley, and Rob Knight. 2018. "Optimizing Taxonomic Classification of Marker-Gene Amplicon Sequences with QIIME 2's Q2-Feature-Classifier Plugin." *Microbiome* 6(1):1–17.

Bolger, Anthony M., Marc Lohse, and Bjoern Usadel. 2014. "Trimmomatic: A Flexible Trimmer for Illumina Sequence Data." *Bioinformatics* 30(15):2114–20.

References

Bolyen, Evan, Jai Ram Rideout, Matthew R. Dillon, Nicholas A. Bokulich, Christian Abnet, Gabriel A. Al-Ghalith, Harriet Alexander, Eric J. Alm, Manimozhiyan Arumugam, Francesco Asnicar, Yang Bai, Jordan E. Bisanz, Kyle Bittinger, Asker Brejnrod, Colin J. Brislawn, C. Titus Brown, Benjamin J. Callahan, Andrés Mauricio Caraballo-Rodríguez, John Chase, Emily Cope, Ricardo Da Silva, Pieter C. Dorrestein, Gavin M. Douglas, Daniel M. Durall, Claire Duvallet, Christian F. Edwardson, Madeleine Ernst, Mehrbod Estaki, Jennifer Fouquier, Julia M. Gauglitz, Deanna L. Gibson, Antonio Gonzalez, Kestrel Gorlick, Jiarong Guo, Benjamin Hillmann, Susan Holmes, Hannes Holste, Curtis Huttenhower, Gavin Huttley, Stefan Janssen, Alan K. Jarmusch, Lingjing Jiang, Benjamin Kaehler, Kyo Bin Kang, Christopher R. Keefe, Paul Keim, Scott T. Kelley, Dan Knights, Irina Koester, Tomasz Kosciolek, Jorden Kreps, Morgan GI Langille, Joslynn Lee, Ruth Ley, Yong-Xin Liu, Erikka Loftfield, Catherine Lozupone, Massoud Maher, Clarisse Marotz, Bryan D. Martin, Daniel McDonald, Lauren J. McIver, Alexey V Melnik, Jessica L. Metcalf, Sydney C. Morgan, Jamie Morton, Ahmad Turan Naimey, Jose A. Navas-Molina, Louis Felix Nothias, Stephanie B. Orchanian, Talima Pearson, Samuel L. Peoples, Daniel Petras, Mary Lai Preuss, Elmar Pruesse, Lasse Buur Rasmussen, Adam Rivers, II Michael S Robeson, Patrick Rosenthal, Nicola Segata, Michael Shaffer, Arron Shiffer, Rashmi Sinha, Se Jin Song, John R. Spear, Austin D. Swafford, Luke R. Thompson, Pedro J. Torres, Pauline Trinh, Anupriya Tripathi, Peter J. Turnbaugh, Sabah Ul-Hasan, Justin JJ van der Hooft, Fernando Vargas, Yoshiki Vázquez-Baeza, Emily Vogtmann, Max von Hippel, William Walters, Yunhu Wan, Mingxun Wang, Jonathan Warren, Kyle C. Weber, Chase HD Williamson, Amy D. Willis, Zhenjiang Zech Xu, Jesse R. Zaneveld, Yilong Zhang, Qiyun Zhu, Rob Knight, and J. Gregory Caporaso. 2018. “QIIME 2: Reproducible, Interactive, Scalable, and Extensible Microbiome Data Science.”

Bonacolta, Anthony M., Michael T. Connelly, Stephanie M Rosales, Javier Del Campo, and Nikki Traylor-Knowles. 2021. “The Starlet Sea Anemone, Nematostella Vectensis, Possesses Body Region-Specific Bacterial Associations with Spirochetes Dominating the Capitulum.” *FEMS Microbiology Letters* 368(3).

Bosch, Thomas C. G. 2012. “Understanding Complex Host-Microbe Interactions in Hydra.” *Gut Microbes* 3(4):345.

Bosch, Thomas C. G., Rene Augustin, Friederike Anton-Erxleben, Sebastian Fraune, Georg Hemmrich, Holger Zill, Philip Rosenstiel, Gunnar Jacobs, Stefan Schreiber, Matthias Leippe, Mareike Stanisak, Joachim Grotzinger, Sascha Jung, Rainer Podschun, Joachim Bartels, Jurgen Harder, and Jens-M. Schroder. 2009. “Uncovering the Evolutionary History of Innate Immunity: The Simple Metazoan Hydra Uses Epithelial Cells for Host Defence.” *Developmental and Comparative Immunology* 33(4):559–69.

References

Bosch, Thomas C. G. and Margaret J. McFall-Ngai. 2011. “Metaorganisms as the New Frontier.” *Zoology (Jena, Germany)* 114(4):185–90.

Brennan, Joseph J., Jonathan L. Messerschmidt, Leah M. Williams, Bryan J. Matthews, Marinaliz Reynoso, and Thomas D. Gilmore. 2017. “Sea Anemone Model Has a Single Toll-like Receptor That Can Function in Pathogen Detection, NF-KB Signal Transduction, and Development.” *Proceedings of the National Academy of Sciences of the United States of America* 114(47):E10122–31.

Buchmann, Kurt. 2014. “Evolution of Innate Immunity: Clues from Invertebrates via Fish to Mammals.” *Frontiers in Immunology* 0(SEP):459.

Buchner, Paul. 1965. *Endosymbiosis of Animals with Plant Microorganisms.* Rev. Eng. ed. New York: Interscience Publishers.

Callahan, Benjamin J., Paul J. McMurdie, Michael J. Rosen, Andrew W. Han, Amy Jo A. Johnson, and Susan P. Holmes. 2016. “DADA2: High-Resolution Sample Inference from Illumina Amplicon Data.” *Nature Methods* 13(7):581–83.

Caporaso, J. Gregory, Justin Kuczynski, Jesse Stombaugh, Kyle Bittinger, Frederic D. Bushman, Elizabeth K. Costello, Noah Fierer, Antonio Gonzalez Peña, Julia K. Goodrich, Jeffrey I. Gordon, Gavin A. Huttley, Scott T. Kelley, Dan Knights, Jeremy E. Koenig, Ruth E. Ley, Catherine A. Lozupone, Daniel McDonald, Brian D. Muegge, Meg Pirrung, Jens Reeder, Joel R. Sevinsky, Peter J. Turnbaugh, William A. Walters, Jeremy Widmann, Tanya Yatsunenko, Jesse Zaneveld, and Rob Knight. 2010. “QIIME Allows Analysis of High-Throughput Community Sequencing Data.” *Nature Methods* 7(5):335–36.

Caspi, Ron, Richard Billington, Carol A. Fulcher, Ingrid M. Keseler, Anamika Kothari, Markus Krummenacker, Mario Latendresse, Peter E. Midford, Quang Ong, Wai Kit Ong, Suzanne Paley, Pallavi Subhraveti, and Peter D. Karp. 2018. “The MetaCyc Database of Metabolic Pathways and Enzymes.” *Nucleic Acids Research* 46(D1):D633–39.

Chaplin, David D. 2010. “Overview of the Immune Response.” *The Journal of Allergy and Clinical Immunology* 125(2 Suppl 2):S3.

Chen, Lihong, Dandan Zheng, Bo Liu, Jian Yang, and Qi Jin. 2016. “VFDB 2016: Hierarchical and Refined Dataset for Big Data Analysis - 10 Years On.” *Nucleic Acids Research* 44(D1):D694–97.

Chiu, Lynn, Thomas Bazin, Marie Elise Truchetet, Thierry Schaeverbeke, Laurence Delhaes, and Thomas Pradeu. 2017. “Protective Microbiota: From Localized to Long-Reaching Co-Immunity.” *Frontiers in Immunology* 8(DEC):1.

Chng, Kern Rei, Tarini Shankar Ghosh, Yi Han Tan, Tannistha Nandi, Ivor Russel Lee, Amanda Hui Qi Ng, Chenhao Li, Aarthi Ravikrishnan, Kar Mun Lim, David Lye, Timothy Barkham, Karthik

Raman, Swaine L. Chen, Louis Chai, Barnaby Young, Yunn Hwen Gan, and Niranjan Nagarajan. 2020. “Metagenome-Wide Association Analysis Identifies Microbial Determinants of Post-Antibiotic Ecological Recovery in the Gut.” *Nature Ecology & Evolution 2020 4:9* 4(9):1256–67.

Clarke, Gerard, Roman M. Stilling, Paul J. Kennedy, Catherine Stanton, John F. Cryan, and Timothy G. Dinan. 2014. “Minireview: Gut Microbiota: The Neglected Endocrine Organ.” *Molecular Endocrinology* 28(8):1221–38.

Clavel, Thomas, Ilias Lagkouvardos, and Bärbel Stecher. 2017. “From Complex Gut Communities to Minimal Microbiomes via Cultivation.” *Current Opinion in Microbiology* 38:148–55.

Collins, A. G. 2002. “Phylogeny of Medusozoa and the Evolution of Cnidarian Life Cycles.” *Journal of Evolutionary Biology* 15(3):418–32.

Coyte, Katharine Z., Jonas Schluter, and Kevin R. Foster. 2015. “The Ecology of the Microbiome: Networks, Competition, and Stability.” *Science* 350(6261):663–66.

Cryan, John F., Kenneth J. O’riordan, Caitlin S. M. Cowan, Kiran V. Sandhu, Thomaz F. S. Bastiaanssen, Marcus Boehme, Martin G. Codagnone, Sofia Cussotto, Christine Fulling, Anna V. Golubeva, Katherine E. Guzzetta, Minal Jaggar, Caitriona M. Long-Smith, Joshua M. Lyte, Jason A. Martin, Alicia Molinero-Perez, Gerard Moloney, Emanuela Morelli, Enrique Morillas, Rory O’connor, Joana S. Cruz-Pereira, Veronica L. Peterson, Kieran Rea, Nathaniel L. Ritz, Eoin Sherwin, Simon Spichak, Emily M. Teichman, Marcel van de Wouw, Ana Paula Ventura-Silva, Shauna E. Wallace-Fitzsimons, Niall Hyland, Gerard Clarke, and Timothy G. Dinan. 2019. “The Microbiota-Gut-Brain Axis.” *Physiological Reviews* 99(4):1877–2013.

Cunliffe, R. N. and Y. R. Mahida. 2004. “Expression and Regulation of Antimicrobial Peptides in the Gastrointestinal Tract.” *Journal of Leukocyte Biology* 75(1):49–58.

Czárán, Tamás L., Rolf F. Hoekstra, and Ludo Pagie. 2002. “Chemical Warfare between Microbes Promotes Biodiversity.” *Proceedings of the National Academy of Sciences of the United States of America* 99(2):786–90.

Darling, J. A., A. M. Reitzel, and J. R. Finnerty. 2004. “Regional Population Structure of a Widely Introduced Estuarine Invertebrate: Nematostella Vectensis Stephenson in New England.” *Molecular Ecology* 13(10):2969–81.

Darling, John A, Adam R. Reitzel, Patrick M. Burton, Maureen E. Mazza, Joseph F. Ryan, James C. Sullivan, and John R. Finnerty. 2005. “Rising Starlet: The Starlet Sea Anemone, Nematostella Vectensis.” *BioEssays : News and Reviews in Molecular, Cellular and Developmental Biology* 27(2):211–21.

Darling, John A., Adam R. Reitzel, Patrick M. Burton, Maureen E. Mazza, Joseph F. Ryan, James C.

Sullivan, and John R. Finnerty. 2005. “Rising Starlet: The Starlet Sea Anemone, Nematostella Vectensis.” *BioEssays* 27(2):211–21.

Datta, Manoshi S., Elzbieta Sliwerska, Jeff Gore, Martin F. Polz, and Otto X. Cordero. 2016. “Microbial Interactions Lead to Rapid Micro-Scale Successions on Model Marine Particles.” *Nature Communications* 7(1):1–7.

David, Lawrence A., Corinne F. Maurice, Rachel N. Carmody, David B. Gootenberg, Julie E. Button, Benjamin E. Wolfe, Alisha V. Ling, A. Sloan Devlin, Yug Varma, Michael A. Fischbach, Sudha B. Biddinger, Rachel J. Dutton, and Peter J. Turnbaugh. 2014a. “Diet Rapidly and Reproducibly Alters the Human Gut Microbiome.” *Nature* 505(7484):559–63.

David, Lawrence A., Corinne F. Maurice, Rachel N. Carmody, David B. Gootenberg, Julie E. Button, Benjamin E. Wolfe, Alisha V. Ling, A. Sloan Devlin, Yug Varma, Michael A. Fischbach, Sudha B. Biddinger, Rachel J. Dutton, and Peter J. Turnbaugh. 2014b. “Diet Rapidly and Reproducibly Alters the Human Gut Microbiome.” *Nature* 505(7484):559–63.

Deines, Peter, Katrin Hammerschmidt, and Thomas C. G. Bosch. 2020a. “Exploring the Niche Concept in a Simple Metaorganism.” *Frontiers in Microbiology* 11.

Deines, Peter, Katrin Hammerschmidt, and Thomas C. G. Bosch. 2020b. “Microbial Species Coexistence Depends on the Host Environment.” *MBio* 11(4):1–13.

DeSantis, T. Z., P. Hugenholtz, N. Larsen, M. Rojas, E. L. Brodie, K. Keller, T. Huber, D. Dalevi, P. Hu, and G. L. Andersen. 2006. “Greengenes, a Chimera-Checked 16S RRNA Gene Database and Workbench Compatible with ARB.” *Applied and Environmental Microbiology* 72(7):5069–72.

Dierking, Katja and Lucía Pita. 2020. “Receptors Mediating Host-Microbiota Communication in the Metaorganism: The Invertebrate Perspective.” *Frontiers in Immunology* 11:1251.

Douglas, A. E. 1998. “NUTRITIONAL INTERACTIONS IN INSECT-MICROBIAL SYMBIOSES: Aphids and Their Symbiotic Bacteria Buchnera.” *Annu. Rev. Entomol* 43:17–37.

Drake, Jake A. 1991. “Community-Assembly Mechanics and the Structure of an Experimental Species Ensemble.” *American Naturalist* 137(1):1–26.

Dumbrell, Alex J., Michaela Nelson, Thorunn Helgason, Calvin Dytham, and Alastair H. Fitter. 2010. “Relative Roles of Niche and Neutral Processes in Structuring a Soil Microbial Community.” *ISME Journal* 4(3):337–45.

Dunn, Casey W., Andreas Hejnol, David Q. Matus, Kevin Pang, William E. Browne, Stephen A. Smith, Elaine Seaver, Greg W. Rouse, Matthias Obst, Gregory D. Edgecombe, Martin V Sorensen, Steven H. D. Haddock, Andreas Schmidt-Rhaesa, Akiko Okusu, Reinhardt Mobjerg Kristensen, Ward C. Wheeler, Mark Q. Martindale, and Gonzalo Giribet. 2008. “Broad Phylogenomic Sampling Improves Resolution of the Animal Tree of Life.” *Nature* 452(7188):745–49.

References

Eberl, G. 2010. “A New Vision of Immunity: Homeostasis of the Superorganism.” *Mucosal Immunology 2010 3:5* 3(5):450–60.

Elias, Sivan and Ehud Banin. 2012. “Multi-Species Biofilms: Living with Friendly Neighbors.” *FEMS Microbiology Reviews* 36(5):990–1004.

Esser, Daniela, Janina Lange, Georgios Marinos, Michael Sieber, Lena Best, Daniela Prasse, Jay Bathia, Malte C. Rühlemann, Kathrin Boersch, Cornelia Jaspers, and Felix Sommer. 2019. “Functions of the Microbiota for the Physiology of Animal Metaorganisms.” *Journal of Innate Immunity* 11(5):393–404.

Faith, Jeremiah J., Janaki L. Guruge, Mark Charbonneau, Sathish Subramanian, Henning Seedorf, Andrew L. Goodman, Jose C. Clemente, Rob Knight, Andrew C. Heath, Rudolph L. Leibel, Michael Rosenbaum, and Jeffrey I. Gordon. 2013. “The Long-Term Stability of the Human Gut Microbiota.” *Science (New York, N.Y.)* 341(6141):1237439.

Faszewski, Ellen E., Annemarie Tyrell, Sujata Guin, and Jane C. Kaltenbach. 2008. “Metamorphic Changes in Localization of Sugars in Skin of the Leopard Frog, Rana Pipiens.” *Journal of Morphology* 269(8):998–1007.

Faust, Karoline and Jeroen Raes. 2012. “Microbial Interactions: From Networks to Models.” *Nature Reviews Microbiology* 10(8):538–50.

Fierer, Noah, Diana Nemergut, Rob Knight, and Joseph M. Craine. 2010. “Changes through Time: Integrating Microorganisms into the Study of Succession.” *Research in Microbiology* 161(8):635–42.

Fieth, Rebecca A., Marie-Emilie A. Gauthier, Joanne Bayes, Kathryn M. Green, and Sandie M. Degnan. 2016. “Ontogenetic Changes in the Bacterial Symbiont Community of the Tropical Demosponge Amphimedon Queenslandica: Metamorphosis Is a New Beginning.” *Frontiers in Marine Science* 3(November):1–20.

Finnerty, John R., Kevin Pang, Pat Burton, Dave Paulson, and Mark Q. Martindale. 2004. “Origins of Bilateral Symmetry: Hox and Dpp Expression in a Sea Anemone.” *Science (New York, N.Y.)* 304(5675):1335–37.

Frank, Peter and J. Sherman Bleakney. 2007. “Histology and Sexual Reproduction of the Anemone Nematostella Vectensis Stephenson 1935.” *Https://Doi.Org/10.1080/00222937600770331* 10(4):441–49.

Franzenburg, Soren, Sebastian Fraune, Sven Kunzel, John F. Baines, Tomislav Domazet-Loso, and Thomas C. G. Bosch. 2012. “MyD88-Deficient Hydra Reveal an Ancient Function of TLR Signaling in Sensing Bacterial Colonizers.” *Proceedings of the National Academy of Sciences of the United States of America* 109(47):19374–79.

References

Franzenburg, Soren, Jonas Walter, Sven Kunzel, Jun Wang, John F. Baines, Thomas C. G. Bosch, and Sebastian Fraune. 2013. “Distinct Antimicrobial Peptide Expression Determines Host Species-Specific Bacterial Associations.” *Proceedings of the National Academy of Sciences of the United States of America* 110(39):E3730-8.

Franzenburg, Sören, Jonas Walter, Sven Künzel, Jun Wang, John F. Baines, Thomas C. G. Bosch, and Sebastian Fraune. 2013. “Distinct Antimicrobial Peptide Expression Determines Host Species-Specific Bacterial Associations.” *Proceedings of the National Academy of Sciences of the United States of America* 110(39):E3730–38.

Fraune, Sebastian, Friederike Anton-Erxleben, Rene Augustin, Soren Franzenburg, Mirjam Knop, Katja Schroder, Doris Willoweit-Ohl, and Thomas C. G. Bosch. 2015. “Bacteria-Bacteria Interactions within the Microbiota of the Ancestral Metazoan Hydra Contribute to Fungal Resistance.” *The ISME Journal* 9(7):1543–56.

Fraune, Sebastian, Sylvain Forêt, and Adam M. Reitzel. 2016. “Using Nematostella Vectensis to Study the Interactions between Genome, Epigenome, and Bacteria in a Changing Environment.” *Frontiers in Marine Science* 3(August):1–8.

Fredman, David, Michaela Schwaiger, Fabian Rentzsch, and Ulrich Technau. 2020. “Nematostella Vectensis Transcriptome and Gene Models v2.0.” Retrieved May 19, 2021 (https://figshare.com/articles/dataset/Nematostella_vectensis_transcriptome_and_gene_models_v2_0/807696).

Friedman, Jonathan and Eric J. Alm. 2012. “Inferring Correlation Networks from Genomic Survey Data.” *PLOS Computational Biology* 8(9):e1002687.

Fritzenwanker, Jens H., Grigory Genikhovich, Yulia Kraus, and Ulrich Technau. 2007. “Early Development and Axis Specification in the Sea Anemone Nematostella Vectensis.” *Developmental Biology* 310(2):264–79.

Fritzenwanker, Jens H. and Ulrich Technau. 2002. “Induction of Gametogenesis in the Basal Cnidarian Nematostella Vectensis(Anthozoa).” *Development Genes and Evolution* 212(2):99–103.

Fu, Limin, Beifang Niu, Zhengwei Zhu, Sitao Wu, and Weizhong Li. 2012. “CD-HIT: Accelerated for Clustering the next-Generation Sequencing Data.” *Bioinformatics (Oxford, England)* 28(23):3150–52.

Genikhovich, Grigory, Patrick Fried, M. Mandela Prünster, Johannes B. Schinko, Anna F. Gilles, David Fredman, Karin Meier, Dagmar Iber, and Ulrich Technau. 2015. “Axis Patterning by BMPs: Cnidarian Network Reveals Evolutionary Constraints.” *Cell Reports* 10(10):1646.

Genikhovich, Grigory and Ulrich Technau. 2009. “The Starlet Sea Anemone Nematostella Vectensis:

An Anthozoan Model Organism for Studies in Comparative Genomics and Functional Evolutionary Developmental Biology." *Cold Spring Harbor Protocols* 2009(9):pdb.emo129.

Gilbert, Jack A., Martin J. Blaser, J. Gregory Caporaso, Janet K. Jansson, Susan V. Lynch, and Rob Knight. 2018. "Current Understanding of the Human Microbiome." *Nature Medicine* 24(4):392–400.

Gould, Alison L., Vivian Zhang, Lisa Lamberti, Eric W. Jones, Benjamin Obadia, Nikolaos Korasidis, Alex Gavryushkin, Jean M. Carlson, Niko Beerenwinkel, and William B. Ludington. 2018. "Microbiome Interactions Shape Host Fitness." *Proceedings of the National Academy of Sciences of the United States of America* 115(51):E11951–60.

Gralka, Matti, Rachel Szabo, Roman Stocker, and Otto X. Cordero. 2020. "Trophic Interactions and the Drivers of Microbial Community Assembly." *Current Biology* 30(19):R1176–88.

Haas, Brian J., Dirk Gevers, Ashlee M. Earl, Mike Feldgarden, Doyle V. Ward, Georgia Giannoukos, Dawn Ciulla, Diana Tabbaa, Sarah K. Highlander, Erica Sodergren, Barbara Methé, Todd Z. DeSantis, The Human Microbiome Consortium, Joseph F. Petrosino, Rob Knight, and Bruce W. Birren. 2011. "Chimeric 16S RRNA Sequence Formation and Detection in Sanger and 454-Pyrosequenced PCR Amplicons." *Genome Research* 21(3):494–504.

Hand, Cadet and Kevin R. Uhlinger. 1992. "The Culture, Sexual and Asexual Reproduction, and Growth of the Sea Anemone Nematostella Vectensis." *Biological Bulletin* 182(2):169.

Hand, Cadet and Kevin R. Uhlinger. 1994. "The Unique, Widely Distributed, Estuarine Sea Anemone, Nematostella Vectensis Stephenson." *Estuaries* 17(2):501.

Hand, Cadet and Kevin R. Uhlinger. 1995. "Asexual Reproduction by Transverse Fission and Some Anomalies in the Sea Anemone Nematostella Vectensis." *Invertebrate Biology* 114(1):9.

Har, Jia Y., Tim Helbig, Ju H. Lim, Samodha C. Fernando, Adam M. Reitzel, Kevin Penn, and Janelle R. Thompson. 2015. "Microbial Diversity and Activity in the Nematostella Vectensis Holobiont: Insights from 16S RRNA Gene Sequencing, Isolate Genomes, and a Pilot-Scale Survey of Gene Expression." *Frontiers in Microbiology* 6:818.

Helm, Rebecca Rae, Stefan Siebert, Sarah Tulin, Joel Smith, and Casey William Dunn. 2013. "Characterization of Differential Transcript Abundance through Time during Nematostella Vectensis Development." *BMC Genomics* 14:266.

Hentschel, Ute, Jorn Piel, Sandie M. Degnan, and Michael W. Taylor. 2012. "Genomic Insights into the Marine Sponge Microbiome." *Nature Reviews. Microbiology* 10(9):641–54.

Hester, Eric R., Katie L. Barott, Jim Nulton, Mark J. A. Vermeij, and Forest L. Rohwer. 2016. "Stable and Sporadic Symbiotic Communities of Coral and Algal Holobionts." *The ISME Journal* 10(5):1157–69.

References

Holmes, Andrew J., Yi Vee Chew, Feyza Colakoglu, John B. Cliff, Eline Klaassens, Mark N. Read, Samantha M. Solon-Biet, Aisling C. McMahon, Victoria C. Cogger, Kari Ruohonen, David Raubenheimer, David G. Le Couteur, and Stephen J. Simpson. 2017. "Diet-Microbiome Interactions in Health Are Controlled by Intestinal Nitrogen Source Constraints." *Cell Metabolism* 25(1):140–51.

Huttenhower, Curtis, Dirk Gevers, Rob Knight, Sahar Abubucker, Jonathan H. Badger, Asif T. Chinwalla, Heather H. Creasy, Ashlee M. Earl, Michael G. Fitzgerald, Robert S. Fulton, Michelle G. Giglio, Kymberlie Hallsworth-Pepin, Elizabeth A. Lobos, Ramana Madupu, Vincent Magrini, John C. Martin, Makedonka Mitreva, Donna M. Muzny, Erica J. Sodergren, James Versalovic, Aye M. Wollam, Kim C. Worley, Jennifer R. Wortman, Sarah K. Young, Qiandong Zeng, Kjersti M. Aagaard, Olukemi O. Abolude, Emma Allen-Vercoe, Eric J. Alm, Lucia Alvarado, Gary L. Andersen, Scott Anderson, Elizabeth Appelbaum, Harindra M. Arachchi, Gary Armitage, Cesar A. Arze, Tulin Ayyaz, Carl C. Baker, Lisa Begg, Tsegahiwot Belachew, Veena Bhonagiri, Monika Bihan, Martin J. Blaser, Toby Bloom, Vivien Bonazzi, J. Paul Brooks, Gregory A. Buck, Christian J. Buhay, Dana A. Busam, Joseph L. Campbell, Shane R. Canon, Brandi L. Cantarel, Patrick S. G. Chain, I. Min A. Chen, Lei Chen, Shaila Chhibba, Ken Chu, Dawn M. Ciulla, Jose C. Clemente, Sandra W. Clifton, Sean Conlan, Jonathan Crabtree, Mary A. Cutting, Noam J. Davidovics, Catherine C. Davis, Todd Z. Desantis, Carolyn Deal, Kimberley D. Delehaunty, Floyd E. Dewhirst, Elena Deych, Yan Ding, David J. Dooling, Shannon P. Dugan, Wm Michael Dunne, A. Scott Durkin, Robert C. Edgar, Rachel L. Erlich, Candace N. Farmer, Ruth M. Farrell, Karoline Faust, Michael Feldgarden, Victor M. Felix, Sheila Fisher, Anthony A. Fodor, Larry J. Forney, Leslie Foster, Valentina Di Francesco, Jonathan Friedman, Dennis C. Friedrich, Catrina C. Fronick, Lucinda L. Fulton, Hongyu Gao, Nathalia Garcia, Georgia Giannoukos, Christina Giblin, Maria Y. Giovanni, Jonathan M. Goldberg, Johannes Goll, Antonio Gonzalez, Allison Griggs, Sharvari Gujja, Susan Kinder Haake, Brian J. Haas, Holli A. Hamilton, Emily L. Harris, Theresa A. Hepburn, Brandi Herter, Diane E. Hoffmann, Michael E. Holder, Clinton Howarth, Katherine H. Huang, Susan M. Huse, Jacques Izard, Janet K. Jansson, Huaiyang Jiang, Catherine Jordan, Vandita Joshi, James A. Katancik, Wendy A. Keitel, Scott T. Kelley, Cristyn Kells, Nicholas B. King, Dan Knights, Heidi H. Kong, Omry Koren, Sergey Koren, Karthik C. Kota, Christie L. Kovar, Nikos C. Kyrpides, Patricio S. La Rosa, Sandra L. Lee, Katherine P. Lemon, Niall Lennon, Cecil M. Lewis, Lora Lewis, Ruth E. Ley, Kelvin Li, Konstantinos Liolios, Bo Liu, Yue Liu, Chien Chi Lo, Catherine A. Lozupone, R. Dwayne Lunsford, Tessa Madden, Anup A. Mahurkar, Peter J. Mannon, Elaine R. Mardis, Victor M. Markowitz, Konstantinos Mavromatis, Jamison M. McCorrison, Daniel McDonald, Jean McEwen, Amy L. McGuire, Pamela McInnes, Teena

Mehta, Kathie A. Mihindukulasuriya, Jason R. Miller, Patrick J. Minx, Irene Newsham, Chad Nusbaum, Michelle Oglaughlin, Joshua Orvis, Ioanna Pagani, Krishna Palaniappan, Shital M. Patel, Matthew Pearson, Jane Peterson, Mircea Podar, Craig Pohl, Katherine S. Pollard, Mihai Pop, Margaret E. Priest, Lita M. Proctor, Xiang Qin, Jeroen Raes, Jacques Ravel, Jeffrey G. Reid, Mina Rho, Rosamond Rhodes, Kevin P. Riehle, Maria C. Rivera, Beltran Rodriguez-Mueller, Yu Hui Rogers, Matthew C. Ross, Carsten Russ, Ravi K. Sanka, Pamela Sankar, J. Fah Sathirapongsasuti, Jeffery A. Schloss, Patrick D. Schloss, Thomas M. Schmidt, Matthew Scholz, Lynn Schriml, Alyxandria M. Schubert, Nicola Segata, Julia A. Segre, William D. Shannon, Richard R. Sharp, Thomas J. Sharpton, Narmada Shenoy, Nihar U. Sheth, Gina A. Simone, Indresh Singh, Christopher S. Smillie, Jack D. Sobel, Daniel D. Sommer, Paul Spicer, Granger G. Sutton, Sean M. Sykes, Diana G. Tabbaa, Mathangi Thiagarajan, Chad M. Tomlinson, Manolito Torralba, Todd J. Treangen, Rebecca M. Truty, Tatiana A. Vishnivetskaya, Jason Walker, Lu Wang, Zhengyuan Wang, Doyle V. Ward, Wesley Warren, Mark A. Watson, Christopher Wellington, Kris A. Wetterstrand, James R. White, Katarzyna Wilczek-Boney, Yuanqing Wu, Kristine M. Wylie, Todd Wylie, Chandri Yandava, Liang Ye, Yuzhen Ye, Shibu Yooseph, Bonnie P. Youmans, Lan Zhang, Yanjiao Zhou, Yiming Zhu, Laurie Zoloth, Jeremy D. Zucker, Bruce W. Birren, Richard A. Gibbs, Sarah K. Highlander, Barbara A. Methé, Karen E. Nelson, Joseph F. Petrosino, George M. Weinstock, Richard K. Wilson, and Owen White. 2012. “Structure, Function and Diversity of the Healthy Human Microbiome.” *Nature* 486(7402):207–14.

Hyun, Jung Kim, James Q. Boedicker, Wook Choi Jang, and Rustem F. Ismagilov. 2008. “Defined Spatial Structure Stabilizes a Synthetic Multispecies Bacterial Community.” *Proceedings of the National Academy of Sciences of the United States of America* 105(47):18188–93.

Ikmi, Aissam and Matthew C. Gibson. 2010. “Identification and in Vivo Characterization of NvFP-7R, a Developmentally Regulated Red Fluorescent Protein of Nematostella Vectensis.” *PloS One* 5(7):e11807.

Ikmi, Aissam, Sean A. McKinney, Kym M. Delventhal, and Matthew C. Gibson. 2014. “TALEN and CRISPR/Cas9-Mediated Genome Editing in the Early-Branching Metazoan Nematostella Vectensis.” *Nature Communications* 5:5486.

Ikmi, Aissam, Petrus J. Steenbergen, Marie Anzo, Mason R. McMullen, Anniek Stokkermans, Lacey R. Ellington, and Matthew C. Gibson. 2020. “Feeding-Dependent Tentacle Development in the Sea Anemone Nematostella Vectensis.” *Nature Communications 2020 11:1* 11(1):1–13.

Jaspers, Cornelia, Sebastian Fraune, A. Elizabeth Arnold, David J. Miller, Thomas C. G. Bosch, and Christian R. Voolstra. 2019. “Resolving Structure and Function of Metaorganisms through a Holistic Framework Combining Reductionist and Integrative Approaches.” *Zoology* 133:81–

87.

Johnke, Julia, Sebastian Fraune, Thomas C. G. Bosch, Ute Hentschel, and Hinrich Schulenburg. 2019. "Bdellovibrio and Like Organisms Are Predictors of Microbiome Diversity in Distinct Host Groups." *Microbial Ecology 2019 79:1* 79(1):252–57.

Jordán, Ferenc, Mario Lauria, Marco Scotti, Thanh Phuong Nguyen, Paurush Praveen, Melissa Morine, and Corrado Priami. 2015. "Diversity of Key Players in the Microbial Ecosystems of the Human Body." *Scientific Reports 2015 5:1* 5(1):1–10.

Karl, Philip J., Adrienne M. Hatch, Steven M. Arcidiacono, Sarah C. Pearce, Ida G. Pantoja-Feliciano, Laurel A. Doherty, and Jason W. Soares. 2018. "Effects of Psychological, Environmental and Physical Stressors on the Gut Microbiota." *Frontiers in Microbiology* 9(SEP).

Kashyap, Purna C., Angela Marcobal, Luke K. Ursell, Samuel A. Smits, Erica D. Sonnenburg, Elizabeth K. Costello, Steven K. Higginbottom, Steven E. Domino, Susan P. Holmes, David A. Relman, Rob Knight, Jeffrey I. Gordon, and Justin L. Sonnenburg. 2013. "Genetically Dictated Change in Host Mucus Carbohydrate Landscape Exerts a Diet-Dependent Effect on the Gut Microbiota." *Proceedings of the National Academy of Sciences of the United States of America* 110(42):17059–64.

Kawai, Taro and Shizuo Akira. 2010. "The Role of Pattern-Recognition Receptors in Innate Immunity: Update on Toll-like Receptors." *Nature Immunology* 11(5):373–84.

Kawasaki, Takumi and Taro Kawai. 2014. "Toll-Like Receptor Signaling Pathways." *Frontiers in Immunology* 0(SEP):461.

Kelava, Iva, Fabian Rentzsch, and Ulrich Technau. 2015. "Evolution of Eumetazoan Nervous Systems: Insights from Cnidarians." *Philosophical Transactions of the Royal Society of London. Series B, Biological Sciences* 370(1684).

Kelsic, Eric D., Jeffrey Zhao, Kalin Vetsigian, and Roy Kishony. 2015. "Counteraction of Antibiotic Production and Degradation Stabilizes Microbial Communities." *Nature* 521(7553):516–19.

Kerr, Benjamin, Margaret A. Riley, Marcus W. Feldman, and Brendan J. M. Bohannan. 2002. "Local Dispersal Promotes Biodiversity in a Real-Life Game of Rock-Paper-Scissors." *Nature* 418(6894):171–74.

Klein, Sylvia, Victoria Frazier, Timothy Readdean, Emily Lucas, Erica P. Diaz-Jimenez, Mitchell Sogin, Emil S. Ruff, and Karen Echeverri. 2021. "Common Environmental Pollutants Negatively Affect Development and Regeneration in the Sea Anemone Nematostella Vectensis Holobiont." *Frontiers in Ecology and Evolution* 9:884.

Koenig, Jeremy E., Aymé Spor, Nicholas Scalfone, Ashwana D. Fricker, Jesse Stombaugh, Rob Knight, Largus T. Angenent, and Ruth E. Ley. 2011. "Succession of Microbial Consortia in the

Developing Infant Gut Microbiome." *Proceedings of the National Academy of Sciences of the United States of America* 108 Suppl 1(Suppl 1):4578–85.

Koropatkin, Nicole M., Elizabeth A. Cameron, and Eric C. Martens. 2012. "How Glycan Metabolism Shapes the Human Gut Microbiota." *Nature Reviews. Microbiology* 10(5):323.

Krueger, Felix. 2021. "TrimGalore: A Wrapper around Cutadapt and FastQC to Consistently Apply Adapter and Quality Trimming to FastQ Files, with Extra Functionality for RRBS Data." Retrieved May 23, 2021 (https://github.com/FelixKrueger/TrimGalore).

Laforest-Lapointe, Isabelle and Marie Claire Arrieta. 2017. "Patterns of Early-Life Gut Microbial Colonization during Human Immune Development: An Ecological Perspective." *Frontiers in Immunology* 8(JUL):788.

Langmead, Ben and Steven L. Salzberg. 2012. "Fast Gapped-Read Alignment with Bowtie 2." *Nature Methods* 9(4):357–59.

Layden, Michael J., Michiel Boekhout, and Mark Q. Martindale. 2012. "Nematostella Vectensis Achaete-Scute Homolog NvashA Regulates Embryonic Ectodermal Neurogenesis and Represents an Ancient Component of the Metazoan Neural Specification Pathway." *Development* 139(5):1013–22.

Layden, Michael J., Fabian Rentzsch, and Eric Röttinger. 2016. "The Rise of the Starlet Sea Anemone Nematostella Vectensis as a Model System to Investigate Development and Regeneration." *Wiley Interdisciplinary Reviews: Developmental Biology* 5(4):408–28.

Leach, Whitney B., Tyler J. Carrier, and Adam M. Reitzel. 2019. "Diel Patterning in the Bacterial Community Associated with the Sea Anemone Nematostella Vectensis." *Ecology and Evolution* 9(17):9935–47.

Ley, Ruth E., Daniel A. Peterson, and Jeffrey I. Gordon. 2006. "Ecological and Evolutionary Forces Shaping Microbial Diversity in the Human Intestine." *Cell* 124(4):837–48.

Li, Heng, Bob Handsaker, Alec Wysoker, Tim Fennell, Jue Ruan, Nils Homer, Gabor Marth, Goncalo Abecasis, and Richard Durbin. 2009. "The Sequence Alignment/Map Format and SAMtools." *Bioinformatics* 25(16):2078–79.

Li, Xiang Yi, Cleo Pietschke, Sebastian Fraune, Philipp M. Altrock, Thomas C. G. Bosch, and Arne Traulsen. 2015. "Which Games Are Growing Bacterial Populations Playing?" *Journal of the Royal Society Interface* 12(108).

Lidicker, William Z. 1979. "A Clarification of Interactions in Ecological Systems." *BioScience* 29(8):475–77.

Litvak, Yael, Mariana X. Byndloss, and Andreas J. Bäumler. 2018. "Colonocyte Metabolism Shapes the Gut Microbiota." *Science (New York, N.Y.)* 362(6418).

References

Liu, Jiwen, Zhe Meng, · Xiaoyue Liu, and Xiao-Hua Zhang. 2019. “Microbial Assembly, Interaction, Functioning, Activity and Diversification: A Review Derived from Community Compositional Data.” *Marine Life Science & Technology* 1:112–28.

Login, Frédéric H., Séverine Balmand, Agnès Vallier, Carole Vincent-Monégat, Aurélien Vigneron, Michèle Weiss-Gayet, Didier Rochat, and Abdelaziz Heddi. 2011. “Antimicrobial Peptides Keep Insect Endosymbionts under Control.” *Science (New York, N.Y.)* 334(6054):362–65.

Longford, Sharon R., Alexandra H. Campbell, Shaun Nielsen, Rebecca J. Case, Staffan Kjelleberg, and Peter D. Steinberg. 2019. “Interactions within the Microbiome Alter Microbial Interactions with Host Chemical Defences and Affect Disease in a Marine Holobiont.” *Scientific Reports* 9(1):1–13.

Love, Michael I., Wolfgang Huber, and Simon Anders. 2014. “Moderated Estimation of Fold Change and Dispersion for RNA-Seq Data with DESeq2.” *Genome Biology* 15(12):550.

Luczynski, Pauline, Karen Anne Mc Vey Neufeld, Clara Seira Oriach, Gerard Clarke, Timothy G. Dinan, and John F. Cryan. 2016. “Growing up in a Bubble: Using Germ-Free Animals to Assess the Influence of the Gut Microbiota on Brain and Behavior.” *International Journal of Neuropsychopharmacology* 19(8):1–17.

Martin, Alyce M., Emily W. Sun, Geraint B. Rogers, and Damien J. Keating. 2019. “The Influence of the Gut Microbiome on Host Metabolism through the Regulation of Gut Hormone Release.” *Frontiers in Physiology* 10(MAR):428.

Martin, Michael U., Holger Wesche, Michael U. artin, and Holger Wesche. 2002. “Summary and Comparison of the Signaling Mechanisms of the Toll/Interleukin-1 Receptor Family.” *Biochimica et Biophysica Acta (BBA) - Molecular Cell Research* 1592(3):265–80.

Martindale, Mark Q., Kevin Pang, and John R. Finnerty. 2004. “Investigating the Origins of Triploblasty: ‘mesodermal’ Gene Expression in a Diploblastic Animal, the Sea Anemone Nematostella Vectensis (Phylum, Cnidaria; Class, Anthozoa).” *Development (Cambridge, England)* 131(10):2463–74.

McCafferty, Jonathan, Marcus Mühlbauer, Raad Z. Gharaibeh, Janelle C. Arthur, Ernesto Perez-Chanona, Wei Sha, Christian Jobin, and Anthony A. Fodor. 2013. “Stochastic Changes over Time and Not Founder Effects Drive Cage Effects in Microbial Community Assembly in a Mouse Model.” *ISME Journal* 7(11):2116–25.

McMurdie, Paul J. and Susan Holmes. 2013. “Phyloseq: An R Package for Reproducible Interactive Analysis and Graphics of Microbiome Census Data” edited by M. Watson. *PLoS ONE* 8(4):e61217.

Medina, M., A. G. Collins, J. D. Silberman, and M. L. Sogin. 2001. “Evaluating Hypotheses of Basal

Animal Phylogeny Using Complete Sequences of Large and Small Subunit RRNA." *Proceedings of the National Academy of Sciences of the United States of America* 98(17):9707–12.

Meibom, Karin L., Melanie Blokesch, Nadia A. Dolganov, Cheng Yen Wu, and Gary K. Schoolnik. 2005. "Chitin Induces Natural Competence in Vibrio Cholerae." *Science (New York, N.Y.)* 310(5755):1824–27.

Meiborn, Karin L., Xibing B. Li, Alex T. Nielsen, Cheng Yen Wu, Saul Roseman, and Gary K. Schoolnik. 2004. "The Vibrio Cholerae Chitin Utilization Program." *Proceedings of the National Academy of Sciences of the United States of America* 101(8):2524–29.

Miller, David J., Georg Hemmrich, Eldon E. Ball, David C. Hayward, Konstantin Khalturin, Noriko Funayama, Kiyokazu Agata, and Thomas C. G. Bosch. 2007. "The Innate Immune Repertoire in Cnidaria--Ancestral Complexity and Stochastic Gene Loss." *Genome Biology* 8(4):R59.

Miller, M. B. and B. L. Bassler. 2003. "Quorum Sensing in Bacteria." *Http://Dx.Doi.Org/10.1146/Annurev.Micro.55.1.165* 55:165–99.

Moran, Yehu, David Fredman, Daniela Praher, Xin Z. Li, Liang Meng Wee, Fabian Rentzsch, Phillip D. Zamore, Ulrich Technau, and Herve Seitz. 2014. "Cnidarian MicroRNAs Frequently Regulate Targets by Cleavage." *Genome Research* 24(4):651–63.

Moran, Yehu, Daniela Praher, David Fredman, and Ulrich Technau. 2013. "The Evolution of MicroRNA Pathway Protein Components in Cnidaria." *Molecular Biology and Evolution* 30(12):2541–52.

Mortzfeld, Benedikt M., Szymon Urbanski, Adam M. Reitzel, Sven Kunzel, Ulrich Technau, and Sebastian Fraune. 2016. "Response of Bacterial Colonization in Nematostella Vectensis to Development, Environment and Biogeography." *Environmental Microbiology* 18(6):1764–81.

Mounier, Jérôme, Christophe Monnet, Tatiana Vallaeys, Roger Arditi, Anne Sophie Sarthou, Arnaud Hélias, and Françoise Irlinger. 2008. "Microbial Interactions within a Cheese Microbial Community." *Applied and Environmental Microbiology* 74(1):172–81.

Mukherjee, Sohini, Hui Zheng, Mehabaw G. Derebe, Keith M. Callenberg, Carrie L. Partch, Darcy Rollins, Daniel C. Propheter, Josep Rizo, Michael Grabe, Qiu Xing Jiang, and Lora V. Hooper. 2014. "Antibacterial Membrane Attack by a Pore-Forming Intestinal C-Type Lectin." *Nature* 505(7481):103–7.

Murillo-Rincon, Andrea P., Alexander Klimovich, Eileen Pemöller, Jan Taubenheim, Benedikt Mortzfeld, René Augustin, and Thomas C. G. Bosch. 2017. "Spontaneous Body Contractions Are Modulated by the Microbiome of Hydra." *Scientific Reports* 7(1):1–9.

Nakashima, Keisuke, Satoshi Kimura, Yu Ogawa, Soichi Watanabe, Satoshi Soma, Toyoji Kaneko, Lixy Yamada, Hitoshi Sawada, Che Huang Tung, Tsai Ming Lu, Jr Kai Yu, Alejandro Villar-

Briones, Sakura Kikuchi, and Noriyuki Satoh. 2018. “Chitin-Based Barrier Immunity and Its Loss Predated Mucus-Colonization by Indigenous Gut Microbiota.” *Nature Communications 2018 9:1* 9(1):1–13.

Nemergut, D. R., S. K. Schmidt, T. Fukami, S. P. O’Neill, T. M. Bilinski, L. F. Stanish, J. E. Knelman, J. L. Darcy, R. C. Lynch, P. Wickey, and S. Ferrenberg. 2013. “Patterns and Processes of Microbial Community Assembly.” *Microbiology and Molecular Biology Reviews* 77(3):342–56.

Nichols, Robert G. and Emily R. Davenport. 2020. “The Relationship between the Gut Microbiome and Host Gene Expression: A Review.” *Human Genetics* 140(5):747–60.

van Nood, Els, Anne Vrieze, Max Nieuwdorp, Susana Fuentes, Erwin G. Zoetendal, Willem M. de Vos, Caroline E. Visser, Ed J. Kuijper, Joep F. W. M. Bartelsman, Jan G. P. Tijssen, Peter Speelman, Marcel G. W. Dijkgraaf, and Josbert J. Keller. 2013. “ Duodenal Infusion of Donor Feces for Recurrent Clostridium Difficile .” *New England Journal of Medicine* 368(5):407–15.

van Nouhuys, Saskia and Illka Hanski. 2005. “Metacommunities of Butterflies, Their Host Plants and Their Parasitoids.” Pp. 99–121 in *Metacommunities - Spatial Dynamics and Ecological Communities*.

O’Hara, Ann M. and Fergus Shanahan. 2006. “The Gut Flora as a Forgotten Organ.” *EMBO Reports* 7(7):688–93.

O’Toole, Paul W. and Ian B. Jeffery. 2015. “Gut Microbiota and Aging.” *Science* 350(6265):1214–15.

Oksanen, Jari, F. Guillaume Blanchet, Michael Friendly, Roeland Kindt, Pierre Legendre, Dan Mcglinn, Peter R. Minchin, R. B. O’hara, Gavin L. Simpson, Peter Solymos, M. Henry, H. Stevens, Eduard Szoecs, and Helene Wagner Maintainer. 2020. *Package “vegan” Title Community Ecology Package Version 2.5-7*.

Oliphant, Kaitlyn and Emma Allen-Vercoe. 2019. “Macronutrient Metabolism by the Human Gut Microbiome: Major Fermentation by-Products and Their Impact on Host Health.” *Microbiome* 7(1):1–15.

Patro, Rob, Geet Duggal, Michael I. Love, Rafael A. Irizarry, and Carl Kingsford. 2017. “Salmon Provides Fast and Bias-Aware Quantification of Transcript Expression.” *Nature Methods* 14(4):417–19.

Pereira, Fátima C. and David Berry. 2017. “Microbial Nutrient Niches in the Gut.” *Environmental Microbiology* 19(4):1366–78.

Pickard, Joseph M., Corinne F. Maurice, Melissa A. Kinnebrew, Michael C. Abt, Dominik Schenten, Tatyana V. Golovkina, Said R. Bogatyrev, Rustem F. Ismagilov, Eric G. Pamer, Peter J. Turnbaugh, and Alexander V. Chervonsky. 2014. “Rapid Fucosylation of Intestinal Epithelium

Sustains Host-Commensal Symbiosis in Sickness." *Nature* 514(7524):638–41.

Pietschke, Cleo, Christian Treitz, Sylvain Forêt, Annika Schultze, Sven Künzel, Andreas Tholey, Thomas C. G. Bosch, and Sebastian Fraune. 2017. "Host Modification of a Bacterial Quorum-Sensing Signal Induces a Phenotypic Switch in Bacterial Symbionts." *Proceedings of the National Academy of Sciences of the United States of America* 114(40):E8488–97.

Pogoreutz, Claudia, Nils Rädecker, Anny Cárdenas, Astrid Gärdes, Christian Wild, and Christian R. Voolstra. 2018. "Dominance of Endozoicomonas Bacteria throughout Coral Bleaching and Mortality Suggests Structural Inflexibility of the Pocillopora Verrucosa Microbiome." *Ecology and Evolution* 8(4):2240–52.

Poole, Angela Z. and Virginia M. Weis. 2014. "TIR-Domain-Containing Protein Repertoire of Nine Anthozoan Species Reveals Coral-Specific Expansions and Uncharacterized Proteins." *Developmental and Comparative Immunology* 46(2):480–88.

Putnam, Nicholas H., Mansi Srivastava, Uffe Hellsten, Bill Dirks, Jarrod Chapman, Asaf Salamov, Astrid Terry, Harris Shapiro, Erika Lindquist, Vladimir V Kapitonov, Jerzy Jurka, Grigory Genikhovich, Igor V Grigoriev, Susan M. Lucas, Robert E. Steele, John R. Finnerty, Ulrich Technau, Mark Q. Martindale, and Daniel S. Rokhsar. 2007. "Sea Anemone Genome Reveals Ancestral Eumetazoan Gene Repertoire and Genomic Organization." *Science (New York, N.Y.)* 317(5834):86–94.

Raimundo, I., R. Silva, L. Meunier, S. M. Valente, A. Lago-Lestón, T. Keller-Costa, and R. Costa. 2021. "Functional Metagenomics Reveals Differential Chitin Degradation and Utilization Features across Free-Living and Host-Associated Marine Microbiomes." *Microbiome* 9(1):1–18.

Rawls, John F., Michael A. Mahowald, Ruth E. Ley, and Jeffrey I. Gordon. 2006. "Reciprocal Gut Microbiota Transplants from Zebrafish and Mice to Germ-Free Recipients Reveal Host Habitat Selection." *Cell* 127(2):423–33.

RC, Edgar. 2010. "Search and Clustering Orders of Magnitude Faster than BLAST." *Bioinformatics (Oxford, England)* 26(19):2460–61.

Reese, Aspen T., Fátima C. Pereira, Arno Schintlmeister, David Berry, Michael Wagner, Laura P. Hale, Anchi Wu, Sharon Jiang, Heather K. Durand, Xiyou Zhou, Richard T. Premont, Anna Mae Diehl, Thomas M. O'Connell, Susan C. Alberts, Tyler R. Kartzinel, Robert M. Pringle, Robert R. Dunn, Justin P. Wright, and Lawrence A. David. 2018. "Microbial Nitrogen Limitation in the Mammalian Large Intestine." *Nature Microbiology* 3(12):1441.

Reichenbach, Tobias, Mauro Mobilia, and Erwin Frey. 2007. "Mobility Promotes and Jeopardizes Biodiversity in Rock-Paper-Scissors Games." *Nature* 448(7157):1046–49.

Reitzel, Adam M., Patrick M. Burton, Cassandra Krone, and John R. Finnerty. 2007. "Comparison of

Developmental Trajectories in the Starlet Sea Anemone Nematostella Vectensis." *Invertebrate Biology* 126(2):99–112.

Reitzel, Adam M., John A. Darling, James C. Sullivan, and John R. Finnerty. 2008. "Global Population Genetic Structure of the Starlet Anemone Nematostella Vectensis." *Biological Invasions* 10(8):1197–1213.

Reitzel, Am, T. Chu, S. Edquist, C. Genovese, C. Church, Am Tarrant, and Finnerty. 2013. "Physiological and Developmental Responses to Temperature by the Sea Anemone Nematostella Vectensis." *Marine Ecology Progress Series* 484:115–30.

Renfer, Eduard, Annette Amon-Hassenzahl, Patrick R. H. Steinmetz, and Ulrich Technau. 2010. "A Muscle-Specific Transgenic Reporter Line of the Sea Anemone, Nematostella Vectensis." *Proceedings of the National Academy of Sciences of the United States of America* 107(1):104–8.

Rentzsch, Fabian, Jens H. Fritzenwanker, Corinna B. Scholz, and Ulrich Technau. 2008. "FGF Signalling Controls Formation of the Apical Sensory Organ in the Cnidarian Nematostella Vectensis." *Development (Cambridge, England)* 135(10):1761–69.

Reshef, Leah, Omry Koren, Yossi Loya, Ilana Zilber-Rosenberg, and Eugene Rosenberg. 2006. "The Coral Probiotic Hypothesis." *Environmental Microbiology* 8(12):2068–73.

Riesgo, Ana, Nathan Farrar, Pamela J. Windsor, Gonzalo Giribet, and Sally P. Leys. 2014. "The Analysis of Eight Transcriptomes from All Poriferan Classes Reveals Surprising Genetic Complexity in Sponges." *Molecular Biology and Evolution* 31(5):1102–20.

Rollins-Smith, Louise A. 1998. "Metamorphosis and the Amphibian Immune System." *Immunological Reviews* 166:221–30.

Rosenberg, Eugene, Ariel Kushmaro, Esti Kramarsky-Winter, Ehud Banin, and Loya Yossi. 2009. "The Role of Microorganisms in Coral Bleaching." *The ISME Journal* 3(2):139–46.

Roswall, Josefine, Lisa M. Olsson, Petia Kovatcheva-Datchary, Staffan Nilsson, Valentina Tremaroli, Marie Christine Simon, Pia Kiilerich, Rozita Akrami, Manuela Krämer, Mathias Uhlén, Anders Gummesson, Karsten Kristiansen, Jovanna Dahlgren, and Fredrik Bäckhed. 2021. "Developmental Trajectory of the Healthy Human Gut Microbiota during the First 5 Years of Life." *Cell Host & Microbe* 29(5):765-776.e3.

Röttinger, Eric. 2021. "Nematostella Vectensis, an Emerging Model for Deciphering the Molecular and Cellular Mechanisms Underlying Whole-Body Regeneration." *Cells 2021, Vol. 10, Page 2692* 10(10):2692.

Rottinger, Eric, Paul Dahlin, and Mark Q. Martindale. 2012. "A Framework for the Establishment of a Cnidarian Gene Regulatory Network for 'Endomesoderm' Specification: The Inputs of Ss-

Catenin/TCF Signaling." *PLoS Genetics* 8(12):e1003164.

Round, June L. and Sarkis K. Mazmanian. 2009. "The Gut Microbiota Shapes Intestinal Immune Responses during Health and Disease." *Nature Reviews Immunology* 9(5):313–23.

Salzman, Nita H., Kuiechun Hung, Dipica Haribhai, Hiutung Chu, Jenny Karlsson-Sjöberg, Elad Amir, Paul Teggatz, Melissa Barman, Michael Hayward, Daniel Eastwood, Maaike Stoel, Yanjiao Zhou, Erica Sodergren, George M. Weinstock, Charles L. Bevins, Calvin B. Williams, and Nicolaas A. Bos. 2010. "Enteric Defensins Are Essential Regulators of Intestinal Microbial Ecology." *Nature Immunology* 11(1):76–83.

Schefe, Jan H., Kerstin E. Lehmann, Ivo R. Buschmann, Thomas Unger, and Heiko Funke-Kaiser. n.d. "Quantitative Real-Time RT-PCR Data Analysis: Current Concepts and the Novel 'Gene Expression's C T Difference' Formula."

Schmitt, Susanne, Peter Tsai, James Bell, Jane Fromont, Micha Ilan, Niels Lindquist, Thierry Perez, Allen Rodrigo, Peter J. Schupp, Jean Vacelet, Nicole Webster, Ute Hentschel, and Michael W. Taylor. 2012. "Assessing the Complex Sponge Microbiota: Core, Variable and Species-Specific Bacterial Communities in Marine Sponges." *The ISME Journal* 6(3):564–76.

Schubert, Alyxandria M., Hamide Sinani, and Patrick D. Schloss. 2015. "Antibiotic-Induced Alterations of the Murine Gut Microbiota and Subsequent Effects on Colonization Resistance against Clostridium Difficile." *MBio* 6(4).

Schwaiger, Michaela, Anna Schonauer, Andre F. Rendeiro, Carina Pribitzer, Alexandra Schauer, Anna F. Gilles, Johannes B. Schinko, Eduard Renfer, David Fredman, and Ulrich Technau. 2014. "Evolutionary Conservation of the Eumetazoan Gene Regulatory Landscape." *Genome Research* 24(4):639–50.

Scotti, M. and F. Jordán. 2010. "Relationships between Centrality Indices and Trophic Levels in Food Webs." *Community Ecology 2010 11:1* 11(1):59–67.

Sebé-Pedrós, Arnau, Baptiste Saudemont, Elad Chomsky, Flora Plessier, Marie Pierre Mailhé, Justine Renno, Yann Loe-Mie, Aviezer Lifshitz, Zohar Mukamel, Sandrine Schmutz, Sophie Novault, Patrick R. H. Steinmetz, François Spitz, Amos Tanay, and Heather Marlow. 2018. "Cnidarian Cell Type Diversity and Regulation Revealed by Whole-Organism Single-Cell RNA-Seq." *Cell* 173(6):1520-1534.e20.

Seemann, Torsten. 2014. "Prokka: Rapid Prokaryotic Genome Annotation." *Bioinformatics* 30(14):2068–69.

Seemann, Torsten. 2020. "ABRicate: Mass Screening of Contigs for Antimicrobial and Virulence Genes." Retrieved May 23, 2021 (https://github.com/tseemann/abricate).

Shade, Ashley, Hannes Peter, Steven D. Allison, Didier L. Baho, Mercè Berga, Helmut Bürgmann,

David H. Huber, Silke Langenheder, Jay T. Lennon, Jennifer B. H. Martiny, Kristin L. Matulich, Thomas M. Schmidt, and Jo Handelsman. 2012. “Fundamentals of Microbial Community Resistance and Resilience.” *Frontiers in Microbiology* 3(DEC).

Shao, Yan, Samuel C. Forster, Evdokia Tsaliki, Kevin Vervier, Angela Strang, Nandi Simpson, Nitin Kumar, Mark D. Stares, Alison Rodger, Peter Brocklehurst, Nigel Field, and Trevor D. Lawley. 2019. “Stunted Microbiota and Opportunistic Pathogen Colonization in Caesarean-Section Birth.” *Nature 2019 574:7776* 574(7776):117–21.

Shetty, Sudarshan A., Ben Kuipers, Siavash Atashgahi, Steven Aalvink, Hauke Smidt, and Willem M. de Vos. 2022. “Inter-Species Metabolic Interactions in an In-Vitro Minimal Human Gut Microbiome of Core Bacteria.” *Npj Biofilms and Microbiomes 2022 8:1* 8(1):1–13.

Sieber, Michael, Lucía Pita, Nancy Weiland-Bräuer, Philipp Dirksen, Jun Wang, Benedikt Mortzfeld, Sören Franzenburg, Ruth A. Schmitz, John F. Baines, Sebastian Fraune, Ute Hentschel, Hinrich Schulenburg, Thomas C.G. Bosch, and Arne Traulsen. 2019. “Neutrality in the Metaorganism.” *PLoS Biology* 17(6):e3000298.

Sieber, Michael, Lucía Pita, Nancy Weiland-Bräuer, Philipp Dirksen, Jun Wang, Benedikt Mortzfeld, Sören Franzenburg, Ruth A. Schmitz, John F. Baines, Sebastian Fraune, Ute Hentschel, Hinrich Schulenburg, Thomas C. G. Bosch, and Arne Traulsen. 2019. “Neutrality in the Metaorganism.” *PLOS Biology* 17(6):e3000298.

Sieber, Michael, Arne Traulsen, Hinrich Schulenburg, and Angela E. Douglas. 2021. “On the Evolutionary Origins of Host-Microbe Associations.” *Proceedings of the National Academy of Sciences of the United States of America* 118(9).

Simon, Jean Christophe, Julian R. Marchesi, Christophe Mougel, and Marc André Selosse. 2019. “Host-Microbiota Interactions: From Holobiont Theory to Analysis.” *Microbiome* 7(1):1–5.

Simon, M., AL Alldredge, F. Azam, M. Simon, AL Alldredge, and F. Azam. 1990. “Bacterial Carbon Dynamics on Marine Snow.” *MEPS* 65:205–11.

Simon, Meinhard, Hans Peter Grossart, Bernd Schweitzer, and Helle Ploug. 2002. “Microbial Ecology of Organic Aggregates in Aquatic Ecosystems.” *Aquatic Microbial Ecology* 28(2):175–211.

Sloan, William T., Mary Lunn, Stephen Woodcock, Ian M. Head, Sean Nee, and Thomas P. Curtis. 2006. “Quantifying the Roles of Immigration and Chance in Shaping Prokaryote Community Structure.” *Environmental Microbiology* 8(4):732–40.

Smith, Patrick M., Michael R. Howitt, Nicolai Panikov, Monia Michaud, Carey Ann Gallini, Mohammad Bohlooly-Y, Jonathan N. Glickman, and Wendy S. Garrett. 2013. “The Microbial Metabolites, Short-Chain Fatty Acids, Regulate Colonic Treg Cell Homeostasis.” *Science (New*

York, N.Y.) 341(6145):569–73.

Souza, Claudiana P., Bianca C. Almeida, Rita R. Colwell, and Irma N. G. Rivera. 2011. "The Importance of Chitin in the Marine Environment." *Marine Biotechnology* 13(5):823–30.

Sprockett, Daniel, Tadashi Fukami, and David A. Relman. 2018. "Role of Priority Effects in the Early-Life Assembly of the Gut Microbiota." *Nature Reviews Gastroenterology & Hepatology* 15(4):197–205.

Stefanik, Derek J., Lauren E. Friedman, and John R. Finnerty. 2013. "Collecting, Rearing, Spawning and Inducing Regeneration of the Starlet Sea Anemone, Nematostella Vectensis." *Nature Protocols* 8(5):916–23.

Steinmetz, Patrick R. H. 2019. "A Non-Bilaterian Perspective on the Development and Evolution of Animal Digestive Systems." *Cell and Tissue Research 2019 377:3* 377(3):321–39.

Subramanian, Sathish, Sayeeda Huq, Tanya Yatsunenko, Rashidul Haque, Mustafa Mahfuz, Mohammed A. Alam, Amber Benezra, Joseph Destefano, Martin F. Meier, Brian D. Muegge, Michael J. Barratt, Laura G. VanArendonk, Qunyuan Zhang, Michael A. Province, William A. Petri, Tahmeed Ahmed, and Jeffrey I. Gordon. 2014. "Persistent Gut Microbiota Immaturity in Malnourished Bangladeshi Children." *Nature 2014 510:7505* 510(7505):417–21.

Tardent, Pierre. 1995. "The Cnidarian Cnidocyte, a Hightech Cellular Weaponry." *BioEssays* 17(4):351–62.

Technau, Ulrich and Robert E. Steele. 2011. "Evolutionary Crossroads in Developmental Biology: Cnidaria." *Development (Cambridge, England)* 138(8):1447–58.

Thiele, Stefan, Bernhard M. Fuchs, Rudolf Amann, and Morten H. Iversen. 2015. "Colonization in the Photic Zone and Subsequent Changes during Sinking Determine Bacterial Community Composition in Marine Snow." *Applied and Environmental Microbiology* 81(4):1463–71.

Tucker, Richard P., Bradley Shibata, and Thomas N. Blankenship. 2011. "Ultrastructure of the Mesoglea of the Sea Anemone Nematostella Vectensis (Edwardsiidae)." *Invertebrate Biology* 130(1):11–24.

Tulin, Sarah, Derek Aguiar, Sorin Istrail, and Joel Smith. 2013. "A Quantitative Reference Transcriptome for Nematostella Vectensis Early Embryonic Development: A Pipeline for de Novo Assembly in Emerging Model Systems." *EvoDevo* 4:16.

Turnbaugh, Peter J., Ruth E. Ley, Michael A. Mahowald, Vincent Magrini, Elaine R. Mardis, and Jeffrey I. Gordon. 2006. "An Obesity-Associated Gut Microbiome with Increased Capacity for Energy Harvest." *Nature* 444(7122):1027–31.

Udayangani, R. M. C., S. H. S. Dananjaya, Chamilani Nikapitiya, Gang Joon Heo, Jehee Lee, and Mahanama De Zoysa. 2017. "Metagenomics Analysis of Gut Microbiota and Immune

Modulation in Zebrafish (Danio Rerio) Fed Chitosan Silver Nanocomposites." *Fish & Shellfish Immunology* 66:173–84.

Vandepas, Lauren. 2018. "Chitin the Good Fight – Identification and Description of Chitin and Its Genes in Cnidaria." Retrieved August 5, 2022 (https://digital.lib.washington.edu/researchworks/handle/1773/43308).

Vellend, Mark. 2010. "Conceptual Synthesis in Community Ecology." *Quarterly Review of Biology* 85(2):183–206.

Vigneron, Aurélien, Florent Masson, Agnès Vallier, Séverine Balmand, Marjolaine Rey, Carole Vincent-Monégat, Emre Aksoy, Etienne Aubailly-Giraud, Anna Zaidman-Rémy, and Abdelaziz Heddi. 2014. "Insects Recycle Endosymbionts When the Benefit Is Over." *Current Biology : CB* 24(19):2267–73.

W, Li and Godzik A. 2006. "Cd-Hit: A Fast Program for Clustering and Comparing Large Sets of Protein or Nucleotide Sequences." *Bioinformatics (Oxford, England)* 22(13).

Wainright, P., G. Hinkle, M. Sogin, and S. Stickel. 1993. "Monophyletic Origins of the Metazoa." *Science* 260(5106):340–42.

Walter, Jens and Ruth Ley. 2011. "The Human Gut Microbiome: Ecology and Recent Evolutionary Changes." *Http://Dx.Doi.Org/10.1146/Annurev-Micro-090110-102830* 65:411–29.

Warner, Jacob F., Vincent Guerlais, Aldine R. Amiel, Hereroa Johnston, Karine Nedoncelle, and Eric Röttinger. 2018. "NvERTx: A Gene Expression Database to Compare Embryogenesis and Regeneration in the Sea Anemone *Nematostella Vectensis*." *Development*.

Wasserman, Stanley and Katherine Faust. 1994. "Social Network Analysis: Methods and Applications."

Watanabe, Hiroshi, Toshitaka Fujisawa, and Thomas W. Holstein. 2009. "Cnidarians and the Evolutionary Origin of the Nervous System." *Development, Growth & Differentiation* 51(3):167–83.

Wei, Zhong, Tianjie Yang, Ville Petri Friman, Yangchun Xu, Qirong Shen, and Alexandre Jousset. 2015. "Trophic Network Architecture of Root-Associated Bacterial Communities Determines Pathogen Invasion and Plant Health." *Nature Communications* 6.

Weiher, Evan and Paul A. Keddy. 1995. "Assembly Rules, Null Models, and Trait Dispersion: New Questions from Old Patterns." *Oikos*. Retrieved May 14, 2021 (https://www.sciencebase.gov/catalog/item/50538693e4b097cd4fce1b66).

Weiland-Bräuer, Nancy, Martin A. Fischer, Nicole Pinnow, and Ruth A. Schmitz. 2019. "Potential Role of Host-Derived Quorum Quenching in Modulating Bacterial Colonization in the Moon Jellyfish Aurelia Aurita." *Scientific Reports* 9(1):1–12.

Weiland-Bräuer, Nancy, Nicole Pinnow, Daniela Langfeldt, Anna Roik, Simon Güllert, Cynthia M. Chibani, Thorsten B. H. Reusch, and Ruth A. Schmitz. 2020. "The Native Microbiome Is Crucial for Offspring Generation and Fitness of Aurelia Aurita." *MBio* 11(6):1–20.

Welch, Jessica L. Mar., Yuko Hasegawa, Nathan P. McNulty, Jeffrey I. Gordon, and Gary G. Borisy. 2017. "Spatial Organization of a Model 15-Member Human Gut Microbiota Established in Gnotobiotic Mice." *Proceedings of the National Academy of Sciences of the United States of America* 114(43):E9105–14.

Wickham, Hadley. 2009. *Ggplot2 - Elegant Graphics for Data Analysis*. Springer-Verlag.

Williams, Leah M., Lauren E. Fuess, Joseph J. Brennan, Katelyn M. Mansfield, Erick Salas-Rodriguez, Julianne Welsh, Jake Awtry, Sarah Banic, Cecilia Chacko, Aarthia Chezian, Donovan Dowers, Felicia Estrada, Yu Hsuan Hsieh, Jiawen Kang, Wanwen Li, Zoe Malchiodi, John Malinowski, Sean Matuszak, Thomas McTigue, David Mueller, Brian Nguyen, Michelle Nguyen, Phuong Nguyen, Sinead Nguyen, Ndidi Njoku, Khusbu Patel, William Pellegrini, Tessa Pliakas, Deena Qadir, Emma Ryan, Alex Schiffer, Amber Thiel, Sarah A. Yunes, Kathryn E. Spilios, Jorge H. Pinzón C, Laura D. Mydlarz, and Thomas D. Gilmore. 2018. "A Conserved Toll-like Receptor-to-NF-KB Signaling Pathway in the Endangered Coral Orbicella Faveolata." *Developmental & Comparative Immunology* 79:128–36.

Williams, R. B. 2007. "A Redescription of the Brackish-Water Sea Anemone Nematostella Vectensis Stephenson, with an Appraisal of Congeneric Species." *Http://Dx.Doi.Org/10.1080/00222937500770051* 9(1):51–64.

Winter, Sebastian E., Christopher A. Lopez, and Andreas J. Bäumler. 2013. "The Dynamics of Gut-Associated Microbial Communities during Inflammation." *EMBO Reports* 14(4):319.

Wu, Guojun, Naisi Zhao, Chenhong Zhang, Yan Y. Lam, and Liping Zhao. 2021. "Guild-Based Analysis for Understanding Gut Microbiome in Human Health and Diseases." *Genome Medicine* 13(1):1–12.

Wu, Liang and Yubin Luo. 2021. "Bacterial Quorum-Sensing Systems and Their Role in Intestinal Bacteria-Host Crosstalk." *Frontiers in Microbiology* 12:101.

Zasloff, Michael. 2002. "Antimicrobial Peptides of Multicellular Organisms." *Nature* 415(6870):389–95.

Zelezniak, Aleksej, Sergej Andrejev, Olga Ponomarova, Daniel R. Mende, Peer Bork, and Kiran Raosaheb Patil. 2015. "Metabolic Dependencies Drive Species Co-Occurrence in Diverse Microbial Communities." *Proceedings of the National Academy of Sciences of the United States of America* 112(20):6449–54.

Zemach, Assaf, Ivy E. McDaniel, Pedro Silva, and Daniel Zilberman. 2010. "Genome-Wide

Evolutionary Analysis of Eukaryotic DNA Methylation." *Science (New York, N.Y.)* 328(5980):916–19.

Zenkert, Claudia, Toshio Takahashi, Mark Oliver Diesner, and Suat Özbek. 2011. "Morphological and Molecular Analysis of the Nematostella Vectensis Cnidom." *PLOS ONE* 6(7):e22725.

Zheng, Danping, Timur Liwinski, and Eran Elinav. 2020. "Interaction between Microbiota and Immunity in Health and Disease." *Cell Research* 30(6):492–506.

Zheng, Junping, Gong Cheng, Qiongyu Li, Siming Jiao, Cui Feng, Xiaoming Zhao, Heng Yin, Yuguang Du, and Hongtao Liu. 2018. "Chitin Oligosaccharide Modulates Gut Microbiota and Attenuates High-Fat-Diet-Induced Metabolic Syndrome in Mice." *Marine Drugs* 16(2).

Zheng, Junping, Xubing Yuan, Gong Cheng, Siming Jiao, Cui Feng, Xiaoming Zhao, Heng Yin, Yuguang Du, and Hongtao Liu. 2018. "Chitosan Oligosaccharides Improve the Disturbance in Glucose Metabolism and Reverse the Dysbiosis of Gut Microbiota in Diabetic Mice." *Carbohydrate Polymers* 190:77–86.

Zhou, Jizhong and Daliang Ning. 2017. "Stochastic Community Assembly: Does It Matter in Microbial Ecology?" *Microbiology and Molecular Biology Reviews* 81(4).

Zimmermann, Bob, Sofia M. C. Robb, Grigory Genikhovich, Whitney J. Fropf, Lukas Weilguny, Shuonan He, Shiyuan Chen, Jessica Lovegrove-Walsh, Eric M. Hill, Katerina Ragkousi, Daniela Praher, David Fredman, Yehu Moran, Matthew C. Gibson, and Ulrich Technau. 2020. "Sea Anemone Genomes Reveal Ancestral Metazoan Chromosomal Macrosynteny." *BioRxiv* 2020.10.30.359448.

Zimmermann, Johannes, Christoph Kaleta, and Silvio Waschina. 2021. "Gapseq: Informed Prediction of Bacterial Metabolic Pathways and Reconstruction of Accurate Metabolic Models." *Genome Biology* 22(1):81.

8 Appendix

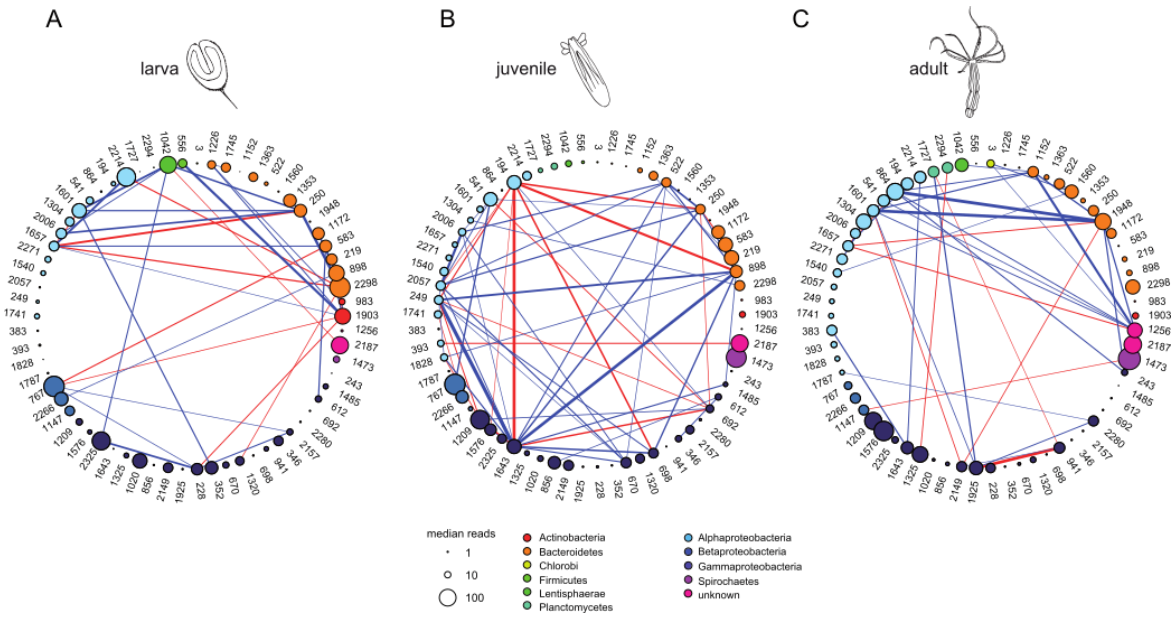

Suppl. Fig. 1 *Microbial co-occurrence network among OTUs during the whole development of N. vectensis. Nodes (N = 66) are the OTUs involved in at least one strong interaction during the whole development or the three developmental stages; their color reflects taxonomic affiliation. The size of the nodes is proportional to the log10 of the median reads (relative abundance of the OTUs) along the whole development. OTUs are arranged by taxonomy and relative abundance (numbers refer to OTU-numbers in Mortzfeld et al., 2016). Links represent the interactions (i.e. significant co-occurrences; pseudo p-value ≤ 0.05) with absolute correlation values above 0.5. Red links are negative interactions, while blue links stand for positive interactions; the thickness of the links is proportional to the strength of the interactions.*

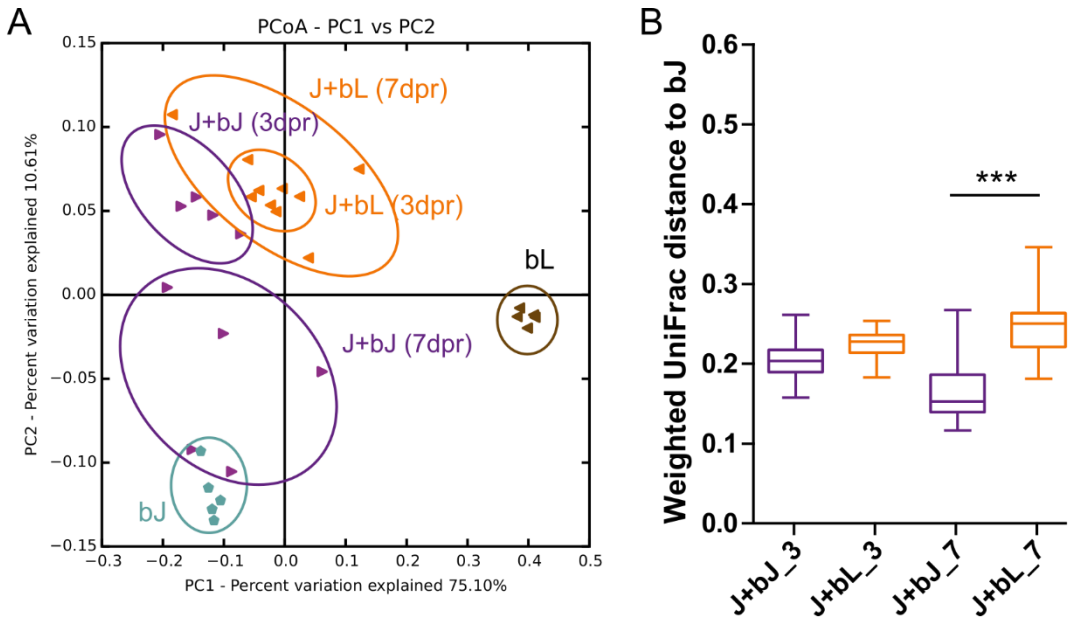

Suppl. Fig. 2 *Juvenile polyps are recolonized differentially with larvae (bL) or juvenile bacteria (bJ). (A) Bacterial communities were clustered using PCoA of the Weighted UniFrac distance matrix. The percent variation explained by the principal coordinates is indicated at the axes. bL – source bacteria of larvae, bJ – source bacteria of juvenile polyps, J+bL – bacterial community of polyps recolonized with bL after 3dpr and 7dpr, J+bJ – bacterial community of polyps recolonized with bJ after 3dpr and 7dpr. (B) Weighted UniFrac distances to bJ after 3dpr and 7dpr. Statistical analysis was conducted using analysis of variance (ANOVA; ***p < 0.001, n = 5).*

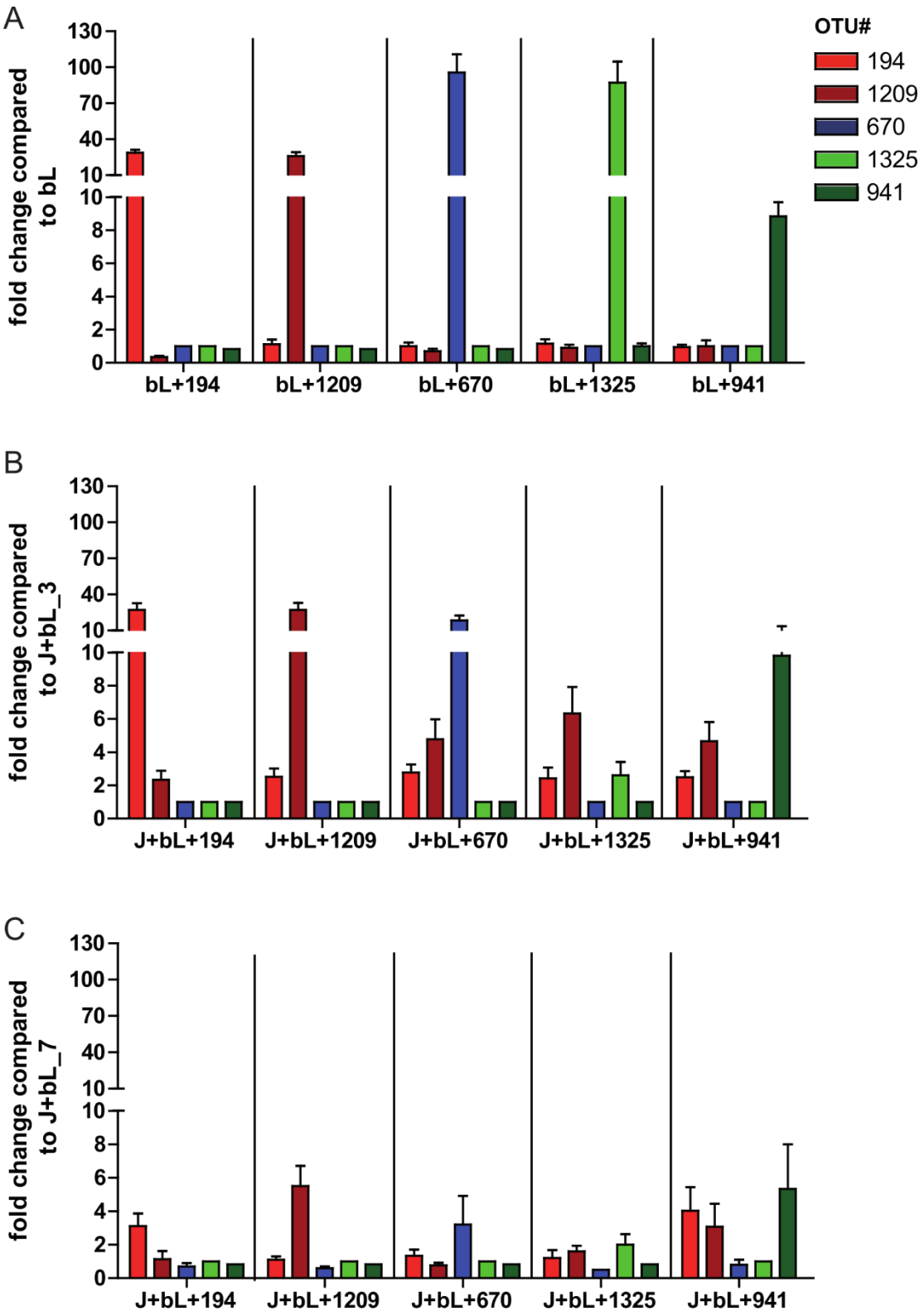

Suppl. Fig. 3 *Overrepresentation of isolates in inocula (A), 3dpr (B) and 7dpr (C) in comparison to control colonization. Fold changes were calculated based on normalized sequencing counts of the representative OTUs (on 97% similarity).*

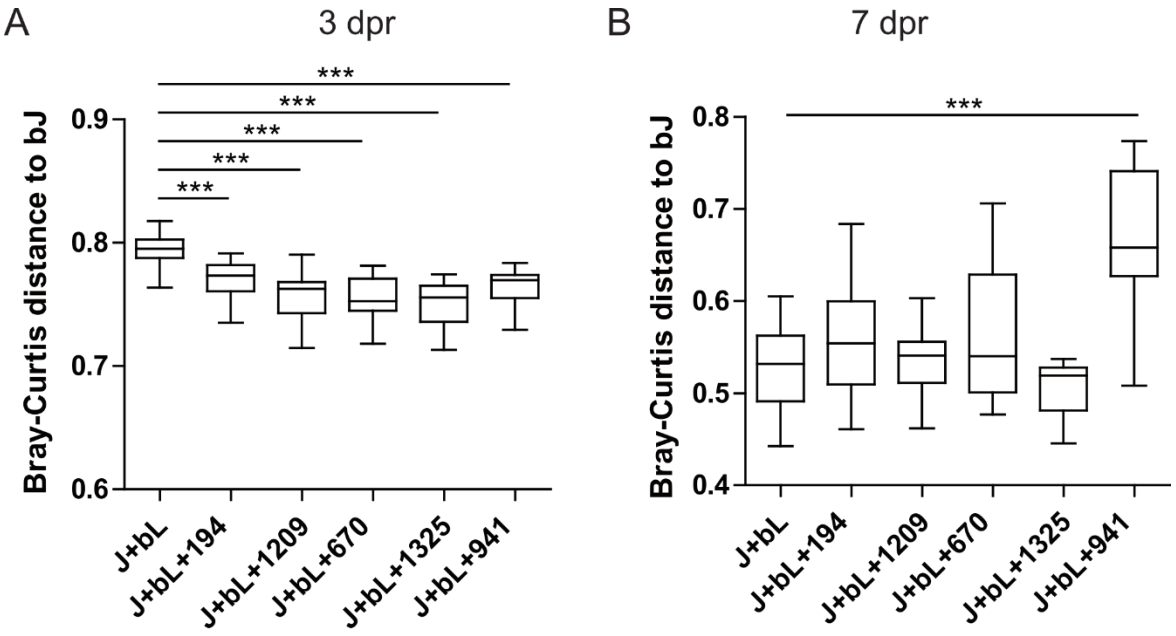

Suppl. Fig. 4 *Bray-Curtis distances to bJ after 3dpr (A) and 7dpr (B) upon recolonization with a mixture of larval bacteria and single bacterial isolates. Statistical analysis was conducted using analysis of variance (ANOVA; ***p < 0.001).*

Suppl. Table 1 *Number of links in the co-occurence network of larvae, juvenile and adult polyps for all OTUs.*

#OTU	whole development	larva	juvenile	adult	taxon
1903		8			Actinobacteria
983		2			Actinobacteria
2298	4	5	1		Bacteroidetes
898	2	2	8		Bacteroidetes
219			1		Bacteroidetes
583		4	1		Bacteroidetes
1172		1			Bacteroidetes
1948	2			7	Bacteroidetes
250		6	8		Bacteroidetes
1353	4	1			Bacteroidetes
1560				3	Bacteroidetes
522			6	1	Bacteroidetes
1363			1		Bacteroidetes
1152				5	Bacteroidetes
1745		1			Bacteroidetes
1226		3			Bacteroidetes
3				2	Chlorobi
556		1			Firmicutes
1042	1	5		1	Lentisphaerae
2294				1	Planctomycetes
1727				2	Planctomycetes
2214	1	2		1	Proteobacteria-alpha
194	1		8	1	Proteobacteria-alpha
864	1			6	Proteobacteria-alpha
541			5	1	Proteobacteria-alpha
1601	1	4		7	Proteobacteria-alpha
1304			1	1	Proteobacteria-alpha
2006		2	5		Proteobacteria-alpha
1657		6		5	Proteobacteria-alpha
2271				1	Proteobacteria-alpha
1540				1	Proteobacteria-alpha
2057			8		Proteobacteria-alpha
249	1		9		Proteobacteria-alpha
1741			1		Proteobacteria-alpha
383				1	Proteobacteria-alpha
393			1		Proteobacteria-alpha
1828			4		Proteobacteria-alpha
1787				1	Proteobacteria-alpha
767	4	4	1		Proteobacteria-beta
2266	1	1	1		Proteobacteria-beta
1147				1	Proteobacteria-beta
1209	5		4		Proteobacteria-gamma

1576	1		2		Proteobacteria-gamma
2325	1	2			Proteobacteria-gamma
1643	1		14	2	Proteobacteria-gamma
1325				1	Proteobacteria-gamma
1020	3				Proteobacteria-gamma
856			1		Proteobacteria-gamma
2149				3	Proteobacteria-gamma
1925				4	Proteobacteria-gamma
228		4			Proteobacteria-gamma
352		1			Proteobacteria-gamma
670			5		Proteobacteria-gamma
1320		1			Proteobacteria-gamma
698			4		Proteobacteria-gamma
941				3	Proteobacteria-gamma
346			1		Proteobacteria-gamma
2157		2			Proteobacteria-gamma
2280				2	Proteobacteria-gamma
692			6		Proteobacteria-gamma
612		1	2		Proteobacteria-gamma
1485			2		Proteobacteria-gamma
243				2	Proteobacteria-gamma
1473	7			1	Spirochaetes
2187	2	1	1		Unknown
1256	1			7	Unknown

Suppl. Table 2 *Clusters with Genome IDs of sequenced bacterial strains of Nematostella, and NCBI database IDs for blasted genomes (97% identity).*

cluster	**genome isolates**	**assembly (NCBI)**		**cluster**	**genome isolates**	**assembly (NCBI)**
cluster0	G21637-S1			**cluster1824**		GCF_001886735.1
cluster1	G21616-S1			**cluster1825**		GCF_000016285.1
cluster10	G21612-S1			**cluster1828**		GCF_001402915.1
cluster100		GCF_002893805.1		**cluster1889**		GCF_002237555.1
cluster1030		GCF_003076415.1		**cluster2**	G21638-S1	
cluster1036		GCF_900187235.1		**cluster20**	G21628-S1	
cluster1040		GCF_006094415.1		**cluster212**		GCF_000010185.1
cluster107		GCF_900474605.1		**cluster23**	G21630-S1	
cluster11	G21609-S1			**cluster24**	G21631-S1	

cluster1101		GCF_008693925.1		**cluster241**		GCF_000208405.1
cluster1164		GCF_000349845.1		**cluster25**	G21632-S1	
cluster1168		GCF_006970865.1		**cluster260**		GCF_001688845.2
cluster1170		GCF_000260985.4		**cluster27**	G21646-S1	
cluster1171		GCF_001895265.1		**cluster3**	G21629-S1	
cluster1172		GCF_003952785.1		**cluster30**	G21597-S1	
cluster1173		GCF_900637825.1		**cluster31**	G21626-S1	
cluster1174	JB_10			**cluster32**	G21636-S1	
cluster1176		GCF_001703595.1		**cluster34**	G21625-S1	
cluster1177		GCF_002310835.1		**cluster35**	G21617-S1	
cluster1179		GCF_003860605.1		**cluster352**		GCF_002763715.1
cluster1182		GCF_002944765.1		**cluster367**		GCF_000217835.1
cluster1183		GCF_003019815.1		**cluster38**	G21619-S1	
cluster1186		GCF_003070865.1		**cluster388**		GCF_008330165.1
cluster1187		GCF_002752675.1		**cluster389**		GCF_002215535.1
cluster1191		GCF_003860525.1		**cluster39**	G21618-S1	
cluster1192		GCF_900638245.1		**cluster390**		GCF_000972725.1
cluster120		GCF_000020605.1		**cluster392**		GCF_902387545.1
cluster1260		GCF_000015305.1		**cluster393**		GCF_900478415.1
cluster1265		GCF_000177535.2		**cluster394**		GCF_003410415.1
cluster1272		GCF_003122385.1		**cluster395**		GCF_003595625.1
cluster1305		GCF_002310795.1		**cluster4**	G21635-S1	
cluster1307		GCF_002966495.1		**cluster40**	G21606-S1	
cluster1309	G21654-S1			**cluster440**		GCF_001688725.2
cluster1311		GCF_003614435.1		**cluster444**		GCF_000478255.1
cluster1313		GCF_000954115.1		**cluster445**		GCF_002173495.1
cluster1315		GCF_001941825.1		**cluster447**		GCF_004006295.1
cluster1316		GCF_000739375.1		**cluster449**		GCF_003966935.1
cluster1318		GCF_002442575.1		**cluster452**		GCF_000698885.1
cluster1323		GCF_002910775.2		**cluster455**		GCF_001590685.1
cluster1331		GCF_000497265.2		**cluster456**		GCF_002356415.1
cluster1472		GCF_000833295.1		**cluster459**		GCF_900635935.1
cluster15	G21599-S1			**cluster50**		GCF_003072625.1
cluster159		GCF_002073435.2		**cluster51**		GCF_002119645.1
cluster1599		GCF_003330885.1		**cluster551**		GCF_000027165.1

cluster16	G21598-S1			**cluster608**		GCF_900638255.1
cluster160		GCF_001689125.2		**cluster612**		GCF_000196315.1
cluster1605		GCF_006385135.1		**cluster62**		GCF_003316915.1
cluster1615		GCF_004564135.1		**cluster667**		GCF_003721455.1
cluster1621		GCF_001543345.1		**cluster668**		GCF_900465055.1
cluster1657		GCF_000013885.1		**cluster672**		GCF_001729525.1
cluster1660		GCF_000067045.1		**cluster674**		GCF_003030985.1
cluster1696		GCF_001678945.1		**cluster703**		GCF_002234495.1
cluster1697		GCF_001620265.1		**cluster708**		GCF_900638535.1
cluster1698		GCF_006740765.1		**cluster749**		GCF_001653935.1
cluster1699		GCF_006517275.1		**cluster750**	G21653-S1	
cluster17	G21627-S1			**cluster752**		GCF_000597785.2
cluster1700		GCF_006351965.1		**cluster753**		GCF_006149185.1
cluster1701		GCF_002222635.1		**cluster754**		GCF_007833295.1
cluster1703	G21655-S1			**cluster759**		GCF_002209245.2
cluster1704		GCF_002850435.1		**cluster761**		GCF_002257605.1
cluster1715		GCF_000021865.1		**cluster764**		GCF_000185965.1
cluster1718	G21611-S1			**cluster8**	G21610-S1	
cluster1719		GCF_004328555.1		**cluster80**		GCF_003288115.1
cluster1727		GCF_004795895.1		**cluster817**		GCF_001275345.1
cluster1734		GCF_000013565.1		**cluster87**		GCF_006704185.1
cluster1737		GCF_002865605.1		**cluster875**		GCF_001010505.1
cluster1738		GCF_003711185.1		**cluster876**		GCF_004295665.1
cluster1743		GCF_004010775.1		**cluster880**		GCF_003006155.1
cluster1745		GCF_003285265.1		**cluster887**		GCF_001266795.1
cluster1746		GCF_002741015.1		**cluster893**		GCF_000709495.1
cluster1747		GCF_001889025.1		**cluster897**		GCF_003611035.1
cluster1748		GCF_002002865.1		**cluster9**	G21601-S1	
cluster1749		GCF_007998985.1		**cluster90**		GCF_900186885.1
cluster1751		GCF_000444995.1		**cluster91**		GCF_000023045.1
cluster1753		GCF_004354345.1		**cluster95**		GCF_000281195.1
cluster18	G21615-S1			**cluster958**		GCF_003344865.1
cluster1820		GCF_001011155.1		**cluster965**		GCF_000024225.1
cluster1822		GCF_001676765.1		**cluster967**		GCF_001590605.1

Suppl. Table 3 *All bacterial isolates tested for their chitin degradation activity with indication if they were predicted chitin degraders and their species level.*

Genome ID	Cryo ID	OTU	Predicted	Species	Chitin Degrading	early/late
G21603-S1	NA_2	1209		*Vibrio alginolyticus*	x	late
G21623-S1	NA_62	1209		*Vibrio alginolyticus*	x	late
G21624-S1	NA_65	1209		*Vibrio alginolyticus*	x	late
G21639-S1	NA_29	1209		*Vibrio alginolyticus*	x	early
G21641-S1	NA_33	1209		*Vibrio alginolyticus*	x	late
G21644-S1	NJ_12	1209		*Vibrio alginolyticus*	x	late
G21621-S1	NA_54	1209		*Vibrio alginolyticus*	x	late
G21615-S1	NP_8	1209	x	*Vibrio alginolyticus*	x	late
G21600-S1	NA_12	1135		*Aeromonas hydrophila*	x	adult/rare
G21616-S1	NA_15	1828	x	*Sulfitobacter sp*	x	late
G21653-S1	A_MB_4	194	x	*Ruegeria pelagia*		juv/rare
G21606-S1	NA_7	524	x	*Vibrio pomeroyi*		late
G21625-S1	NA_68	243	x	*Vibrio shilonii*		early
G21612-S1	NP_3	2325	x	*Vibrio diazotrophicus*		late
G21614-S1	NP_5	2325		*Vibrio diazotrophicus*		
G21635-S1	NP_25	2325		*Vibrio diazotrophicus*		late
G21648-S1	NP_18	2325		*Vibrio diazotrophicus*		
G21633-S1	NP_22	2325		*Vibrio diazotrophicus*		early
G21617-S1	NA_85	776		*Sphingomonas sp*		
G21630-S1	NJ_41	1304		*Kiloniella laminariae*		early
G21632-S1	NJ_43	1486		*Henriciella barbarensis*		late

G21610-S1	NJ_3	2324		*Roseovarius arcticus*		early
G21646-S1	NP_16	386		*Shewanella affinis*		early
	JB_053_A2-LB-5	941		*Pseudomonas peli*		late
G21626-S1	NA_71	2280		*Marinobacter algicola*		late
G21627-S1	NA_74	93		*Hoeflea alexandrii*		late
G21607-S1	NA_9	2214		*Sulfitobacter sp*		
G21596-S1	NA_44	2226		*Microbacterium koreense*		
G21601-S1	NA_14	941		*Pseudomonas peli*		early

9 List of Publications

Domin, Hanna, Yazmín H. Zurita-Gutiérrez, Marco Scotti, Jann Buttlar, Ute Hentschel Humeida, and Sebastian Fraune. 2018. “Predicted Bacterial Interactions Affect in Vivo Microbial Colonization Dynamics in *Nematostella*.” *Frontiers in Microbiology* 9(APR):1–12.

10 Extracted parts of published manuscripts

Chapter 2.1, chapter 3.1, and chapter 3.2, as well as appropriate method subchapters were extracted from the following publication:

Domin, Hanna, Yazmín H. Zurita-Gutiérrez, Marco Scotti, Jann Buttlar, Ute Hentschel Humeida, and Sebastian Fraune. 2018. “Predicted Bacterial Interactions Affect in Vivo Microbial Colonization Dynamics in *Nematostella*.” *Frontiers in Microbiology* 9(APR):1–12.

As already stated in the manuscript itself, the authors contributed as follows:

HD, YZ-G, MS, UHH, and SF contributed to conception and design of the study. HD, YZ-G, and JB performed the research. HD, YZ-G, and SF performed the statistical analysis. HD, YZ-G, MS, and SF wrote the first draft of the manuscript. All authors contributed to manuscript revision and read and approved the submitted version.

11 Acknowledgments

Zunächst möchte ich mich bei Professor Sebastian Fraune bedanken. Dafür, dass ich nicht nur meine Masterarbeit im Rahmen dieser Doktorarbeit weiterführen durfte, sondern auch dafür, dass ich Teil des Düsseldorf-Teams sein durfte. Er hat mir nicht nur ermöglicht mich als Wissenschaftlerin weiterzuentwickeln, sondern auch einen Blick hinter die Kulissen des wissenschaftlichen Arbeitens zu werfen. Ich danke ihm weiterhin für seine exzellente Leitung, Betreuung und Menschlichkeit.

Ich danke Professor Ute Hentschel-Humeida und Dr. Katja Dierking für die Bereitschaft Teil meines TAC-Komitees in Kiel zu sein. Ich danke Professor Martin Beye für die Übernahme der Mentorenrolle während meiner Zeit in Düsseldorf. Außerdem danke ich Professor Ilka Axmann für die Übernahme der zweiten Berichterstattung.

Ich möchte weiterhin Professor Thomas Bosch dafür danken, dass ich meine Doktorarbeit in seinen Laboren beginnen durfte. Ich danke auch dem SFB1182, durch den meine Arbeit und so viel wissenschaftlicher Austausch ermöglicht wurde. Ich möchte auch der gesamten Kieler Arbeitsgruppe unter Prof. Boschs Leitung danken. Dort habe ich so viel gelernt, dass der Umzug nach Düsseldorf und das Aufbauen der neuen Gruppe leicht überwindbar klang.

Ich möchte weiter Dr. Jan Taubenheim und Timo Minten danken. Wir sind zusammen von Kiel nach Düsseldorf gezogen und haben Büro, Fortschritt, Frust und Abende geteilt. Jan hat mir darüber hinaus lebensrettend viel mit bioinformatischer Datenanalyse geholfen. Mit Timo teile ich schon länger ein Büro als ich jemals mit jemandem teilen musste und mit keinem anderen hätte ich das so lange ausgehalten.

Ich danke Dr. Johannes Zimmermann für die fruchtvolle Kollaboration an der Analyse der Bakterien-Bakterien-Interaktionen. Ich danke Dr. Sebastian Hänsch für die kompetente Einführung in das Benutzen eines konfokalen Mikroskops.

Mein Dank gilt natürlich auch der gesamten OrgInt-Arbeitsgruppe, für niemanden back ich so gern wie für euch.

Ganz besonderer Dank gilt meinen Eltern Annette und Uwe und meinem Gespons Markus, für die Ermutigungen auf dem Weg, und die Möglichkeit des Rückzugs und Krafttankens.

12 Eidesstattliche Erklärung

Ich versichere an Eides statt, dass die Dissertation von mir selbstständig und ohne unzulässige fremde Hilfe unter Beachtung der Grundsätze zur Sicherung guter wissenschaftlicher Praxis an der Heinrich-Heine-Universität Düsseldorf erstellt worden ist.

Ferner erkläre ich, dass ich in keinem anderen Dissertationsverfahren mit oder ohne Erfolg versucht habe, diese Dissertation einzureichen.

Düsseldorf, den _____